Energy, Mines and Resources Canada

Énergie, Mines et Ressources Canada

CANMET

Canada Centre for Mineral and Energy Technology

Centre canadien de la technologie des minéraux et de l'énergie

Mining Research Laboratories

Laboratoires de recherche minière

Canada

A REVIEW OF AIRBORNE PARTICLE SAMPLING WITH SPECIAL REFERENCE TO LONG-LIVED RADIOACTIVE DUST

J. BIGU ELLIOT LAKE LABORATORY

MRL 90-054(TR) MARCH 1990

Report in compliance with the Atomic Energy Control Board (AECB) Contract No. 4.108.1, entitled 'Comparison of Radioactive Aerosol Sampling Instruments', Phase I.

...ument was prepared primarily ...ion and internal ...purposes. It does not ...represent a final expression of the opinion of the Canada Centre for Mineral and Energy Technology (CANMET)

Ce document a été préparé principalement pour fin de discussion et de documentation interne. Il ne représente nullement l'expression définitive de l'opinion du Centre canadien de la technologie des minéraux et de l'énergie (CANMET)

MICROMEDIA

139pp

90-07126/

A REVIEW OF AIRBORNE PARTICLE SAMPLING WITH SPECIAL REFERENCE TO LONG-LIVED RADIOACTIVE DUST

J. Bigu*

ABSTRACT

This report reviews some basic aspects related to the sampling of airborne particles with special reference to Long-Lived Radioactive Dust (LLRD). Although succinct and at an elementary level, the report covers a number of areas of practical interest such as the production of aerosols, the dynamics of suspended particles, the physical and chemical characteristics and properties of dust clouds, and the inhalation and measurement of dust. It is followed with a brief review of dust sampling instrumentation, and with a short account of the work done on LLRD in Canada with a few references to work done outside this country. This work has been sponsored by the Atomic Energy Control Board (AECB) as part of a contract entitled "Comparison of Radioactive Aerosol Sampling Instruments" (Contract No. 4.108.1).

Key words: Aerosols; Radioactivity; Long-Lived Radioactive Dust; Sampling.

*Research Scientist and Radiation/Respirable Dust/Ventilation Section Head, Elliot Lake Laboratory, CANMET, Energy, Mines and Resources Canada, Elliot Lake, Ontario, Canada, P5A 2J6

ÉTUDE DU PRÉLÈVEMENT DE PARTICULES EN SUSPENSION DANS L'AIR, PARTICULIÈREMENT DES POUSSIÈRES RADIOACTIVES DE LONGUE PÉRIODE

J. Bigu*

RÉSUMÉ

Le présent rapport étudie certains aspects fondamentaux du prélèvement de particules en suspension dans l'air, particulièrement des poussières radioactives de longue période (PRLP). Bien qu'il soit succinct et de niveau élémentaire, le rapport traite d'un certain nombre de sujets d'intérêt pratique, comme la production d'aérosols, la dynamique des particules en suspension, les caractéristiques physiques et chimiques et les propriétés des nuages de poussière, et l'inhalation des poussières ainsi que les mesures portant sur celles-ci. Viennent ensuite une brève étude des instruments de prélèvement de poussières et un bref compte rendu des travaux effectués sur les PRLP au Canada, avec quelques mentions portant sur les travaux effectués à l'étranger. L'activité a été financée par la Commission de contrôle de l'énergie atomique (CCEA) dans le cadre du contrat "Comparison of Radioactive Aerosol Sampling Instruments" (comparaison des instruments de prélèvement d'aérosols radioactifs) (contrat n° 4.108.1).

Mots-clés : aérosols; radioactivité; poussière radioactive de longue période; prélèvement.

*Chercheur scientifique et chef de la section Rayonnement/poussière inhalable/ventilation du Laboratoire d'Elliot Lake, CANMET, Énergie, Mines et Ressources Canada, Elliot Lake (Ontario), Canada, P5A 2J6.

FOREWORD

The review given here does not pretend to be complete or exhaustive. For this purpose, the interested reader should consult the numerous bibliography references available on the several subjects dealt with in this report. However, whenever possible, an extensive list of references has been given for further reading and consultation.

With regard to the section on Dust Sampling Instrumentation, it should be noted that mention of any particular type of instrument or instrument manufacturer does not necessarily mean their endorsement. Furthermore, and for reasons of space, only a fraction of the commercially available dust instrumentation and dust techniques in current use has been discussed. The discussions have centered mainly on techniques and instrumentation the Elliot Lake personnel, i.e., the author, is directly acquainted with thorough direct experimental experience, or reference. Other biases may also be noted. Again, for more documentation the reader should refer to several excellent bibliographical sources listed at the end of the report.

Finally, the views expressed in this report do not necessarily reflect the views of the sponsoring agency (AECB), or Energy, Mines and Resources Canada (Elliot Lake Laboratory, Mining Research Laboratories, CANMET).

The author is grateful to K.P. Ho (AECB project's manager, and scientific liaison officer for this contract) for his interest, support and availability.

CONTENTS

	Page
ABSTRACT	i
FOREWORD	ii
INTRODUCTION	1
AIRBORNE PARTICULATE MATTER CLASSIFICATION	2
PRODUCTION OF AEROSOL CLOUDS	4
DYNAMICS OF SUSPENDED PARTICLES	8
A. Particle Sedimentation	10
B. Particle Inertial Deposition (Impaction)	13
C. Particle Adhesion and Reentrainment	16
CHARACTERISTICS AND PROPERTIES OF DUST CLOUDS	20
A. Particle Size Distribution	21
B. Particle Shape	23
ELECTRICAL CHARACTERISTICS OF DUST CLOUDS (WITH PARTICULAR REFERENCE TO LONG-LIVED RADIOACTIVE DUST, LLRD)	26
OPTICAL PROPERTIES OF DUST PARTICLES	30
A. Rayleigh Scattering	33
B. Fraunhofer Diffraction Region	34
C. Mie Scattering	34
CHEMICAL COMPOSITION AND CHEMICAL CHARACTERISTICS OF AEROSOL CLOUDS	35
INHALATION OF DUST	37
HEALTH EFFECTS OF DUST	40
THE MEASUREMENT OF DUST	42
A. Criteria for the Measurement of Airborne Particulate Matter	42
B. Instrumentation for Dust Measurements	44
DUST SAMPLING INSTRUMENTATION	50
A. Inertial and Gravitational Dust Collectors	50
B. Dust Collection by Filtration	62
C. Electrostatic and Thermal Particle Collectors	63
D. Optical Particle Counters (OPC)	66
E. Other Types of Particle Counters and Particle Sizers	71
LONG-LIVED RADIOACTIVE DUST STUDIES IN CANADA	72
A. Long-Lived Radioactive Dust Studies Conducted at the Elliot Lake Laboratory	74
B. Long-Lived Radioactive Dust Studies Conducted by Other Organizations in Canada	79
C. Long-Lived Radioactive Dust Studies Outside Canada	80
FINAL COMMENTS	81
REFERENCES	84

TABLES

No		Page
1.	Terminal velocities, relaxation times and diffusivities of spherical particles of unit density at 1 atm and 20°C (11,12,14) ..	95
2.	Cascade impactor data for several mechanical operations in a uranium mill	96
3.	Cascade impactor data for several physico-chemical operations in a uranium mill	97
4.	Data for several mining operations	98
5.	Dust and radioactive dust data taken in several underground uranium mines	99
6.	Effect of dust abatement methods on AMAD, MMAD and [LLRD]	100
7.	Effect of dust abatement methods on MMAD, AMAD and [LLRD]	101

FIGURES

1.	Drag coefficient versus Reynolds number for spheres, cylinders and disks	102
2.	Drag coefficient versus Reynolds number	102
3.	Impaction of efficiencies for cylinders, spheres, ribbons and disks	103
4.	Theoretical impaction efficiency on cylinders at low Reynolds numbers	103
5a.	Particle electrical charge versus particle diameter	104
5b.	Particle electrical charge versus particle diameter limit	105
6.	Total and regional deposition fractions for various sizes of inhaled airborne spherical particles with physical density of 1.0 g/cm^3 in the human respiratory tract as calculated by the International Commission on Radiological Protection (ICRP)Task Group on Lung Dynamics for nasal breathing at a rate of 15 breaths per minute and tidal volume of 1450 cm^3	106
7.	Selected data reported for the deposition in the entire respiratory tract of monodisperse aerosols inhaled by persons via the nose from Giacomelli-Maltoni et al., Heyder et al., George Breslin, and Shanty compared with predicted values calculated by the ICRP Task Group on Lung Dynamics for tidal volumes of 750 cm^3 and 1450 cm^3	107
8.	Selected data reported for the deposition in the entire respiratory tract of monodisperse aerosols inhaled by persons through the mouth from Giacomelli-Maltone et al., Altshuler et al., Heyder et al., George and Breslin, Foord et al., Shanty, and Lippmann and Albert compared with predicted values calculated by the ICRP Task Group on Lung Dynamics for tidal volumes of 750 cm^3 and 1450 cm^3	108

9. Selected data reported for the deposition in the human tracheobronchial region as the fraction of monodisperse aerosols entering the trachea reported by Foord et al., Lippmann and Albert, Chan and Lippmann, and Stahlhofen et al., compared with predicted values calculated by the ICRP Task Group on Lung Dynamics for tidal volumes of 750 cm^3 and 1450 cm^3 109

10. Selected data for pulmonary gas exchange region deposition of monodisperse aerosols inhaled through the mouth by people reported by Altshuler et al., George and Breslin, Foord et al., Shanty, and Lippmann and Albert, compared with predicted values calculated by the ICRP Task Group on Lung Dynamics for tidal volumes of 750 cm^3 and 1450 cm^3 110

11. Nasal Inhalation Deposition: Total and regional deposition fractions for aerosols entering the nose for various sizes of inhaled airborne spherical particles with physical density of 1 g/cm^3 in the human respiratory tract as calculated by the ICRP Task Group on Lung Dynamics for nasal breathing at a rate of 15 breaths per minute and tidal volume of 750 mL 111

12. Oral Inhalation Deposition: Total and regional deposition fractions for aerosols entering the mouth for various sizes of inhaled airborne spherical particles with physical density of 1 g/cm^3 in the human respiratory tract as calculated by the ICRP Task Group on Lung Dynamics with the head airway deposition function given by Raabe for oral breathing at a rate of 15 breaths per minute and tidal volume of 750 mL 112

13. Flow patterns in a cyclone collector 113

14. Fraction of solid particles deposited in the AIHL cyclone as a function of particle aerodynamic diameter 114

15. Schematic of two impactor stages showing large and small particle trajectories 115

16. A single-jet, five-stage cascade impactor 116

17. Sierra/Marple series 210 ambient cascade impactor 117

18. Marple personal sampler, series 290 117

19. Top view of a cylindrical duct aerosol centrifuge with particle trajectories 118

20. Schematic of the conifuge 118

21. Calibration curves for the Stober spiral duct centrifuge at different rotation rates and at different total flow rates 119

22. CLIMET Model CI-7300 optical particle counter optical system 120

23a. LLRD α-activity concentration in mine air. Same general area of an U/G U-mine collected over several months, Elliot Lake Laboratory .. 121

23b. LLRD α-activity concentration in mine air. Different mines, different locations (taken over two years), Elliot Lake Laboratory. 121

24. Percentage cumulative LLRD α-particle activity corresponding to dust of size $<D_{p,50}$ versus EAD for several independent measurements by cascade impactors 122

25. Cumulative α-particle activity versus Equivalent Aerodynamic Diameter for long-lived radioactive dust and thoron progeny, for different days. (Conveyor belt) 123

26a. TnD α-spectrum from a radioactive dust sample. Also shown is the α-spectrum from a RnD + TnD reference source 124

26b. LLRD α-spectrum from a radioactive dust sample from U/G U-mine (tentative identification). Silicon barrier detector, under vacuum 124

26c. LLRD γ-spectrum, taken with a HPGe, from a radioactive dust sample. 124

27. Alpha-particle spectra corresponding to different mill operations.. 125

28. Frequency (distribution) versus α-particle activity concentration for LLRD samples collected in an U/G U-mine. Also shown are the frequency percentages of the total number of measurements (Mine A). 126

29. Frequency (distribution) versus α-particle activity concentration for LLRD samples collected in an U/G U-mine. Also shown are the frequency percentages of the total number of measurements (Mine B). 127

30. LLRD α-particle activity versus quartz dust mass for the period 1983-1985 (Mine A) 128

31. LLRD α-particle activity versus quartz dust mass for the period 1983-1985 (Mine B) 129

32. Diffusion coefficient for particles of diameter D_p 130

33. Electrical mobility for particles of diameter D_p 131

34. Electrical mobility for particles of diameter D_p, and slip factor for particles of diameter D_p 132

INTRODUCTION

Mining operations generate dust within a wide size range - from submicron size to well beyond the respirable size range (1). Of particular interest, from the occupational and health physics standpoints, is dust in the respirable size range (<1-10 μm) because once inhaled, a fraction of it will be deposited in the respiratory system (2-5).

In underground uranium mines and uranium mills, dust emissions contain certain radionuclides. These radionuclides have been identified by a variety of methods, such as α- and γ-spectrometry, neutron activation analysis, particle induced X-ray emissions, fluorescence, and spectrophotometry (6-9). The radionuclides identified include the parents of the natural uranium and thorium decay chains (^{238}U, ^{235}U, ^{232}Th) and their short-lived and long-lived decay products (^{234}U, ^{230}Th, ^{226}Ra, ^{222}Rn, ^{228}Ra, ^{228}Th, ^{218}Po, ^{214}Pb, ^{214}Bi, ^{212}Pb, ^{212}Bi, ^{210}Pb and ^{210}Po) (6-9).

The inhalation of dust generated in mining and milling operations poses a potential health hazard, and if the dust contains radionuclides, inhalation can pose an even greater potential occupational health concern (10).

Dust that contains long-lived radionuclides is commonly referred to as Long-Lived Radioactive Dust (LLRD). However, because of the decay of these radionuclides into short-lived radioisotopes, short-lived radioactivity is also associated with LLRD. The most hazardous type of radiation associated with LLRD is α-particle emissions.

Because of the health risks associated with the inhalation of LLRD, its accurate quantification and characterization is of utmost importance. Sampling methods and techniques, and sampling instrumentation for accurate quantification and characterization of dust and of its associated radioactivity is of great practical interest in order to determine occupational exposures, and in ascertaining that LLRD control methods operate efficiently.

There is a significant information gap regarding the performance and accuracy of LLRD sampling techniques and sampling instrumentation. This report deals with the above subjects and was requested by the Atomic Energy Control Board (AECB) as part of a contract awarded to CANMET (E.M.R.) entitled "Comparison of Radioactive Aerosol Sampling Instruments", Contract No. 4.108.1.

AIRBORNE PARTICULATE MATTER CLASSIFICATION

The classification of airborne particulate matter is a subject of great difficulty. The discussion that follows is entirely based on the definitions and discussions by Green and Lane (11), and Friedlander (12).

Aerosols, i.e., airborne particulate matter, are formed either by the conversion of gases to particulate matter or by disintegration of solids and liquids. Aerosols may also result from the resuspension of powdered materials or the break-up of agglomerates. Aerosol formation from the gas phase tends to produce much finer particles than disintegration processes, except when condensation phenomena occur directly on existing particles. Aerosols formed directly from gases are usually of submicron size.

Attempts made in the past to classify disperse systems in gases on the basis of their origin, nature, shape, and particle size have met with great difficulty. Disperse systems in gases have been broadly, and rather popularly, classified (sometimes with somewhat conflicting meanings) into the following categories:

1. Dusts,
2. Smokes,
3. Mists,
4. Fumes, and
5. Haze.

Dusts consist of solid particles dispersed in a gas phase as a result of mechanical disintegration processes such as dust clouds formed by disintegrating minerals and rocks during mechanical processes involving blasting, crushing, grinding, drilling, etc., or by subjecting powders to strong aerodynamic forces such as those produced by an air blast. Dusts tend to be highly heterogeneous systems of poor stability and highly irregular particle shape, which contain more large particles than smokes and mists.

Mists are made up of liquid droplets usually formed by the condensation of vapour. However, mists can also be produced by the atomization of a liquid. The liquid droplets, regardless of whether they are formed by atomization or condensation, may carry substances in solution or particles in suspension. Mists, particularly those of natural origin, consist of particles up to, or greater than, 10 μm in size. The particle number content of mists is usually low.

In smokes, and also in fumes, particles are generally smaller in size than dust particles, and are formed from the gas phase. Smokes cover a wide variety of gaseous disperse systems consisting of particles of low vapour pressure which settle slowly under gravitational forces. Smokes are particularly characterized by their mode of formation. There is a variety of ways in which smokes can be formed, by combustion, destructive distillation, volatilization and condensation, chemical and photochemical reactions, and electrical and mechanical pulverization.

Fumes usually refer to the case when a smoke is formed simultaneously with the production of a gas or a vapour. Sometimes this term is also used to indicate the cloud of particles formed over a substance by vapour phase or other reaction.

Haze is usually a combination of particles or atmospheric pollution, dust, and atmospheric droplets.

Fogs and smogs are terms used to mean, in general, the following. When

the suspensoid (suspended particles) in mist is of sufficient concentration to reduce the visual range significantly, then it is fog. Smog is referred to as the aerial system formed when fog occurs in the presence of atmospheric pollution from domestic and industrial chimneys, although the term has also been used to classify other noxious atmospheric suspensions.

PRODUCTION OF AEROSOL CLOUDS

Aerosols of a wide size range are produced artificially in the laboratory for scientific, technical, medical or other practical purposes. Aerosols are also produced by natural processes on the surface of the earth and in the biosphere, or as a result (or as a by-product) of industrial operations and other mechanisms. The following are some common processes of aerosol production:

1. condensation from the vapour phase;
2. mixing of vapour-laden gas streams at different temperatures;
3. chemical interactions and reactions in the gas phase;
4. combustion;
5. electric arcing;
6. photolysis;
7. dispersion;
8. attrition, disruptive, or impulsive forces;
9. atomization.

From the aerosol family the one member of most interest in the context of this study is dust. More specifically, we are interested in radioactive dust in the respirable size range, that is, radioactive dust particles of size large enough that no appreciable penetration in the nose or mouth takes place because of rapid gravitational settling, or any other physical or chemical selective removal mechanism, by the above. In general, respirable dust

fraction is understood to be dust in the size range from ~1 μm to 10 μm. This size range is, however, somewhat arbitrary and can be extended slightly downward and upward.

Radioactive dusts are mainly found near:

1. radioactive (materials) deposits;
2. uranium/thorium mines;
3. uranium/thorium mills;
4. uranium/thorium refineries;
5. nuclear fuel fabrication cycle facilities;
6. nuclear installations;
7. other sources.

From all the classifications and categories so far described and discussed, the one of particular interest here is respirable dust containing long-lived radionuclides of the natural U and Th radioactive family series. These dusts are mainly encountered in U/Th mine atmospheres and in U/Th mill atmospheres, and they will be the major thrust of this report.

Radioactive dusts are generated in the above environments preferentially by the following processes:

1. physical disintegration or fragmentation;
2. dispersion;
3. reentrainment.

Among physical disintegration or fragmentation processes the following are most important: blasting, drilling, crushing, milling or grinding. The physical disintegration or fragmentation of a solid substance is brought about by applying shearing and tensile stresses slowly, such as in milling processes, or by a crushing pressure applied gradually by means, of say, rollers, or abruptly, e.g. in blasting operations, or in powerful impact machinery. In all cases, the applied forces cause solid fragmentation by cracking or splitting the material along 'weakness' planes or surfaces. In

some dusts, it is possible to distinguish between two kinds of particles represented by small, i.e., relatively large fragments, and by fine particles released from the recently formed surfaces by micro-scale cracking as the material is torn apart.

Dispersion processes are to be understood here as the dispersion of dusts from a liquid suspension, resuspension, or by pneumatic vibration or percussion of discrete dust sources. Examples of these processes are ore loading, unloading and mucking operations. Another example is ore transportation by conveyor belts and other operations.

Reentrainment is defined here as the dispersion of thin layers of dust deposited over extended surfaces by aerodynamic forces. An example of reentrainment is the dispersion of dust particles deposited on mine wall surfaces by the flow of mine air, particularly under turbulent conditions, i.e., high Reynolds number.

The behaviour of aerosol clouds depend on a number of important considerations and physical phenomena such as:

1. Interaction of airborne particles with gas constituents.
2. Interaction of particles with other suspended particles.
3. Motion of particle clouds or particles under the influence of external forces.
4. Motion of particles with respect to flow boundaries or obstacles.

The motion of particles suspended in a stationary or flowing gas is determined by external forces that act on the particles, and on the kinetic properties of the gas phase. The following physical phenomena result in transport, deposition or motion of aerosol particles:

1. Electric fields;
2. Magnetic fields;
3. Gravitational fields;
4. Laminar and turbulent shear gradients;

5. Inertial forces;
6. Centrifugal or vortex flow;
7. Drag forces;
8. Coriolis forces;
9. Concentration gradients in molecular species in the gas phase, i.e., diffusiophoresis;
10. Thermal gradients, i.e., thermophoresis;
11. Acoustic forces, i.e., alternating pressure fields;
12. Photophoresis; and
13. Other phenomena.

In the presence, or the absence, of one or more of the above physical phenomena, the suspended particles in the gas phase undergo the following physical mechanisms:

1. Diffusion.
2. Convective transport.
3. Sedimentation.
4. Coagulation.
5. Nucleation.
6. Adhesion and reentrainment.

Items 1 to 3 and 6 represent transport across walls or boundaries within a given control volume, whereas 4, 5, and sometimes 6, take place within this element of volume. Items 4 and 5 result in an increase in size of the original particle. For particles of size equal to or larger than about 1 μm, i.e., dusts, diffusion phenomena can be neglected. This is so because the particle size is much larger than the mean free path of the gas molecules. Hence, particle motion is governed by convective transport and sedimentation. The next few sections will deal with some aspects of particle dynamics. However, before leaving this section a few definitions and clarifications will be given.

The term adhesion is given to the physical mechanism whereby aerosol particles deposit on a solid surface by the action of a force arising from the particle and the surface properties, interface geometrical considerations, and condensed gas constituents (13). Adhesion forces for particles in the size range 1-7000 μm are within 10^{-9} Kg-force (a few millidynes) to about 1.0×10^{-5} Kg-force (~10 dynes), respectively. Particles of size about 2 μm have dimensions near the size of irregularities of the deposition surface. Much larger particles make few contacts at points on the deposition surface. Furthermore, these particles have weights that exceed the adhesion force.

Coagulation of airborne particles take place when particles collide with one another resulting in larger particles forming. The forces and mechanisms responsible for coagulation are various, and include thermal, acoustical, electromagnetic, inertial, gravitational, molecular and hydrodynamical forces.

Nucleation refers to condensation of a vapour phase by the presence of foreign airborne particles.

DYNAMICS OF SUSPENDED PARTICLES

A number of physical phenomena such as electrical mobility, thermophoresis, and diffusiophoresis, which are relevant for particles in the submicron size range in still air or in special apparatus, are not important for larger particles, i.e., particles of size equal or greater than about 1 μm. The reason for this lies in the much larger mass of large particles. As a result larger particles are easily swept along by air currents or settle rapidly in air at rest, forming sediments. Hence, removal or loss of suspended large particles ($\gtrsim$1 μm) takes place preferentially by the following processes:

1. Sedimentation;

2. Impaction (inertial deposition);

3. Adhesion and reentrainment.

The above mechanisms are influenced by external force fields and airflow conditions. Items 1 to 3 are of great practical importance in the context of this report because these mechanisms play a very dominant role in:

1. Measurement, characterization and monitoring of dust clouds in working environments;
2. Behaviour of instrumentation used in the assessment of particulate matter; and
3. Choice of monitoring and measuring dust instrumentation.

A brief discussion on each of the main physical processes by which large particles are removed from air suspensions are given below. However, before doing so it is important to distinguish between the following regimes of particle motion (14):

1. Particles moving with an air stream at a low rate of flow;
2. Particles settling at appreciable speeds but having negligible inertia;
3. Particles having negligible settling rate but appreciable inertia;
4. Particles having appreciable inertia and settling rate.

Items 2 and 4 are important in the context of the present study. Items 1 and 3 are mostly applicable to smaller particles, i.e., $<<1$ μm.

Inertial effects are characterized by the stop-distance, d_s of the particle given by (14):

$$d_s = \tau v_o \qquad (1)$$

where, v_o is the velocity with which the particle is projected in still air. The variable τ is a relaxation time, and is defined as the time a particle needs to adapt itself, i.e., relax, to an external applied force.

The stop distance, d_s, in Equation 1 is the distance within which the particle comes to rest when projected at the speed v_o in air at rest. For particles which follow Stokes law of resistance τ is given by:

$$\tau = m/6\ \pi a\eta = 2\ a^2\sigma/9\ \eta \qquad (2)$$

where,

m is the mass of the particle,

a is the radius of the particle,

η is the viscosity of air, and

σ is the density of the particle.

The terminal velocity (rate of fall), v_s, or a heavy particle in air due to gravity is:

$$v_s \simeq g\tau \qquad (3)$$

where g is the acceleration due to gravity.

Values for v_s and τ for particles of several sizes are given in Table 1. These data are for spherical particles of unit density and in air at NTP (normal temperature/pressure conditions), P = 1 atm, T = 20°C.

A. PARTICLE SEDIMENTATION

When a spherical particle within the size range usually found in dusts, mists and smokes, falls through a viscous fluid, it is acted on by gravity forces (F_g), inertial forces, and viscous drag forces (F_D). If the particle is of a large size compared with the mean free path of the gas molecules, e.g., air, but is not so large that inertial effects must be taken into account (or under laminar flow conditions), then:

$$F_D = F_g \qquad (4)$$

$$\text{where, } F_D = 3\ \pi\eta_f\ v_s\ D_p, \text{ and } F_g = (\pi/6)\ D_p{}^3(\rho_p - \rho_f)g \qquad (5)$$

where, in Eqs. 5:

η_f is the viscosity of the fluid (in this case air),

v_s is the terminal or settling velocity of the particle,

D_p is the diameter of the particle,

ρ_p is the density of the particle, and

ρ_f is the density of the fluid (in this case air).

Equations 4 and 5 are used sometimes to estimate the size of the falling particle, D_p, from experimental measurements of the settling velocity, v_s. Conversely, the latter can be derived if D_p is known, namely:

$$v_s = \frac{(\rho_p - \rho_f) g D_p^2}{18 \eta_f} \tag{6}$$

Equation 6 indicates that the settling velocity increases as the square of the particles' diameter, and hence increases very rapidly with particle size. It is clear from the above discussion that Eq. 6 is only valid for a still fluid (air) or for very low airflow conditions, i.e., $v \simeq 0$, where v is the linear velocity of the fluid. (Table 1 gives terminal velocities data, and other data, as a function of the particle diameter.)

The above discussion and the expression for v (see Eq. 6) are only valid for viscous, streamline, or Stokes' law region, i.e., for airflow conditions for which the Reynolds number (Re) is very low, i.e., up to about 0.1. (The Reynolds number is given by the expression $Re = (v_p D_p \rho_p / \mu_f)$, where v_p is the velocity of the particle.)

Outside the viscous flow region, the terminal velocity of the particle, v_s, is given by:

$$v_s = (2\ G/A\ \rho_p\ C_D)^{1/2} \tag{7}$$

where, G is the external force applied to the particle, i.e., electrostatic, gravitational, etc.,

A is the projected surface area of the particle perpendicular to the direction of motion (for a sphere $A = \pi D_p^2/4$),

C_D is the drag coefficient. This coefficient assumes different form for different airflow conditions, i.e., different values for the Reynolds number.

If the external force applied to the particles is that due to gravity, Eq. (7) becomes:

$$v_s = [4\ D_P\ (\rho_P - \rho_f)g/3\ \rho_P\ C_D]^{1/2} \qquad (8)$$

Expressions for C_D for several Re regions are given below (15):

1. $C_D = 24/Re$ for $Re \leq 0.1$,

2. $C_D \simeq 10\ Re^{1/2}$ for $30 < Re < 300$ (Allen's region),
   or more accurately:
   $C_D = (Re/24) + 4/(Re)^{1/3}$,

3. $C_D = 29.6\ Re^{(0.554\ \ln Re\ -\ 0.983)}$ for $0.1 < Re < 3500$.

Other expressions for other regions of Re can be found in the above reference. Useful graphs showing C_D as a function of Re are given in Figs. 1 and 2.

Because dust clouds and other aerosols are usually bounded by walls such as man-made vessels, natural enclosures, e.g., caverns, and semi-natural enclosures, such as, mine galleries, it is of great practical interest to determine the decay of particle concentration from sedimentation for some common geometries or enclosures. The following expressions have been taken from Billings and Gussman (13).

1. Enclosed Rectangular Vessel. The differential equation describing the depos. ion rate of particles uniformly stirred in an enclosed rectangular vessel is given by:

$$dn/dt = - n v_s t/h \qquad (9)$$

where, n is the particle concentration,

t is time, and

h is the height of the vessel.

Integration of Eq. 9 over time, gives:

$$n = n_o\ e^{-v_s t/h} \qquad (10)$$

2. Enclosed Spherical Vessel. For an enclosed spherical vessel of diameter d, the particle concentration function assumes the following form:

$$n = n_o\, e^{-3\, v_s t/4\, d} \qquad (11)$$

3. Horizontal Cylindrical Tube. The loss of particles flowing through a horizontal cylindrical tube of radius r under laminar flow conditions is given by:

$$n/n_o = 1 - \frac{2}{\pi}[2\,\omega\,\Omega + \arcsin\,\omega^{1/3} - \omega^{1/3}\Omega] \qquad (12)$$

where, $\omega = 3\, v_s L/8\, r v_m$, and $\Omega = (1-\omega^{2/3})^{1/2}$, and

L is the length of the tube,

v_m is the mean velocity of the air flow.

Under turbulent flow conditions Eq. 12 becomes:

$$n/n_o = e^{-2 v_s L/\pi v_m r} \qquad (13)$$

where, in Eqs. 12 and 13, n_o is the particle inlet concentration, i.e., the concentration at the tubes' entrance. In Eqs. 10 and 11, n_o represents the initial particle concentration, i.e., the concentration at $t = 0$.

Equations 10 and 11 show that, as expected, particle losses decrease with increasing vessel size. The same geometrical arguments apply equally well to the case of cylindrical tubes (Eq. 12 and 13).

B. PARTICLE INERTIAL DEPOSITION (IMPACTION)

Because of their inertia, particles above a certain size are not able to follow the motion of their accelerating suspension (gas) medium. Inertial effects become important for particles of size larger than about 1 μm, and may lead to particle deposition by obstructing material surfaces. For instance, when a material surface, i.e., obstacle, is introduced into a flowing aerosol cloud, particles of small size are able to follow the gas flow lines around the object, whereas particles of large size are not able to change their direction, and are, therefore, intercepted (deposited on) by the obstacle. In all cases, it is the acceleration of the gas, e.g., air stream, that leads to

inertial deposition. Unlike diffusion, which is a stochastic process, inertial deposition is a deterministic process.

The parameter that characterizes impaction phenomena is the Stokes number (St) or Impaction parameter (Ip). The Stokes number is defined as the dimensionless ratio of the stop distance (the finite distance travelled by a particle of size D_p projected into the stationary fluid with a velocity v) to a characteristic dimension of the obstacle of the flow geometry, e.g., the diameter of a cylindrical rod or sphere introduced into the airflow, or the viscous sublayer thickness. The expression for St is:

$$St = \rho_p D_p^2 v/18 \eta_f D \tag{14}$$

where, in Eq. 14, D is the diameter of the sphere, cylinder, disk, or width of, say, a ribbon.

Another important parameter in inertial impaction phenomena is the impaction efficiency, η_I, which is defined as the ratio of the volume of gas cleared of particles by the collecting element, i.e., obstacle, to the total volume swept out by the collector. The impaction efficiency is a complex function of the Stokes number, the Reynolds number, and the interception diameter, R, defined (12) as:

$$R = D_p/L \tag{15}$$

where, L is the characteristic length of the collector. In other words, the impaction efficiency depends on airflow conditions, particle size, the geometry of the system, and other considerations.

Impaction of spherical particles on obstacles of simple geometries such as spheres, cylinders, ribbons and discs transverse to the direction of fluid flow has been investigated, both theoretically and experimentally. These studies are of great practical interest; for example, flow around single cylinders is taken as the model on which particle filtration by a fibrous filter is based. Furthermore, the cylindrical model is the geometry of interest for inertial deposition on pipes, wires, and other similar objects in

a fluid flow.

Jet impaction is a particular case of inertial impaction on, in general, simple geometries. In this case, a particulate stream is drawn into a nozzle where the gas and particles are accelerated to great velocities and then directed against an adjacent flat surface. As the gas flow diverges after impaction, suspended particles tend to continue in a forward direction because of their inertia. A velocity difference develops between the gas and the suspended particles. This difference in velocity depends on the size of the particle; larger particles suspended in the gas flow impact upon the plate and are removed from the stream, whereas smaller particles are carried aside and continue on with the gas.

Inertial impaction on spheres is of great interest in air pollution and cloud physics studies where the collection (collision) efficiency of drops (e.g., water droplets) moving through a dust cloud is of importance. This process is also important in scrubbers which use this mechanism of particle deposition for the purpose of cleaning the air at the work place.

Another practical application based on particle inertial deposition principles is the cyclone separator, which is often used for the removal of large particles from process gases. The dust laden gas enters an annular space through a tangential inlet. The gas acquires a rotating motion and particles suspended in it are removed on the outer walls of the separator by centrifugal forces.

Inertial deposition of particles on surfaces depends, as previously indicated, on fluid flow conditions. Under turbulent conditions, large particles suspended in a stream of gas flowing parallel to a material surface deposit on the latter because of the fluctuating velocity components perpendicular to the material surface. Suspended particles are not able to follow the eddy motions and are projected onto the surface of the obstacle through the relatively motionless fluid close to the obstacle's surface. The

particle deposition rate depends on the relative rates of particle transport and reentrainment.

Experimental impaction efficiency data for several geometrical objects (cylinders, spheres, discs and long ribbons) in an air stream are shown in Fig. 3. The Figure shows the impactor efficiency (η_I) versus the impaction parameter (I_P). The latter is related to η_I through $I_P = S_F\ St$, where, S_F is the so-called Slip Factor.

The data shown in Fig. 3 represent objects with a characteristic dimension (diameter or width) ranging from 0.1 cm to 2 cm, immersed in a fluid of linear velocity in the range 2 ms^{-1} to 6 ms^{-1} and Re = 165 - 8500, where dibutyl phalate particles of diameter 20, 30 and 40 μm were sprayed. As the graphs show, the impaction efficiency increases, although in a rather complex fashion, with increasing Stokes number.

Figure 4 shows the theoretical impaction efficiency versus the impaction parameter for cylinders of different Reynolds (Re) numbers. For very low values of the Re, i.e., Re $\lesssim$0.2, a linear relationship between η_I and I_P is obtained. Departure from linearity or quasi-linearity is clear at higher values of Re.

Impaction (inertial deposition) is an important physical mechanism of particle removal on which some dust monitoring and measuring instruments are based.

C. PARTICLE ADHESION AND REENTRAINMENT

Solid particles attach themselves to material surfaces by binding forces which depend on the physical and chemical properties of the substrate (material surface) and the solid particles, e.g., dust particles. In addition, adhesion forces also depend on environmental variables such as relative humidity and temperature, and airflow conditions.

There are a number of forces which contribute to the adhesion of dust particles to substrates such as:

1. Van der Waals forces;
2. Electrostatic forces;
3. Surface tension forces;
4. External force fields; and
5. Other forces.

Van der Waals forces include attractive forces between molecules (in dust particles and substrates) possessing permanent electrical dipole and quadrupole moments, forces of attraction arising from the electrical induction or polarization of molecules by static dipole and quadrupole electric fields of other (nearby) molecules, and dispersion (i.e., nonpolar Van der Waals, or London-van der Waals forces) forces. Among these three types of forces, namely, dipole, induction, and dispersion forces, the latter is usually the major contributing factor.

The London-van der Waals dispersion force, $F_{L,V}$, between two molecules a distance r apart is given by the following equation:

$$F_{L,V} = \lambda\, r^{-7} \tag{16}$$

where, λ is the van der Waals force for attraction and r is the distance between the molecules.

The attractive force described by Eq. 16 decreases rapidly with the molecular separation distance, and is only effective within several molecular diameters. The force of attraction between a spherical particle of diameter D_p at a distance r from a material surface has been given by:

$$F_{L,V} = (\pi^2\, n^2\, \lambda\, D_p/12) r^{-2} \tag{17}$$

where, n is the number of atoms per cm^{-3}. Equation 17 has been derived from the attraction force for two molecules derived by Hamaker and Bradley (16,17).

The nature of the material surfaces enters into the calculation of the London-van der Waals dispersion constant, λ. Furthermore, the electrical and

chemical characteristics and properties of the materials determine the strength and sites of electrostatic charge or ion transfer, if any of these mechanisms are applicable. Hence, it is not surprising to find that forces of adhesion for different material surfaces can vary by a factor of ten for the same particle size (18).

Equation 17 shows that if London-van der Waals dispersion forces are responsible for adhesion phenomena, than the force of attraction between a substrate and a spherical particle of dust is proportional to the particle diameter.

The binding force between a particle and a substrate can be affected a great deal by the electrostatic charge on the particle, the substrate, or both. Unfortunately, there is little information available on the effect of this charge on the binding force between particles and the substrates.

Particles can also be bound to material surfaces by surface tension forces. For perfectly 'smooth' surfaces and spherical particles of size D_P it can be shown that if a film of liquid exists between the particle and a surface in physical contact, the adhesion force, F_A, due to the liquid film is given by:

$$F_A = 2\pi \gamma D_P \qquad (18)$$

where, γ is the surface tension of the liquid film. The expression for F_A given by Eq. 16 represents the maximum force which could be experienced as a result of the liquid film. Equation 16 is only valid at relative humidities near 100%. Adhesion forces between particles and material surfaces in moisture unsaturated air are considerably lower than the values given by Eq. 16.

Adhesion forces are affected by a variety of external force fields such as electric fields and temperature gradients. In addition, adhesion is also affected by other factors such as surface contamination, particle shape, surface roughness, state of particle aggregation, and the contact time between

particles and substrates.

The reentrainment (resuspension) of particles adhered to a substrate exposed to a moving fluid is a common natural phenomenon. Reentrainment is associated with the aerodynamic detachment of particles of size less than about 100 μm attached to material surfaces by adhesion forces. Particle reentrainment is initiated by fluid flows whose velocity exceeds some threshold value. Furthermore, this threshold flow velocity decreases with increasing particle size. Reentrainment is commonly explained as the balance of forces acting on the resuspending particle. In the classical theory of reentrainment, a solid particle adhering to a substrate will be dislodged when the removal force provided by the drag and lift of the fluid stream on the particle is larger than adhesive binding forces. The drag force, F_D, acting on a stationary particle in a moving fluid is given by:

$$F_D = C\rho_f \, v_f^2 \, A_p/2 \tag{19}$$

where, C is the drag coefficient,

ρ_f is the density of the fluid,

A_p is the particle projected area, and

v_f is the velocity of the fluid.

More recently, Reeks et al. (19) have advanced a new theoretical approach to reentrainment phenomena in which they recognize the importance of the turbulent energy transferred to the particle from the resuspending flow. Such a transfer takes place through the aerodynamic lift force which fluctuates randomly in time. In this statistical model of particle reentrainment, a particle in contact with a material surface is in a constant state of vibration, building up energy until this energy is sufficient to detach the particle from the material surface. The theory postulates that this accumulation of energy takes place most efficiently at driving frequencies close to the natural frequency of the motion, i.e., resonant energy transfer, where it is limited by the energy dissipation in the local

fluid and material surface, i.e., fluid and mechanical damping.

The above researchers have shown that the threshold flow velocity for detachment (desorption) in this theory can be significantly lower than that based on a balance of adhesive and aerodynamic forces. Furthermore, it can be theoretically predicted (experimentally observed) that after some initial time (<1 s) the reentrainment rate of particles varies almost inversely as the time.

The long-term reentrainment rate constant, R, based on the above model is given by:

$$R \sim \omega_o \exp [-Q/(2\langle PE\rangle)] \qquad (20)$$

where, ω_o is the typical frequency of vibration of the particle,

Q is the height of the surface adhesive potential well, and

<PE> is the average potential energy of the particle in the potential well.

Reentrainment is an important mechanism that plays an important role in dust monitoring and measuring instruments.

CHARACTERISTICS AND PROPERTIES OF DUST CLOUDS

The great majority of natural and artificially produced aerosols possess considerable polydispersity. However, polydispersity is only one of the many characteristics of airborne small particles; chemical diversity and physical diversity are other attributes of natural and artificial aerosols. In general, aerosols, such as dust clouds, can be characterized by the following:

1. Particle size distribution,
2. Particle shape,
3. Particle and particle cloud chemical composition,
4. Chemical properties of the dust cloud,
5. Physical characteristics such as electrical charge distribution

and optical properties (e.g., scattering).

The above topics have been dealt with extensively in the literature, however, a brief discussion of the above items will be given below for the sake of completeness.

A. PARTICLE SIZE DISTRIBUTION

There are a number of ways the size distribution of an airborne particle assemble can be expressed. The fraction of the total number of particles having diameters which lie between D_p and D_p+dD_p can be written:

$$df = f(D_p)\, dD_p \tag{21}$$

subject to the condition:

$$\int_o^\infty f(D_p)\, dD_p = 1 \tag{22}$$

The function $f(D_p)$ represents the particle size frequency distribution curve.

A similar expresion can be written for the weight distribution:

$$dW = W(D_p)\, dD_p \tag{23}$$

subject to the condition:

$$\int_o^\infty W(D_p)\, dD_p = 1 \tag{24}$$

where the function $W(D_p)$ represents the particle weight frequency distribution.

The functions $f(D_p)$ and $W(D_p)$ are related by the following expression (20):

$$W(D_p) = \beta\, m(D_p)\, f(D_p) \tag{25}$$

where $m(D_p)$ is the mass of the particle with diameter D_p and β is a proportionality factor which can be determined by the equation:

$$\int_o^\infty W(D_p)dD_p = 1 = \beta \int_o^\infty m(D_p)f(D_p)dD_p = \beta\, \bar{m} \qquad (26)$$

where $\bar{m}$ represents the arithmetic mean of the masses of the dust particles.

From the above expression it is simple to arrive at the following equality:

$$W(D_p) = (m(D_p)/\bar{m})\ f(D_p) \qquad (27)$$

A number of empirical, semi-empirical and theoretical expressions have been suggested to represent the size distributions of aerosols. However, because of the great complexity of aerosol formation and dispersion processes, no precise theoretical approach is available (except for a few cases) to derive accurate expressions representing actual particle size distribution in a number of cases of practical interest. However, if dispersion is attained by comminution processes such as crushing and grinding (milling), the particle size distribution appears to follow a log normal relationship. Materials such as quartz, granite, pulverized silica, soda, ash, alumina, and clay, among other materials, give size distributions that can be represented satisfactorily by the logarithmic form of the normal law (21).

The normal distribution law, or Gaussian error curve, is one of the most important laws in nature. However, as indicated above, it is rare for particle sizes to be distributed equally about a mean as the normal distribution requires. Although such a distribution has been found in condensation systems, particularly in so-called monodisperse aerosols, more often there is a skewness of the distribution and the probability curve follows a geometric or logarithmic form of the normal distribution. According to the log normal distribution, Eq. 21 can be represented by:

$$f(D_p)\ dD_p = \frac{1}{\log \delta\ \sqrt{2\pi}} \exp\ -\left[\frac{(\log D_p - \log D_{p,g})^2}{2(\log \delta)^2}\right] d\log D_p \qquad (28)$$

where, $(\log \delta)^2 = \overline{(\log D_p - \log D_{p,g})^2}$, and $\log D_{p,g} = \overline{\log D_p}$.

In the last two expressions, $D_{p,g}$ is the geometrical mean of the

particle diameter.

The number of particles of diameter between $D_{P,1}$ and $D_{P,2}$, say $n(D_{P,1}, D_{P,2})$ can be calculated according to:

$$n(D_{P,1}, D_{P,2}) = \sum_i n_{D_{P,i}} \int_{D_{P,1}}^{D_{P,2}} f(D_P)dD_P \qquad (29)$$

where, $\Sigma\, n_{D_{P,i}} = N$ is the total number of particles,

and $f(D_P)dD_P$ is given by Eq. 28.

Particle weight (mass) distribution and other particle distributions can be written by analogy with Eqs. 28 and 29.

B. PARTICLE SHAPE

Airborne particles are found in a variety of shapes. The British Standards Institute has prepared a standard terminology for the description of particle shapes (22):

1.	Acicular	needle shaped
2.	Angular	sharply etched or having a roughly polyhedral shape
3.	Crystalline	a geometric shape freely developed in a liquid
4.	Dendritic	having a branched crystalline shape
5.	Fibrous	regularly or irregularly thread-like
6.	Flaky	flake-like
7.	Lamellar	plate-like
8.	Granular	having approximately equidimensional but irregular shape
9.	Irregular	lacking any symmetry
10.	Modular	having rounded, irregular shape
11.	Spherical	globular shape.

Fuchs (20) divided the shape of airborne particles into three classes determined by their relative dimensions along three axes perpendicular to one

another:

1. Isometric particles, in which all three dimensions are roughly the same, e.g., spherical, regular polyhedral, and particles approximating these forms or shapes;
2. Particles having much greater lengths in two dimensions than in the third dimension, e.g., platelets, scales and leaves; and
3. Particles with great length in one dimension such as prisms, needles and threads.

The determination of particle size, except for the odd case where spherical particles are involved, is a difficult process. The data obtained in the experimental measurements depend to some extent upon the physical principles used in the determination procedure, and the conventions employed in the definition of particle size, which become necessary because of the irregular shape of the particles. In this regard the use of, for example, 'equivalent', 'average' and 'projected' geometrical variables such as particle diameter and surface area, and shape factors, are frequently employed useful concepts (21). In addition, because all laws describing the properties of aerosols are expressed for particles of spherical shape, the degree of irregularity is usually assessed by the deviation of the particle shape from spherical, i.e., the coefficient of sphericity, which is defined as the ratio of the surface area of a sphere with the same volume as the given particle to the surface area of the particle. For instance, the coefficient of sphericity is 0.846 for an octahedron, 0.806 for a cube, 0.670 for a tetrahedron, and, of course, 1 for a spherical particle (20).

The boundary of a particle defines its shape. There are several mathematical methods to extract boundary information from (for) particles. Several workers have proposed, and used, the idea that a dimensionless description of the profile (boundary) of a particle could be obtained from a Fourier analysis of a waveform representing the profile (23-25). Schwartz and

Shane (23) have suggested that one could generate a wave function characteristic of the particle profile using a rotating vector transform procedure. For this, a reference point within the particle profile is needed. This point is identified by circumscribing particles in the smallest possible circle. The centre of this circle is taken as the reference point. The magnitude of the vector drawn from the centre of the circle to the periphery of the profile of the particle is then measured as a function of the angle swept by this vector, thereby generating a waveform. Because this waveform can be treated as one complete cycle (vector sweeps from 0 to 360^{o}) of a continuous periodic function, it can be subjected to Fourier analysis.

The external morphology of a particle profile can be investigated by generating a geometric signature waveform based on the Feret diameter (FEDI) of a profile. To generate the FEDI signature form, the particle profile is rotated through the angle describing the orientation of the profile relative to a fixed direction in space. As the profile is rotated, the magnitude of the projected length is taken as defining the amplitude of the waveform. All values of the projected length are normalized relative to the maximum FEDI. (Note: for convenience, the reference direction is usually taken parallel to the maximum projected length of the profile.) It is important to notice that the waveform generated is independent of the location of the point of rotation with respect to the location of the profile. Furthermore, the FEDI waveform can be appreciated by considering the physical significance of the area under the FEDI waveform graph. Also, a dimensionless estimate of the perimeter of the profile can be gained by integrating the area defined by the FEDI waveform.

Some researchers have generated characteristic signature waveforms from the diffraction patterns of particle profiles (26,27) using, for instance, optical pattern recognition systems operating on optical (laser) diffraction principles (28). Frequently, this method employs Fourier analysis techniques.

Some workers have explored the possibility of using the method in the description of a variety of shapes such as geological fossils, chromosomes, viruses, and the like (29).

More recently, the theory of fractals has been used to characterize or describe highly convoluted and rugged boundaries occurring in nature (30). Mandelbrot (30) has shown that it is useful to consider the nature of a rugged curve as being described by a mathematical dimension that has fractional values. He calls this dimension the fractal dimension of the system.

The fractal theory was developed by Mandelbrot (31), and provides an entirely new approach to the characterization of many natural and engineered systems devoid of regularity or definite form. Fractal geometry is a natural description for disordered objects ranging from macromolecules to the surface of the earth. Fractals and fractal geometry have been used by a number of workers to characterize particle aggregates, polymers, ceramic materials, dusts, and the like (22,32,33). It is a rapidly expanding field of research which will most likely prove very useful to the shape characterization of dust particles.

The discussions presented in the above sections indicate that the experimental and theoretical determination of particle size distribution of a dust cloud is not devoid of complexity. It is clear that information on size distribution is to some extent uncertain because of particle shape and morphological considerations.

ELECTRICAL CHARACTERISTICS OF DUST CLOUDS (WITH PARTICULAR REFERENCE TO LONG-LIVED RADIOACTIVE DUST, LLRD)

Field and laboratory measurements have shown that aerosols and industrial dusts carry an electrical charge (34-41). The electrical charge associated with dust clouds, particularly in the respirable size range, is of interest from the health standpoint because it influences the deposition of

these particles in the human respiratory system (42). It is also important because it affects the collection efficiency and collection characteristics of dust monitoring and measuring instruments (43,44).

The electrical charge on airborne particles depends mainly on the following:

1. method of production;
2. interaction of the particles with their gaseous-phase environment.

Piezoelectric, triboelectric, and possibly, exoelectron effects are believed to be responsible for the electrical charge developed in dust produced during rock crushing (breaking), blasting, drilling, and milling operations. Friction, collisions, bouncing, and rock (particle) 'shaking' are believed to play an important role in the production of charge during transportation of rock and mineral ores, and other mining and milling operations. The above apply equally well to a variety of other industrial and laboratory dust production methods, or methods which generate dust as an unwanted by-product.

In addition to their methods of production, dust clouds can acquire electrical charge through interactions with the gaseous environment as follows. Uranium (U) and thorium (Th) minerals are widely, and more or less uniformly distributed in the crust or outer layers of the earth. Uranium-238, ^{235}U, and ^{232}Th are the parents of the three naturally-occurring radioactive decay chains. Through a series of decay steps, ^{238}U, ^{235}U, and ^{232}Th decay eventually to ^{222}Rn, ^{219}Rn, and ^{220}Rn, respectively. These three elements are radioactive gases which find their way from the earth's crust to the biosphere by diffusion and transport mechanisms. Once in the atmosphere, they further decay into their short-lived decay products, also known as daughters, descendents, or progeny.

The short-lived decay products of ^{222}Rn and ^{220}Rn, formed initially in an atomic, positively charged state, rapidly combine with atmospheric aerosols

(41,45-49). As aerosols are found in positively, negatively, and neutrally charged states, the resulting atmosphere consists of a complex mixture of charged and neutral particles of size covering a wide range. Because of the electrical charge associated with dust clouds, these particles can be influenced by external electric and magnetic fields (20,50-53), thereby providing a means to reduce radiation levels in working environments. The electrical characteristics of radioactive and non-radioactive aerosols, and industrial dusts, have been investigated by several workers (34-41).

Aerosols in the submicron range and airborne dust in the respirable range interact with bipolar and unipolar atmospheres in a rather complex way. For radioactive and non-radioactive aerosols and dust found in an electrically charged state in underground uranium mines, and other radioactive environments, the following competing mechanisms of interaction are operative:

1. Diffusion charging (54),
2. Electrical neutralization (55),
3. Electrical self-charging effects (56),
4. α-particle recoil (57 and refs. therein), and
5. electron charge transfer.

Charge neutralization occurs because of ion-pairs produced by ionization of, say, mine air, by ^{222}Rn and ^{220}Rn progeny. Self-charging effects are caused by radionuclides contained in aerosols and dust particles. Diffusion charging arises from attachment or adsorption of ions from ion-pairs produced in mine air by ^{222}Rn and ^{220}Rn progenies. Alpha-particle recoil arises from α-particle emission by some long-lived radioactive dust nuclides, ^{222}Rn, ^{220}Rn, and some of their short-lived decay products. Electron charge transfer is brought about by transfer of free electrons from one molecular species (or ions) to another.

The above processes are further complicated in certain environments such as uranium mines because dusts contain, in addition to long-lived

radionuclides such as ^{238}U, ^{232}Th, and ^{226}Ra, the following:

a) Short-lived decay products of ^{222}Rn and ^{220}Rn formed by the radioactive decay of U and Th radioisotopes. These products are being formed continuously because of the presence of their long-lived parents;

b) Short-lived decay products of ^{222}Rn and ^{220}Rn attached to the surface of airborne particles.

Items (a) and (b) are not only important in connection with self-charging effects, but they also affect neutralization and diffusion-charging mechanisms.

The maximum electrical charge that can be carried by a particle is limited by the physical properties of the particle. Three electrical limits have been recognized, namely, the electron limit, the ion limit, and the Rayleigh limit. For a spherical particle, the limit of charge is given by (50).

$$n_p = D_p^2 \, E_s/4e \tag{30}$$

where, E_s is the electric surface field intensity at which emission of electrons and ions takes place, n_p is the number of elementary units of charge corresponding to the electron or ion limit, and e is the elementary unit of charge. Surface field intensities of the order of 10^7 V/cm are usually required for the spontaneous emission of electrons, whereas a somewhat larger field intensity (~2 x 10^8 V/cm) is necessary for the emission of, say, positive ions.

An electrically charged liquid drop will disintegrate when the (outward) pressure produced by the electric field at the surface of the drop is equal to or greater than the inward pressure produced by the surface tension, S_T. The limiting charge in this case was first given by Rayleigh (in 50) as:

$$n_p = [(2 \pi S_T)^{1/2} / e] \, D_p^{1.5} \tag{31}$$

Equations 30 and 31 give the theoretical maximum electrical charge that

an airborne particle can carry. The values given by these expressions are, therefore, limiting, extreme values. Under normal circumstances, however, the electrical charge acquired by particles is much less and is governed by Boltzmann's distribution law of classical statistical mechanics. According to this law, the fraction of particles of size D_p carrying n_p elementary units of charge, say, $F(n_p)$, is given by:

$$F(n_p) = (1/\Sigma) \exp [-(n_p e)^2 / D_p k T] \quad (32)$$

where, in Eq. (32) k is the Boltzmann constant, and T is the absolute temperature of the particle assembly. The symbol Σ stands for the expression below:

$$\Sigma = \sum_{-\infty}^{+\infty} \exp [-(n_p e)^2 / D_p k T] \quad (33)$$

Equation 32 is valid when the mobility of the positive and negative ions are equal, and when the particle cloud is in equilibrium with bipolar ions. When the mobility of the positive and negative ions are not equal, a different expression must be used. The particle charge limits and the Boltzman distribution versus particle size are shown in Fig. 5.

The electrical charge of dust clouds is a property that has been widely used in the design of cleaning systems such as electrostatic charge dust precipitators and other gas cleaning devices.

The electric charge characteristics of LLRD clouds has been investigated by Bigu (40).

OPTICAL PROPERTIES OF DUST PARTICLES

The interaction of radiation and particles dispersed in a gas phase has been the subject of numerous investigations. Suspended particles in a gas scatter, reflect and absorb electromagnetic radiation to a degree which depends on their size, shape, nature, and the wavelength of the incident

radiation. Absorption and scattering of radiation by particles are two important physical mechanisms which have been used extensively to measure the concentration of dust particles. These two interaction mechanisms are defined below.

Absorption is defined as the process whereby the incident radiant energy is transformed, upon interacting with the particle, into other forms of energy, such as heat, energy of chemical reaction, or radiation of a with wavelength.

Scattering is defined by the process in which the electromagnetic energy received is reradiated by the particle in the same wavelength. The reradiation process may take place in all directions but usually with different intensities in different directions.

In an optical range, light attentuation by absorption is the predominant mechanism for black smokes, whereas scattering processes dominate for water droplets.

Electromagnetic radiation propagates in matter according to the refractive index, m, of the material. In general, m is a complex quantity which according to electromagnetic theory can be written as:

$$m^2 = \epsilon\mu - j(4\pi\sigma\mu/\omega) \tag{34}$$

where, ϵ, μ, and σ are, respectively, the dielectric constant, magnetic permeability, and electrical conductivity of the material. The symbol $\omega = 2\pi f$, is the angular frequency, and f is the frequency of the radiation. The symbol $j = (-1)^{1/2}$.

Equation 34 is also often written as:

$$m = n - j\,n' \tag{35}$$

where, n and n′ are, respectively, the real and imaginary part of the complex refractive index, m.

The absorbing properties for bulk material are related to the quantity $4\pi n'/\lambda$, the absorption coefficient, where λ is the wavelength of the

radiation. For a non-absorbing medium, $\sigma = 0$, and $m = n = (\epsilon\mu)^{1/2}$.

A dispersion or suspension of particles removes electromagnetic radiation, e.g., light, from an incident beam by scattering, and also by absorption, if the particles are made of absorbing material. This total removal of flux from the beam in traversing the particle suspension is called the extinction. The extinction is given by the Bouguer Law:

$$I_T = I_o \text{ ext.}(-N\, C_{ext}\, l) \tag{36}$$

where, $C_{ext} = C_{sca} + C_{abs}$ is the total cross-section for extinction. The symbols C_{sca} and C_{abs} stand, respectively, for the scattering and absorption cross-sections. In Eq. 36, N represents the number of particles per unit volume, and l is the path length.

The theory for calculating the extinction cross-section, C_{ext}, from basic principles is referred to as the Lorentz-Mie theory. This theory enables the calculation of C_{ext} in terms of the index of refraction of the particle relative to the medium in which it is suspended, the observation angle through which the radiation is scattered by the particle, and a size parameter, Z, which for a sphere of diameter D_p, assumes the form:

$$Z = \pi D_p/\lambda \tag{37}$$

where, λ is the wavelength of the scattered radiation.

The scattering of electromagnetic radiation of wavelength λ by particles of arbitrary shape and size is a subject of great difficulty. Substantial simplifications in the theory can be introduced if spherical particles of diameter D_p are assumed. However, scattering phenomena are highly dependent on λ/D_p. Again, considerable simplification can be introduced for the two limiting cases:

a) $D_p/\lambda \ll 1$, i.e., $D_p \ll \lambda$, Rayleigh scattering

b) $D_p/\lambda \gg 1$, i.e., $D_p \gg \lambda$, Diffraction Fraunhofer region

As a rule of thumb the above regions are given by the following approximations:

1) $D_p < 0.1\ \lambda$, Rayleigh region

2) $D_p > 4\ \lambda$, Diffraction Fraunhofer region.

A more meaningful parameter, p, for distinguishing the above regions has been suggested by van de Hulst (58) which takes into consideration both the refractive index, m, the size of the particle, D_p, and the wavelength, λ, of the radiation:

$$p = 2\ \pi\ D_p(m-1)/\lambda \tag{38}$$

The above parameter permits the following classification:

$p < 0.3$, Rayleigh region

$p \gg 30$, Diffraction (Fraunhofer) region.

The most difficult case to solve is that for which $D_p \simeq \lambda$, or $p \simeq 1$. This region is usually referred to as the Lorentz-Mie region.

A. RAYLEIGH SCATTERING

The wavelength of visible light is about 0.5 μm. For particles much smaller than this wavelength, the local electric field, E, in the particle produced by the electromagnetic wave is approximately uniform at all times. This applied electric field induces in the particle an electrical dipole moment, P:

$$P = \alpha \cdot E \tag{39}$$

where, α is the polarizability of the particle, usually a tensor.

From the energy of the electric field produced by the oscillating dipole (notice that as E oscillates, P also oscillates), an expression can be derived for the scattered radiation, I_s:

$$I_s = [(1 + \cos^2 \Theta)\ k^4\ \alpha^2/2\ r^2]I_o \tag{40}$$

where, Θ is the scattering angle,

I_o is the intensity of the incident radiation,

k is the wave number ($k = 2\pi/\lambda$), and

r is the distance from the particle.

Equation 40 applies to particles of arbitrary shape and is symmetrical with respect to the direction of the incident beam. For an isotropic spherical particle of volume V it can be shown (12, p. 126):

$$\alpha = 3(m^2 - 1)\ v/4\ \pi(m^2 + 2) \tag{41}$$

an expression that can readily be substituted into Eq. 40.

B. FRAUNHOFER DIFFRACTION REGION

Fraunhofer diffraction theory is derived from fundamental optical principles. It can be shown that for a sphere of diameter D_p, the intensity of the scattered radiation, I_s, of wavelength λ is given by (58):

$$I_s = (G^2/\lambda^2 r^2)\ |D(\theta,\varphi)|^2\ I_o \tag{42}$$

where, $G = \pi(D^2_p/4)$ is the geometric area of the particle shadow, and:

$$D(\theta,\varphi) = 2\ J_1(z \sin \theta)/z \sin \theta \tag{43}$$

where, J_1 is the first order spherical Bessel function, and the angles θ and φ are spherical coordinate systems having the usual meanings. The rest of the variables in Eqs. 42 and 43 have been defined previously.

An interesting phenomenon for particles for which $D_p >> \lambda$ is the so-called extinction paradox. In this case a large particle removes from the beam twice the amount of radiation (e.g., light) intercepted by its geometric cross-sectional area (58).

C. MIE SCATTERING

The complete analytical solution for spherical particles of diameter comparable with λ was first developed by Mie in 1908. The intensity of the scattered radiation in this case is given by:

$$I_s(\theta) = (\lambda^2/8\ \pi^2\ r^2)\ (i_1 + i_2) \tag{44}$$

where, i_1 and i_2 are defined in terms of the coefficients of the electric and magnetic waves, a_n and b_n, respectively, and the result is expressed in a rather complex equation involving Hankel, Bessel, and Legendre functions as well as the refraction index m, and the parameter $k = \pi D_p/\lambda$.

Total scattering, S, by one particle for unit intensity is given by:

$$T = (\lambda^2/2\pi) \sum_{n=1}^{\infty} (2n + 1) (|a_n|^2 + |b_n|^2) \qquad (45)$$

Because scattering of light by particles and other forms of electromagnetic radiation, is dependent on λ and the size of the particle, optical instrumentation has been developed for characterizing particle size distribution.

CHEMICAL COMPOSITION AND CHEMICAL CHARACTERISTICS OF AEROSOL CLOUDS

Particulate clouds are so widespread in nature that is virtually impossible to cover, even succinctly, a fraction of this topic here. Particulate clouds are generated as a result of:

1. Meteorological phenomena (fog, mist, haze, smog),
2. Domestic, commercial, manufacturing and industrial operations,
3. Human activities (cooking, smoking),
4. Mass transportation systems,
5. Vehicle traffic, and
6. Other phenomena, operations or activities.

Particulate clouds can be divided into two main groups, namely, chemical and biological (e.g., microbial aerosols). According to their nature, particulate clouds can produce damage to:

1. Buildings,
2. Materials,
3. Vegetation,

4. Human health.

The effect of particulate clouds on biological and inanimate matter depends on a variety of factors, which include the following:

1. Chemical and/or biological nature of the cloud,
2. Particle size and size distribution,
3. Particle shape,
4. Particle concentration,
5. Particle radioactivity, and
6. Particle electrical charge.

Of particular interest are particulate clouds which constitute a potential health hazard to humans. In this context the health hazard associated with the particulate cloud may arise from its:

1. Flammability,
2. Explosive potential, or
3. Toxicity.

Conservatively speaking, there are several hundred thousand chemical substances (compounds) or biological aerosols (spores, fungi, viruses, microbial matter and the like) which are proven to be either toxic to varying degrees or potentially hazardous (toxic) to human health.

Because virtually any chemical or biological substance in the solid state can be reduced to small particles by a variety of chemical, physical, or mechanical processes and methods, the variety of aerosols in nature, e.g., in the working place, is bewildering. Vapours, and other substances in the gaseous state, are by definition, airborne, and hence, contribute their potentially deleterious effect on humans, other biological systems, inanimate matter and buildings.

Although of great practical interest from the epidemiological, toxicity, pollution, environmental, and health physics standpoints, the chemical and biological characteristics of airborne particles as encountered

in nature, the work place, and at home, will not be pursued any further in the context of this report.

INHALATION OF DUST

When air is inhaled, airborne particulate matter deposits on the respiratory tract regions in a manner which depends mainly on the geometry and physical characteristics of the different respiratory system regions, and the aerodynamic diameter of the particles. It is important for the sake of clarity to define the following dynamic situations (59).

1. Deposition - This term refers specifically to the collection of inhaled airborne particles by the respiratory tract and to the initial regional patterns of these deposited particles.
2. Clearance - This refers to the subsequent translocation, transformation and removal of deposited particles from the respiratory tract.
3. Retention - This term refers to the temporal distribution of uncleared particulate matter.

The respiratory tract can be divided into the three following main regions:

1. Head Air Region (HAR). This region comprises the following anatomical structures: nose, mouth, nasopharynx, oropharynx and laryngopharynx;
2. Tracheobronchial Region (TBR). This region includes the following anatomical structures: larynx, trachea, bronchi, and bronchioles.
3. Gas Exchange Region (GER). This region comprises the respiratory bronchioles, the alveolar ducts, the alveolar sacs, and the alveoli.

Inertial deposition is the dominant mechanism of deposition of particles larger than about 3 μm in aerodynamic diameter in the head airways or tracheobronchial airway regions. In this process, the airborne particles, because of their inertia, do not follow changes in direction or speed of air

streamlines and they may collide with the wall of the airway where they are deposited. Aerodynamic separation of the inertial type may be characterized in terms of an 'impaction' parameter given by D_p^2Q where Q is the average inspiratory flow rate.

Deposition by diffusion can also occur in the nose, mouth and pharyngeal airways for very small particles as a result of Brownian motion. Diffusional deposition in the gas exchange region of the lung is the predominant collection mechanism for particles smaller than 0.5 μm.

Inspirability criteria have been generated from the results of wind tunnel experiments to investigate the efficiency with which airborne particles entered the nose and/or the mouth of a life-size mannequin during simulated breathing.

Human deposition data in the respiratory system have been collected from volunteers inhaling test aerosols through either mouthpieces or nose tubes using monodisperse, insoluble, and stable aerosols of different sizes (see for instance refs. 59 and 60).

Theoretical 'lung' models have also been developed to estimate the expected deposition with respect to particle size of particles. The most widely used models of regional deposition versus particle size have been developed by the International Commission on Radiological Protection (ICRP) Task Group on Lung Dynamics. Although the purpose of these models was to estimate radiation exposure from inhaled radioactive aerosols, the ICRP aerosols deposition models are widely applied to environmental and occupational aerosols. Because considerable variability in anatomical and respiratory parameters may occur among individuals in the population, the above models refer to an individual prototype of the following characteristics: 70 kg body weight, 1.75 m height, 1.8 m^2 body surface area, and a breathing rate of 15 breaths per minute (bpm). Theoretical data predicted by these models and experimental data collected from human

volunteers are presented in Figs. 6 to 12.

Figures 7 and 8 show total experimental and theoretical particle deposition (i.e., deposition in HAR + TBR + GER) data versus d_{ar} (particle aerodynamic resistance diameter) for nasal and mouth breathing, respectively. Theoretical data have been calculated according to the ICRP Task Group on Lung Dynamics models for two tidal volumes (TV), namely: TV = 750 cm^3, and TV = 1450 cm^3. Experimental data by several workers were obtained for several BPM (breaths per minute). (Note: the aerodynamic resistance diameter is about equivalent to the aerodynamic diameter except ~0.08 μm larger. The particle aerodynamic diameter, d_a, is equivalent to the diameter of a unit density sphere, 1 gcm^{-3}, having the same settling velocity, under gravity, as the particle in question of whatever shape and density.)

Figures 9 and 10 show similar types of data to that of Figs. 7 and 8 except for the tracheobronchial (TB) and pulmonary (P) regions, respectively.

Figures 11 and 12, show theoretical particle deposition data calculated according to the ICRP lung model (TV = 750 cm^3, BPM = 15) for nasal and oral inhalation, respectively. These figures show total particle deposition (HAR + TBR + GER) as well as the regional deposition fractions in the different respiratory tract regions, i.e., nasal-pharyngeal (or oro-pharyngeal), tracheobronchial (TB), and pulmonary (alveolar).

Inspection of the above figures shows the following features of interest regarding the dependence of particle deposition versus particle size:

1. Substantial differences between nasal and oral breathing;
2. Different regions of the pulmonary tract have different deposition characteristics;
3. Particle deposition within a given pulmonary track region or section is highly dependent on particle size;
4. Particle deposition characteristics depend on tidal volume (TV) and breathing rate (BPM).

The deposition of airborne particulate matter in the respiratory system is a subject of great complexity. For an in-depth study of this subject the reader should consult the relevant literature (see for instance refs. 59, 60, and refs. therein.

HEALTH EFFECTS OF DUST

It is not the intention of this report to discuss or describe in any significant detail the medical, biological, toxic or epidemiological aspects of dust inhalation. Not only is this an extremely complicated subject, best dealt with by specialists in these fields, but it is of only marginal relevance in the context of this report. Suffice to say that dust monitoring programs, and the like, have been established at the work place and urban areas because of the well known potential health hazard and adverse effects associated with the inhalation of airborne particulate matter.

Broadly speaking, the interaction of airborne particulate matter and living systems is dependent on the following:

1. Physical and geometrical properties, characteristics, and chemical composition of particles;
2. Regions where particles are absorbed, adsorbed, deposited, or react in the respiratory tract;
3. Solubility of particulate matter in body fluids;
4. Biological and/or radioactive half-life of particles in biological structures;
5. Chemical affinity of particles and biological tissues or cells.

Apart from microbiological aerosols, two broad types of deleterious effects may be distinguished arising from the inhalation of airborne particulate matter:

1. Non-localized or systemic effects which are caused by suspensions

(dispersions) which act as systemic poisons or cause loss of function, e.g., pesticides, Pb dusts, etc.; and

2. Localized effects in the respiratory system.

Systemic effects are less particle size dependent than localized effects, i.e., effects in the respiratory system. Deposition of particulate matter in certain regions of the respiratory tract (lungs) give rise to a group of diseases commonly known as pneumoconiosis.

Radioactivity associated with airborne particulate matter represents an additional health hazard to the respiratory system. This is important for the uranium industry (mines, mills, refineries, and so on) where long-lived and short-lived radionuclides are frequently associated with respirable dust clouds, e.g., silica dust. Extended inhalation of airborne radioactive matter can induce lung cancer.

Because of the potentially adverse effects associated with the inhalation and ingestion of radioactive and non-radioactive dust clouds, careful monitoring of dust concentration levels at the work place and in living areas is vitally important.

Accurate dust concentration monitoring and dust characterization studies are indespensable for air quality control purposes. Because of this, techniques, methods and instrumentation used for monitoring, characterization, control and engineering purposes are fields of great practical interest and relevance. The next few sections will be devoted to:

1. Criteria for the measurement of airborne particulate matter (dust clouds);
2. Techniques and methods for characterizing dusts;
3. Instrumentation used for the measurement and characterization of dust clouds;
4. Review of work conducted in Canada regarding the evaluation of instrumentation used in the measurement and characterization of Long-

Lived Radioactive Dust (LLRD); and

5. Review of the work carried out in Canada and other countries with regard to the characterization and measurement of LLRD at the work place (uranium related industries).

THE MEASUREMENT OF DUST

A. CRITERIA FOR THE MEASUREMENT OF AIRBORNE PARTICULATE MATTER

In a previous section, the dust deposition (inhalation) characteristics of the respiratory system have been discussed. Also, the need for dust sampling and dust monitoring has been repeatedly emphasized as a means of assessing the potential health hazards associated with the occupational exposure of humans to dusty environments. Sampling, monitoring and characterization of dusty atmospheres can be regarded as important preventive measures which can, at the same time, also assist greatly in the design, implementation and evaluation of air quality control measures aimed at reducing unnecessary human exposure to potentially hazardous situations.

Because the health effects or nuisance effects arising from exposure to dusty atmospheres very much depend on the location where particulate matter deposits on the respiratory tract, it is important to design instrumentation with similar dust deposition characteristics to that of the respiratory tract. In other words, size-selectivity has to be introduced into the response of the instrument in order to be useful from the occupational and health physics standpoints.

Size selective standards have been established to address the problems associated with lung disease caused by dust inhalation, e.g., pneumoconiosis. The standards for respirable dust are reviewed below.

In 1952 the British Medical Research Council (BMRC) adopted a

definition of respirable dust as that dust reaching the alveolar region. The BMRC selected the horizontal elutriator (described in a different section) as a practical size selector. Furthermore, it defined respirable dust as that passing an ideal horizontal elutriator, and selected the elutriator cut-off to provide the best match to experimental human respiratory tract deposition data available at that time. The respirable fraction was defined in terms of the settling velocity of the particles by the expression: $C/C_o = v/v_{2s}$, where C and C_o are the particle concentrations of falling speed v in the respirable fraction and in the whole dust cloud, respectively, and v_{2s} is a constant equal to twice the settling velocity in air of a spherical particle of unit density and 5 μm in diameter.

The U.S. Atomic Energy Commission (AEC) established a second standard in 1961. The Office of Health and Safety defined respirable dust, in terms of respirable particulate mass (RPM), as the fraction of the inhaled dust which penetrates to the non-ciliated portions of the gas exchange region. This definition was intended only for insoluble dust particles which exhibit prolonged lung retention, and was, therefore, not intended for dusts with appreciable solubility in body fluids and chemical toxicants. With this in mind, respirable dust was defined with a 50% respirable cut-size at an aerodynamic diameter of 3.5 μm. Other specified fractions were 0% at 2 μm, 25% at 2.5 μm, 75% at 5 μm, and 100% at 10 μm.

The American Conference of Governmental Industrial Hygienists (ACGIH) in 1968 adopted size-selective characteristics similar to AEC differing only at 2 μm where it allows for 90% passing the first stage collector instead of 100%. This small difference was aimed at recognizing the characteristics of real particle separators.

The criteria presented above are applicable to deposition in the alveolar region or the non-ciliated portions of the gas exchange region. However, different criteria and standards have been defined for particles

which deposit in the head airways and the tracheobronchial airways. In these areas of the respiratory system, deposition of dust can cause diseases such as nasal and bronchial cancers, and chronic bronchitis. Criteria and standards for this type of deposition have been addressed by the U.S. Environmental Protection Agency (EPA), and the International Standards Organization (ISO).

In 1981, the Office of Air Quality Planning and Standards recommended to the EPA the selection of a cut-size for a pre-collector with d_{50} (50% cut-size) for a particle aerodynamic diameter of 10 μm.

The ISO referred to the dust fraction drawn in by the nose or mouth as the 'inspirable' fraction; the fraction collected in the head airway as the 'extra-thoracic' fraction; whereas the fraction penetrating through the larynx was called 'thoracic', which was further subdivided into 'tracheobronchial' and 'alveolar'. The recommendations by the ISO were presented with two options, namely, one with a d_{50} cut of 15 μm for penetration into the trachea, and one with a d_{50} cut of 10 μm. The latter gave a more unbiased cut between head and chest fractions and was voted by 85% of the ISO membership.

In addition to the above criteria, other criteria have been adopted for specific dust occupational hazards such as those derived from the inhalation of cotton dust, asbestos and other dusts (59).

B. INSTRUMENTATION FOR DUST MEASUREMENTS

Because of physical constraints as well as practical limitations in the design of particle measuring instrumentation, there is often an inherent limitation or bias in the response of the instrument to either particle size or particle concentration, or both. In this sense, any instrument possesses some degree of particle size selectivity. Some instrumentation, however, has been purposely designed with specific particle size selectivity in order to

match the deposition characteristics of particulate matter in some regions of the respiratory tract. This type of instrumentation is particularly useful in occupational exposure studies.

Dust instrumentation can be classified in a variety of ways depending on some specific feature or attribute of an instrument or group of instruments. Similarly, there are a number of different operating physical principles on which dust instrumentation can be based depending on the specific type of dust measurement of interest such as particle concentration, particle size distribution, and so on.

Broadly speaking, dust instrumentation can be divided into two main categories, namely:

1. Instrumentation for particle size characterization (with or without built-in size selectivity to match deposition characteristics in biological structures).
2. Instrumentation to determine particle concentration within a broad particle size range, e.g., 'respirable range', either by particle number or, more often, by mass.

In addition to items 1 and 2, instrumentation can be further classified into that of a continuous 'sampling', or intermittent (discrete) sampling nature. Usually, continuous sampling instrumentation provides real time data, i.e., data are displayed and/or can be accessed in real time, in other words, instantaneously or almost instantaneously at the time of the measurement. Intermittent or discrete sampling is usually referred to as grab-sampling.

Depending on the degree of complexity, type of measurement, and other practical and experimental considerations, the design of instrumentation can range from fully automated (e.g., microprocessor controlled) to requiring a great deal of manual intervention, e.g., most cascade impactors.

Before proceeding, the reader should be aware that no single technique or instrument covers all particle sizes of interest, nor, within a given size

range is any instrument or single technique capable of handling all the field conditions where air samples are to be taken. Hence, the brief discussion that follows is only intended to be of a very general nature and for illustration purposes only. The reader interested in pursuing the subject of particle instrumentation further is advised to consult the pertinent literature (22,61-66, and refs. therein).

The techniques most widely used in the characterization of airborne particulate matter can be divided as follows:

1. Scattering techniques (ST),
2. Impaction techniques (IT),
3. Sieving techniques (SIT), and
4. Other techniques (OT).

Each of the above categories can be further subdivided into the following:

1. Scattering Techniques. This category can be divided into the following:
   a) Classical Light Scattering (CLS) in which the time-average light scattering is used to determine weight average molecular weight, z-average mean square radius of gyration, shapes, and interaction of particles with size range from 0.01 μm to 10 μm.
   b) Fraunhofer Diffraction (FD) - normally using a laser (He-Ne) as the light source, can cover the particle size range from ~2 μm to 175 μm.
   c) Particle Counting (PC) - in this technique, the light scattered from a single particle is a function of the particle size and of its index of refraction. This method covers well above the respirable dust range, i.e., up to >10 μm.
   d) Laser Doppler Velocimetry (LDV) and Laser Doppler Anemometry (LDA) - these two techniques have traditionally been used to measure particle velocities. More recently, however, LDV and LDA have been used to study

the size information contained in the Doppler signal. The above techniques find particular application when it is important to determine particle size non-perturbately under laminar or turbulent flow conditions, e.g., particles formed in flames.

2. Impaction Techniques. This category can be subdivided into the following classes:

a) Jet Impactors - in which particles are forced through an orifice at high velocity. A plate or impactor surface is placed at right angles to the jet exit. Particles impact on this surface where they deposit.

b) Virtual Impactors - in this type of device or technique, the solid impaction surface used in jet impactors is substituted by a slowly pumped stagnant air void. This is done because of the particle-surface interaction problems associated with inertial impactors such as particle bounce, particle reentrainment, and collection surface overload.

c) Cascade Impactors - consist of a collection of jet impactors, as described above. The mechanical configuration of the device consists of a series of impactor stages (see below).

d) Cyclones - in this device, the particle cloud enters the unit and is whirled downward; large particles impinge on the wall, slide down, and are finally collected.

e) Centrifugal Classifiers - size classification is attained when particles entering the device spin in the 'sensitive volume' by centrifugal forces.

3. Sieving Techniques. These techniques use screens of different openings in order to attain particle size separation. The latter can be achieved by either using one screen of a given opening size at a time, and repeating the particle screening procedure with subsequent ever decreasing opening

size screens, or alternatively, stacking a series of screens of decreasing opening size (top to bottom) and conducting the screening operation simultaneously. In each case, screening is only accomplished by shaking the material placed on the screen(s) by means of specially designed 'shakers'. Some specific uses of sieving techniques include:

i) preparation of powders with relatively broad particle size ranges for injection into special chambers to generate dust clouds;

ii) classification or sizing of relatively large amounts of powders. Efficient particle sizing is, however, limited to the large particle size range.

Sieving techniques are not suitable for in situ monitoring or measurement of dust clouds at, say, the working place.

4. Other Techniques. There are a number of techniques other than those discussed above which are of varying degrees of practical interest in the context of this report. Some of these techniques include image analysis, microscopy, photon correlation spectroscopy (PCS), particle chromatography, hydrodynamic chromatography, condensation nuclei counting methods, and electric aerosol classifiers among other devices or techniques.

Of all the techniques examined above only a few are extensively used in the characterization of dust clouds in mines, mills and other working locations. The choice of these specific techniques is most often based on solid technical grounds, and also on practical and economical considerations. Most of the techniques and instrumentation in common use in mines, mills, and other work sites emphasize the measurement of dust mass over a particle size range or ranges as opposed to particle number over the same size range(s). Which concept or measurement is most appropriate or meaningful from the occupational, hygiene and health point of view is somewhat debatable, and beyond the scope of this report.

The most widely used techniques, or instrumentation, under field conditions, e.g., mines and mills, are light scattering devices, cascade impactors, and cyclones. In certain cases it is of interest to study the response to dust clouds of devices which were not originally designed or intended for dust collection and dust characterization purposes, and to compare the results with standard methods of dust characterization such as cascade impactors, cyclones, and light scattering (techniques) devices. For example, in the area of personal α-particle dosimetry it is important to determine the dust collection characteristics of the dosimeter sampling head in order to ascertain whether the information obtained under dust exposure conditions would be suitable for dust quantification purposes. If this were the case, the combined use of a personal dosimeter for airborne radioactivity and dust quantification purposes would result in a considerable simplification of the experimental procedures and protocols. It is also of interest to compare the dust collection characteristics of a conventional open face filter through which samples are drawn by means of a sampling pump at the same flow rate as, say, cyclones are operated.

The preceding discussion on techniques and measurements referred to 'conventional' dust. However, the main concern here is Long-Lived Radioactive Dust (LLRD), a unique and rather interesting albeit complex case, which requires both size characterization and radioactivity characterization, the latter as a function of particle size. It should be noted that the particle (or mass) concentration versus particle size distribution and the distribution of radioactivity associated with a given particle size (or size range) versus particle size do not necessarily need to be the same. In fact, these distributions which are characterized, respectively, by the Mass Median Aerodynamic Diameter (MMAD) and the Activity Median Aerodynamic Diameter (AMAD), are different. Despite the above subtle differences, LLRD is determined by the same means as 'ordinary' dust except that additional

radioactivity measurements are required as described in a subsequent section of this report.

The following section will be devoted to a description and discussion of a reduced number of techniques and instruments, some of which will be extensively used in phase II of the present project (Comparison of Radioactive Aerosol Sampling Instruments). Although this discussion is mostly limited to the instruments and techniques which will be used in the experimental phase of the project, and only represent a fraction of the instrumentation available in the market, they are the most widely used, and therefore, quite representative of the state of the art in dust characterization.

DUST SAMPLING INSTRUMENTATION

This section will deal with a description and discussion of dust sampling instrumentation of most common use. This section will be divided into subsections each dealing in turn with instrumentation operating on different dust collection principles.

A. INERTIAL AND GRAVITATIONAL DUST COLLECTORS

Impactors, cyclones, elutriators, impingers and aerosol centrifuges are included in this category. Unlike filters, these dust collectors distinguish between particle sizes. Single stage impactors, cyclones and elutriators are often used as a precut, to remove large particles from the dust cloud, in size-selective dust sampling. These respirable dust mass collectors are usually followed by a suitable filter for dust collection and have been designed to follow the respirable dust collection efficiency curves discussed in the preceding section. In some cases a single-stage impaction head is used to provide adequate dust size separation in PM_{10} (Particulate Matter below a

10 μm cut size) dust sampling instruments. Horizontal elutriators have been designed following either the respirable or the thoracic deposition curves to measure the mass of dust available for deposition in the tracheobronchial (TB) region.

A battery of impactors in series (i.e., cascade impactors), cascaded cyclones as well as horizontal elutriators, and aerosol centrifuges 'classify' airborne particles according to their aerodynamic diameter, i.e., the key variable or parameter for gravitational and inertial dust collection devices. Each stage of a cascade impactor, or cascaded cyclone enables both dust mass distribution or chemical composition versus particle size to be ascertained. Furthermore, horizontal elutriators, and aerosol centrifuges 'classify' particle size of dust clouds over a continuous particle size spectrum thereby permitting the determination of aerodynamic shape factors for particles of irregular shapes. The theory of operation and other important related matters for inertial and gravitational sampling devices are discussed, in turn, below.

1. Cyclone Sampling Devices. The principle of operation of a cyclone is illustrated graphically in Fig. 13. These devices consist of a cylindrical or conical chamber, or both, upstream of a filter/filter holder assembly and an air sampling pump. Air is drawn in tangentially near the top of the chamber and is forced to spiral down the outer region of the chamber, reversing its flow at the bottom of the chamber and spiralling up the inner region of the same to an exit tube located at the top of the cyclone chamber. Airborne particles large enough, i.e., with sufficient inertia, are not able to follow the airflow pattern (streamlines) and impact onto the internal walls of the cyclone chamber where these particles are either retained or migrate to the bottom of the cyclone chamber.

A complicating factor in the description of cyclones is that the flow pattern inside the cyclone chamber is complex, often turbulent, particularly

for small cyclones such as those required for air sampling purposes. Because of this, there is no precise theoretical framework to describe the performance of small cyclones. For large (industrial) cyclones, such as those used in industry to remove dust particles from process stream, agreement between theory and experiment is significantly better. The prediction of cyclone performance is often made with reference to empirically developed correlations.

Pertinent to the central question of cyclone design and performance is the relationship between the cyclone cut point and its physical dimensions, airflow rate, gas viscosity, and temperature. Another important question is the shape of the particle collection efficiency versus the particle size distribution. The effect of airflow rate on the relationship between cyclone collection efficiency (and the cut point, D_{50}, of the cyclone) and particle aerodynamic diameter for a specific type of cyclone, namely, the AIHL cyclone, is illustrated in Fig. 14 (67). The graph is self-explanatory, and hence, does not require further discussion.

A useful empirical relationship between a cyclone cut point, D_{50}, and the air sampling rate, Q, applicable to many of the cyclones in common use is given below (68):

$$D_{50} = k\, Q^{n} \tag{46}$$

where, n and k are numerical factors which are empirically determined and vary for different cyclones.

Another useful relationship relating D_{50}, the physical dimensions of the cyclone and the airflow rate has been given (69):

$$D_{50}/D = k_d(Re/1000)^{-0.83} \tag{47}$$

where, Re, the Reynolds number, is given by $Re = 4\rho Q/\pi\mu D_o$ in which ρ and μ are the air density and viscosity, respectively, and D_o is the outlet tube diameter. The symbol D stands for the diameter of the cyclone body, and k_d is a dimensionless constant which varies from 1.4×10^{-4} to 4.5×10^{-4} depending

on the type of cyclone.

Very often, as in our case, cyclones are used as a particle precut device to another dust collector such as an impactor or a filter. The use of cyclones for air sampling purposes offers a number of advantages such as low cost and ease of operation. Cyclones have no moving parts, no problems with particle bounce and reentrainment, and do not require special collecting surfaces or coating materials. Cyclones do require, however, a constant airflow rate to ensure a sharp cut point D_{50}. Furthermore, electrostatic effects play a significant role in their sampling efficiency (44,70), and whenever possible, non-conducting materials should be avoided in their design and construction.

Nylon cyclones will be used in Phase II of this project, and electrostatic effects are expected to arise. As indicated above, cyclones are used in this work as a means of removing large dust particles (>10 μm), approximately), collecting the smaller size fraction on a downstream silver membrane filter (5 μm pore size) for dust sampling and quantification purposes.

2. Cascade Impactors. Devices that remove airborne particles through mechanical impaction processes, i.e., particle deposition occurring when airflow streamlines bend sharply as the airflow bypasses a solid object, are known as impactors. The name cascade impactor refers to the case where a number of single stage impactors are stacked together in series, each stage impactor having different particle cut size characteristics.

A single stage impactor essentially consists of an air inlet into a cylindrical chamber where laminar flow is maintained. The cylindrical chamber becomes a conical chamber where the airflow streamlines converge and the airflow is accelerated towards a short, small diameter, orifice (i.e., nozzle) where a dust laden air impaction jet is formed. This high velocity jet

impacts on an obstacle (impactor plate) facing the jet a distance away. By varying the diameter of the nozzle and the distance between the latter and the impactor plate, impaction stages of different cut size characteristics can be built. It is not uncommon to find cascade impactors which are designed with multiple nozzles for each impactor stage.

The principle of operation of a two-stage cascade impactor is depicted graphically in Fig. 15, where the effect of mechanical impaction on particle collection is illustrated for the first (upper) impactor stage. This mechanical process can be extended to any reasonable number of impaction stages of different collection characteristics. Because larger particles are removed from dust laden air by impaction mechanisms first, impaction stages following the first stage need to be designed in such a way as to permit increasingly smaller particle sizes to be removed as the air stream progressively flows and reaches subsequent impaction stages. This is normally accomplished by varying the distance between the impactor stage nozzle(s) and the impaction plate while simultaneously varying the diameter of the nozzle(s). Smaller particle cut size values are obtained by progressively decreasing both simultaneously. By proper design, cascade impactors provide the means for accurate size distribution analysis. The mechanical configuration of a multi-stage cascade impactor is shown in Fig. 16.

In order to facilitate analyses of the data, cascade impactors normally use (removeable) substrates made up of filter material which are placed on the impaction plates. Hence, after sampling, the substrates can be weighed or counted for radioactivity to determine mass and/or radioactivity size distribution. Although impaction plates are usually of circular shape, they are often designed with radial slots of different shapes (e.g., rectangular and oval) to improve their performance. Furthermore, a backup filter is placed at the exit of the cascade impactor to collect particles that penetrate the last stage, i.e., particles smaller than the last stage can remove.

Measurements on the backup filter are necessary in the calculations.

As with cyclones, cascade impactor performance is characterized by collection efficiency curves for each stage and airflow rate. Collection efficiency curves for the two cascade impactor types which will be used in phase II of this project, namely, the 10-stage Sierra Model 210 ambient cascade impactor, and the 8-stage Marple personal cascade impactor, Model 290, are shown in Figs. 17 and 18, respectively. An important parameter in collection efficiency curves for cascade impactors is the cut-point diameter, D_{50}, which corresponds to the point on each collection efficiency curve for which a collection efficiency of 50% is attained. The cut-point diameter can be calculated theoretically according to Eqs 48 and 49 for round jet impactors and slotted impactors, respectively (71):

$$D^2_{50}\, C_S = 9\, \pi\, \eta_a\, n\, D^3_j\, St_{50,C}/4\, \rho\, Q \qquad (48)$$

for round jet impactors, and

$$D^2_{50}\, C_S = 9\, \eta_a\, n\, lw^2\, St_{50,r}/\rho\, Q \qquad (49)$$

for rectangular slotted impactors.

In the above expressions, C_s is the Cunningham slip factor given by the expression:

$$C_S = 1 + (\lambda/D_p)\, [2.514 + 0.8\, \exp(-0.55\, D_p/\lambda)] \qquad (50)$$

where, D_p is the physical diameter for spherical particles, and

λ is the mean free path of the air.

The slip factor C_S is an empirical factor which accounts for the reduction of the drag force on particles caused by the 'slip' of the gas (air) molecules at the particle surface. For $D_p > 5\ \mu m$, $C_S \sim 1$, whereas for $D_p < 5\ \mu m$, $C_S > 1$.

Furthermore, in Eqs. 48 and 49:

η_a is the air viscosity,

n is the number of jets or slots,

D_j is the diameter of the round jet

l and w are, respectively, the length and width of the rectangular slots,

ρ is the particle density,

Q is the sampling volumetric airflow rate,

St_{50} is the Stokes number corresponding to D_{50} (the subindices C and r stand, respectively, for circular orifices and rectangular slots).

The Stokes number for these particular cases (see also Eq. 14) is given by:

$$St = \rho\ D^2_P\ C_S\ v/9\ \eta_a\ A \qquad (51)$$

where, A is the jet diameter, or width, and v is the mean velocity in the jet. For circular jet impactors and slotted impactors St_{50} are, approximately, 0.24 and 0.59, respectively (71).

In order for cascade impactors to operate satisfactorily, their particle collection curve characteristics should be as steep as possible to emininate cross-over of the collection curves for different cascade stages. (It should be noted that the shape of the impactor collection efficiency curves depend on the Reynold's number $Re = \rho_a\ vA/\eta_a$, where the symbol a stands for air).

A major experimental difficulty with the use of cascade impactors is particle bounce and reentrainment. For these two reasons sometimes the substrates of the impactor stages are coated with some material such as grease so that particles stick to their surface. (Particle bounce and reentrainment are topics that have been dealt with in earlier sections of this report. The interested reader should consult these sections and references therein.)

As for the case of cyclones, airflow rate Q is an important parameter which determines D_{50}. Constancy of Q is an absolute must for accurate dust size characterization using cascade impactors.

3. Elutriators. This type of device uses gravitational settling as a laminar

flow to separate airborne particles by aerodynamic diameter. There are two kinds of elutriators, namely, vertical elutriators and horizontal elutriators.

A vertical elutriator consists of a vertical duct through which dust laden air is slowly drawn upwards by means of a sampling pump. Particles with sedimentation velocities greater than the airflow velocity in the vertical duct cannot follow the airflow and settle out. Particles of size sufficiently small penetrate the duct and are collected by a downstream filter situated at the exit of the elutriator. The particle penetration characteristics of a vertical elutriator can be calculated under laminar flow conditions if the airflow profile is known. Vertical elutriators find their use in some epidemiological studies and in the monitoring of, say, cotton dust in cotton mills (72). There are basically two types of vertical elutriators, i.e., cylindrical and conical elutriators (73).

Horizontal elutriators are more widely used for dust monitoring or characterization purposes than vertical elutriators. The principle of operation of horizontal elutriators is as follows. Air travels, under laminar flow conditions, through a set of closely spaced parallel horizontal plates. Particles with settling velocities greater than the ratio of the plate separation, h, to transit time, t_t, i.e., h/t_t, will be removed from the airflow. Smaller particles will be removed from the airflow by the parallel plates with an efficiency of less than 100%. Particles that penetrate the elutriator plates are collected by means of a downstream filter situated at the exit of the elutriator. The 50% penetration efficiency for a horizontal elutriator takes place when the following relationship is satisfied:

$$\rho C_S D^2_P = (hQ/2nSL)(18\eta g) \qquad (52)$$

where n is the number of parallel plates, L is the length of the plates with a rectangular cross-sectional area S. The symbol g stands for the gravitation constant. The other variables have already been defined.

Broadly speaking, the penetration, P, for particles with a settling

velocity, V_s, in a horizontal elutriator can be expressed as follows (74):

$$P = 1 - (V_s A_h/Q) \quad \text{for} \quad V_s < Q/A_h \tag{53}$$

for $V_s > Q/A_h$, $P = 0$.

As for the case of cascade impactors, horizontal elutriators enable particle size characterization of dust clouds. However, in order to obtain reliable data, the following are prerequisites.

1. Constant volumetric airflow rate, Q, during the sampling period,
2. Constant spacing, h, between parallel plates,
3. Laminar flow conditions, and
4. Airflow should be in the right range to eliminate thermal convection and re-entrainment effects. Adjustment of h may be necessary in conjunction with Q adjustments to remove unwanted effects.

If only two parallel plates are used, horizontal elutriators can be used as particle spectrometers (73). The theory of vertical and horizontal elutriators is dealt with in ref. (73).

4. Aerosol Centrifuges. These devices discriminate particle size by subjecting particle clouds to large centrifugal forces, i.e., particles entering the sampler (centrifuge) are forced to spin at high velocity in order to acquire high values for the centrifugal force. There are a number of particle centrifuge designs (74-83), such as spiral duct centrifuges, cylindrical duct centrifuges, high flow rate centrifuges (drum centrifuge), and conifuges and annular duct centrifuges. The operating characteristics and particle size ranges of these devices have been summarized elsewhere (71).

The variable of interest for a particle centrifuge is the deposition distance, L_D, which is defined as the distance along the centrifuge walls at which a particle of a specific diameter, D_p, will deposit. For an annular centrifuge this distance is (71):

$$L_D = [\ln(R_2/R_1)/h_d(R_2 - R_1)][9\ \eta\ Q/2\ \pi^2 f^2 \rho_p\ D^2_p\ C_S] \tag{54}$$

where, R_1 and R_2 are, respectively, the external and internal radii of the annular centrifuge,

h_d is the height of the duct, and

f is the frequency of rotation.

The other variables have been described previously.

For a more detailed description of particle centrifuges the reader is advised to consult the specialized literature (75-83). In order to give the reader an idea of the operating principles and characteristics of particle centrifuges, illustrations pertaining to a cylindrical duct aerosol centrifuge and a conifuge are reproduced in Figs. 19 and 20, respectively. In addition, the characteristics of a spiral duct centrifuge (Stöber centrifuge) are also given in Fig. 21.

Particle centrifuges can attain very high particle size resolution. Their operating (total) airflow rates are usually in the order of 1-20 L/min, except for high flow rate centrifuges which operate at a particle flow rate between 5×10^3 L/min and 2×10^4 L/min. The particle size range that a particle centrifuge can cover depends on the centrifuge type, but it can be as low as 0.05 μm for some types, to above 6 μm for other types. However, to the knowledge of the author, no single centrifuge can cover the size range 0.05 to 6 μm simultaneously.

5. Other Variants of the Above Dust Collectors. Cyclones, cascade impactors, particle centrifuges, and elutriators constitute the major kinds of dust sampling devices operating on inertial and gravitational principles. However, it is possible to combine more than one type of the above devices, or one of these devices with a device operating on a different dust collection principle, in order to accomplish some specific purpose. For example, it is not uncommon to combine a cyclone with a cascade impactor or horizontal elutriator in order to remove the large size particle fraction from a dust

cloud. Furthermore, a single stage virtual impactor upstream of an optical particle counter (OPC) can be used to improve the operating capabilities of the latter (84).

Some types of impactor devices do not use collection plates or substrates to collect dust fractions in different particle size ranges. Instead a 'probe' or collection nozzle is placed below the impactor jet(s) which samples only a small fraction of the flow whereas the rest of the flow bypasses the probe. This type of impactor is commonly referred to as a virtual impactor and operates as follows (85). In the above impactor jet/probe configuration, the air streamlines above the probe tip are similar to those of a conventional impactor stage. Hence, dust particles are separated by cut-point size into two main streams, namely, the small or minor flow, which is sampled by the collection nozzle (tip of the probe), and the large or major airflow which bypasses the probe altogether. The minor flow through the probe carries the large particle size fraction from the total sample flow as well as small particles from the minor flow, whereas the major flow, which bypasses the probe, carries only the finer particle size fraction. In both cases, the airflows pass through filters where the particles are collected and later weighed or counted. Some models are provided with a rotary tray where a number of filters are placed for automatic sampling. Because the total flow is divided into two flows this type of virtual impactor is known as the dichotomous sampler (86).

The problems of particle bounce and particle reentrainment or blow-off in cascade impactors have been indicated. A theoretical study (87) has shown that it is possible to use electret substrates in cascade impactors to reduce the above mechanisms. In this study the authors show that particle bounce and blow-off can be reduced by increasing the force of attraction of particles to the substrates. The argument goes as follows. Uncharged particles are attracted to the electret fibres by induced dipole and van der Waals forces

while charged particles experience an additional Coulombic force. The magnitude of these forces depends on the electric surface charge density of the electret, the dimensions of the electret fibres, the particle size and on its electrical charge. To the knowledge of the author the suggestion of using electret substrates in cascade impactors has neither been thoroughly investigated experimentally nor implemented in commercial devices.

Conventional cascade impactors are designed and built to operate as a number of single stage impactors of varying cut-size characteristics, assembled in series. A variant of the common series cascade impactor has been designed, built and tested (88), in which cascade stages are assembled in parallel rather than in series. This different mechanical configuration has a number of advantages but also some disadvantages. Among the latter is the necessity of using an independent sampling pump for each parallel impactor stage, thereby requiring that several airflow rates have to be carefully controlled instead of just one as for the case of the series cascade impactor. However, the parallel cascade impactor has the advantage of permitting independent calibration of each stage which, according to the author, can lead to more accurate measurements.

In certain cases, technological advances in miniaturization, detector design, processing methods and techniques, and other advances have made it possible to design and build fully automated cascade impactors whose means of dust evaluation is somewhat different than traditional methods, such as manual weighing after sampling. Such a case pertains to a series cascade impactor which uses piezoelectric crystals as impactor substrates. Every piezoelectric crystal used in (each) impactor stage has a different natural frequency. Deposition of dust particles on the impactor substrates shift its natural frequency by an amount proportional to the mass deposited. Automatic measurement of these frequency shifts permit automatic calculation of dust particle mass on each substrate and rapid particle size distribution

calculation by internally implemented software in conjunction with microprocessor controlled hardware. Because of the sensitivity of the method, complete particle characterization is possible (including sampling) in, at most, a few minutes. The instrument is known under the commercial name PC-1, and is manufactured by California Instruments (U.S.A.).

B. DUST COLLECTION BY FILTRATION

Filtration is the most common technique for particle sampling. Its wide use is due to its great simplicity and low cost. In its simplest version, dust sampling by filtration consists of an open face filter housing a suitable filter through which air is sampled by means of a constant flow rate sampling pump. In this configuration, total dust will be sampled, i.e., particles of all size ranges, or at least within a broader size range than necessary or useful for occupational and/or epidemiological studies. Quite often, an impaction stage of some sort is used upstream of the sampling train in order to remove particles larger than above a certain size range, i.e., $>10\mu m$. (This sampling configuration is similar to the cyclone sampler previously discussed.)

There are a variety of filter materials available for air sampling. The most common filter types are glass fibre and cellulose fibre filters. Because of their particular molecular structure and bulk characteristics, these filters cannot be used to provide particle size selectivity. That is, in a majority of cases these filters are used as 'absolute' filters in the sense that all particles incident on the filter material will be removed by it. It is possible, however, to use other types of filter materials that enable particle size selectivity. For example, polycarbonate-type materials have very defined pore sizes which permit these filters to be used in a similar fashion as graded mesh screens or cascade impactor stages to gain

information on particle size distribution.

The reader who wishes to learn more about filter materials and filter holder characteristics is recommended to consult ref. 89. Filtration, despite its deceiving simplicity, is a subject of great technical difficulty. For more on the subject the reader should consult refs. 90 and 91, and references therein.

C. ELECTROSTATIC AND THERMAL PARTICLE COLLECTORS

Electrostatic and thermal particle samplers differ from other collection mechanisms in that the forces acting to separate or remove airborne particles are of an electrical and thermal nature, respectively, rather than gravitational or inertial as discussed in a previous section.

1. Thermal Particle Collectors. Thermal particle collectors or precipitators are devices based on Aitken's (92) experimental observation that particles suspended in a gas medium move collectively in the direction of a temperature gradient, i.e., thermophoresis. A thermal precipitator removes particles from a dust cloud by passing the latter through a narrow gap or channel having a relatively high temperature gradient perpendicular to the direction of the airflow. Particles subjected to the temperature gradient move in the direction of decreasing temperature causing them to deposit on an appropriate collecting surface located on the walls of the precipitator gap (channel).

In its simplest design, a thermal particle collector would consist of a heated wire (heating can be realized by passing a current through the wire according to standard methods) placed radially across a cylindrical cavity through which air is drawn through a slit located on the side of the cavity. The airflow is directed perpendicularly to the wire and after passing through the cylindrical cavity is removed from the latter at the opposite end of the

slit. Thermophoretic particle flow is collected on the end plates of the collector cavity. Such a design (93,94) and modifications of it have been used in commercial and research devices (95,96).

Some thermal precipitators are equipped with an impactor stage, elutriator or cyclone upstream of the precipitator inlet to remove coarse particles from the main airflow stream. Provided that a sufficiently strong thermal gradient is produced, thermal precipitators can collect particles in the size range 0.01 μm to 5 μm. Particles larger than 5 μm are more difficult to collect because of inertial and gravitational effects that interfere with thermophoretic mechanisms. One advantage of thermal precipitators is that the electrical state of particles seems to play little role, and hence does not interfere with thermophoretic processes. Thermal precipitators are also highly efficient submicron particle collectors. However, thermal precipitators have, in general, poor size selection characteristics.

2. Electrostatic Particle Collectors. Industrial electrostatic particle collectors are widely used in the removal of dusts produced in industrial processes. The principle of operation of dust sampling (monitoring) devices using electrostatic means is, however, essentially the same as that employed in industrial cleaning operations, and involves two quite distinct and separate processes, namely:

a) Electrical charging of the particulate cloud; and

b) Application of an electric field to the charged particles in order to produce particle acceleration in the direction of opposite polarity, and hence, induce particle removal from the airflow.

Although there are a variety of methods that can be used for electrical charging of particles only two of these methods are in common use:

1. Electrical charging by means of ionizing radiation (e.g., β- and α-particles) produced by some radioactive sources;

2. Electrical charging by high voltage corona discharge.

From the two charging methods indicated above, corona discharge is by far the most efficient, faster and more controllable method. The details of electrostatic charging have been reviewed by several workers (50,97-99).

The collection of charged particles is affected by Coulomb forces exerted by applying an electric field to the charged particle cloud. The migration velocity of charged particles by an electric field can be calculated by equating the Stokes force (viscous force) and the Coulomb force (electrostatic force). Relatively simple calculations can be made to determine the particle collection efficiency under streamline flow characteristics. Collection efficiencies under turbulent flow conditions can be calculated by probability theory.

There are a number of factors that affect the collection efficiency of charged particles such as: operating parameters (voltage, current), airflow conditions, sampling flow rate, particle size, particle shape, and particle electrical characteristics as well as the carrier gas (air) parameters, e.g., temperature, relative humidity, barometric pressure, and chemical composition.

A very popular arrangement for electrostatic sampling collectors uses the point-to-plane electrode configuration with a needle point as the corona emitting electrode and the plane electrode as the grounded collector plate. It is not uncommon to attain a 60-80% particle collection efficiency over the size range 0.02 μm to 5 μm with some commercially available air sampling electrostatic collectors.

The distance that a charged particle will travel along the axis of an electrostatic precipitator before reaching a grounded collection plate depends on a number of variables including the particle size and the linear air velocity, among other factors. By proper design it is, therefore, possible to build an air sampling electrostatic collector with particle size distribution capabilities (see, for instance, ref. 95).

D. OPTICAL PARTICLE COUNTERS (OPC)

In a majority of the cases, (i.e., instruments or devices) reviewed above the dust sampling device itself is used only to collect particles for subsequent gravimetric, microscopic or chemical analysis. The use of such devices constitutes merely a first or intermediate step in the sometimes long (experimental) procedural chain necessary for the estimation of particle concentration and/or particle size distribution. In this regard the use of this type of instrumentation requires a great deal of manual operation, and is both time-consuming and expensive. Except for a notable exception, namely, the automated piezoelectric cascade impactor, the instruments considered in this section are more complex than the instrumentation considered in former sections. In the instrumentation discussed in this section, particle sampling and analysis of the data are carried out within the instrument and the variable of interest can be obtained (virtually) in real-time, on command. Quite often these instruments are called direct-reading instruments, and in most cases use optical means, e.g., light-scattering, light-extinction, and other light phenomena, as a means of particle detection. Because of the complexity of some of these phenomena, e.g., light-scattering and the number of ways it can be utilized for obtaining particle size information, a large number of instruments have been developed using these principles. However, because of the abundance of different instruments the discussion that follows will be limited to a few instruments, among them the ones which will be used in phase II of this project.

1. Aerodynamic Particle Sizer (APS). A particle sizer developed by T.S.I. Inc. (U.S.A.) under the commercial name APS-33 operates as follows. Airborne particles moving at a constant velocity are introduced through an orifice into a sheath airstream moving at a higher constant velocity. Upon entering this

higher velocity air stream the particles accelerate, with the smaller particles accelerating more rapidly than the larger particles. The particles then pass individually through a detector zone consisting of a laser beam which is split into two parallel planes. In this configuration, each particle produces two light scattering pulses which are detected by a photomultiplier in the forward direction of the incident beam. The two light pulses define a time interval for the particle to move the fixed distance between the two parallel beams of the laser source. The time interval measured represents the characteristic time-of-flight of the particle. This time information is stored in a multichannel accumulator and is used to derive aerodynamic size by means of a microcomputer. Because each particle size provides a different time-of-flight, polydisperse dust clouds can be readily analyzed. The particle size range of the APS-33 is 0.5 to 15 μm. Air is sampled at a flow rate of 1 L/min and is accelerated by the air sheath flow of 4 L/min.

2. Light Extinction Particle Sizers. Arguably, the simplest optical phenomenon employed for particle size and analysis is that of light absorption or extinction in which suspended dust particles flow individually through an illuminated sensing zone, reducing the amount of light reaching a photodiode. The relation between the voltage output, V, of the photodiode and the particle cross-section, A_p, is simply given by the following relationship: $V = A_p V_o/A_d$, where V_o is the photodiode voltage in the absence of suspended particles, and A_d is the cross-sectional area of the detector (photodiode) in the direction of incident beam. It follows from the above expression that V is related to the particle size, thereby providing a means for size discrimination. One such instrument that operates on this principle is the HIAC Model PA-720 manufactured in the U.S.A.

3. Time-Averaged Light Scattering Particle Monitors. Light scattering

phenomena can be divided into two major classes depending on the mode of application to particle size analysis. The first category is time-averaged scattering, where either the intensity of the scattered light or it spatial distribution (i.e., Fraunhofer diffraction) is measured. The second category is time-fluctuation scattering, which includes the analysis of the spectral distribution of the scattered radiation as well as Photon Correlation Spectroscopy.

A number of instruments have been designed that operate on light scattering principles. A few of these instruments will be briefly described here. This by no means should be construed as endorsement of these instruments over other instruments not described here. The same applies equally well to any other type of instrumentation discussed in this report or not described at all for reasons of space, or any other reason. Usually, the descriptions and discussions on instrumentation in this report are those which refer to instruments in use at the Elliot Lake Laboratory (ELL), or to instrumentation with which the ELL personnel are directly aquainted through direct or indirect experimentation and/or use. More extensive and complete descriptions of particle instrumentation can be found in the relevant literature (61-63,66).

The HIAC/ROYCO 5000 Series (Models 5100 and 5300) and Model 4130 are three instruments that operate on light scattering principles. These instruments cover the approximate particle size range 0.25-0.5 μm (for the lower limit) up to 20 μm. The Model 5100 uses a He-Ne laser as the light source and a photodiode as a light receptor. The size range is 0.25-10 μm, and the sampling flowrate is 28 L/min. The light scattered (90^{o} scattering particle detector) is collected over the range 60^{o} to 120^{o} with a size sensitivity of 0.25 μm. This model (contrary to Models 5300 and 4130) is a total particle counter, i.e., it does not provide particle size discrimination, and hence, particle size distribution.

The HIAC/ROYCO Models 5300 and 4130 enable particle size distribution measurements through six size range 'windows' covering the size ranges 0.5 to 20 μm (Model 5300) and 0.3 to 20 μm (Model 4130). The model 5300 uses a halogen lamp light source whereas Model 4130 uses a He-Ne laser light source. Both instruments operate at a sampling flow rate of ~28 L/min. The Model 5300 has been designed as a clean room particle sizer for low particle concentration measurements. Model 4130 collects particle scattered light over the angle range 30^{o} to 170^{o} by means of an ellipsoidal mirror. The three instruments described above are fully automated, and they are equipped with a built-in printer where data are displayed.

Another light scattering particle sizer is the Model CI-7300 manufactured by Climet Instruments Co. (U.S.A.) (see Fig. 22). This is a microprocessor based six channel particle counter which uses a quartz-halogen light source and particle light scattering through a wide angular range from 15^{o} to 150^{o}. The standard sampling flow rate is ~28 L/min although other flow rates are optional, down to 0.28 L/min. The instrument counts at 6 particle ranges with thresholds at 0.3 μm, 0.5 μm, 0.7 μm, 1.0 μm, 5.0 μm, and 10 μm. Cumulative and differential particle counts are available. The CI-7300 is equipped with temperature and relative humidity probe, air velocity probe, thermal printer, RS-232 serial port, analog and digital outputs, and interface to control multiport samplers. This instrument will be used in phase II of this project with a nominal sampling flow rate of 2.8 L/min. Climet Instruments also manufactures other particle monitors of interest.

Another company which specializes in particle sizers is Particle Measuring Systems Inc. (U.S.A.), which manufactures a number of laser (He-Ne) based instruments covering the size range from less than 1 μm to above 12 μm, depending of the model. The following are models of interest DS-LAS-250X (0.2 to 12 μm), DS-LAS-X (0.09 to 3 μm), DS-LPC-555 (0.3 to 5 μm), and LPC-525 (0.2 to 5 μm). The sampling flow rate varies with the model.

Insitec (U.S.A.) manufactures a particle-counter-sizer-velocimeter Model PCSV which operates on light scattering and intensity deconvolution principles. It covers a particle size range of 0.2 to 200 μm. The Model PCSV-E can accomodate flow streams of up to 1.5 m in diameter. Two laser beams are focused to form two independent measurement volumes which provide a wide dynamic range for particle size measurements.

GCA Corporation (U.S.A.) manufactures a personal dust particle monitor, the MINIRAM (for Miniature Real-Time Aerosol Monitor) Model PDM-3. This instrument is an ultra-compact personal size airborne particulate monitor based on the detection of scattered light in the near infrared. The MINIRAM uses a pulsed GaAlAs light emitting source, which generates a narrow-band emission centered at 880 nm with a power output of 2 mW. Infrared light scattered by dust particles in the approximate size range 0.1 to 10 μm is sensed over an angle of 45^{o} to 95^{o} from the forward direction by means of a silicon-photovoltaic hybrid detector with an internal low-noise amplifier. The MINIRAM is a light scattering device of the nephelometric type, i.e., the instrument continuously senses the combined scattering from the population of particles present within its ~1 cm^3 sensing volume, whose dimensions are large compared with the average separation between the individual dust particles. The MINIRAM has a sensing chamber through which air surrounding the instrument passes freely as a result of air transport caused by convection, ventilation, personnel motion or circulation. This device does not require a sampling pump for its operation because the rate at which air passes through the sensor does not influence the particle concentration measurement. This is because the detection is performed on every 'parcel' of air traversing the fixed sensing volume.

The MINIRAM is a fully automated particle monitor which provides data update every 10 s and also average particle concentration over a daily working shift, i.e., 8 h. The instrument operates in conjunction with an external

printer. It gives particle concentration data but it has no size discrimination capabilities. The MINIRAM is one of the dust instruments which will be used in phase II of this project.

Other particle sizers covering the particle size range of interest here are manufactured by TSI (U.S.A.) and other North American and European firms. TSI manufactures a laser diode based instrument covering the size range 0.5 to 20 μm at a sampling flow rate of 2.8 L/min (Model TSI 3755).

E. OTHER TYPES OF PARTICLE COUNTERS AND PARTICLE SIZERS

In addition to the types of instrumentation discussed in the above sections, there is a variety of devices which operate on principles different than those described in items A to D. One such case is Photon Correlation Spectroscopy, particle sizers that are based on electrostatic separation methods, and methods based on nuclear particle attenuation principles, e.g. by β-particle attenuation.

Airborne particle mass concentration instruments have been designed which are sensitive to the collected dust mass by means of the attenuation of β-particles. In this type of instrumentation, the particles are drawn through an orifice and impact on a suitable material surface. This impaction surface is located between a β-particle radioactive source and a β-particle counter. The attenuation of β-radiation is proportional to the mass collected on the impaction surface.

This will end the present discussion on dust particle instrumentation. For more details about this type of instrumentation the reader should consult the relevant bibliography (61-63,66 and refs. therein).

LONG-LIVED RADIOACTIVE DUST STUDIES IN CANADA

The Elliot Lake Laboratory (Mining Research Laboratories, CANMET, E.M.R) has played a leading role in the quantification and characterization of Long-Lived Radioactive Dust (LLRD) generated in Canadian underground uranium mines and uranium mill operations. During the last decade, numerous investigations were undertaken at the Elliot Lake Laboratory (ELL). More specifically, studies have been conducted in order to determine the:

1. Production of LLRD for a wide range of mining and milling operation conditions.
2. Effect of dust control measures and techniques on the reduction of LLRD generated in the course of a variety of mining operations.
3. Relationship of LLRD and total dust and silica dust.

Among the most important mining and milling operations monitored and studied in item 1 were: crushing, drilling, mucking, slushing, leaching, and ore transportation by conveyor belts, as well as milling and all major physico-chemical operations usually performed in the extraction and refinement of uranium in uranium mills. The latter included precipitation, decantation, extraction, concentration processes, drying, and packaging.

Several technologies have also been investigated aimed at controlling and/or reducing LLRD emissions from various mining operations. These technologies include wet scrubbers, electrostatic precipitators, such as charged water sprays, fan/filter systems, and water sprays.

In addition to the above, extensive radionuclide identification studies have been carried out by means of α-particle spectrometry and γ-ray spectrometry using NaI(Tl) and high purity Germanium detectors, respectively.

Apart from the work carried out by the ELL, LLRD characterization studies have also been done in Canada by several external contractors such as the Canadian Institute for Radiation Safety (CAIRS) and MacLaren Plansearch

Inc. under contract with AECB. In addition, other LLRD related studies (also sponsored by the AECB) have been conducted, such as solubility of long-lived airborne particulates in simulated lung fluid, and health effects of inhaled uranium ore dust.

In the work conducted at the Elliot Lake Laboratory (ELL), the following variables were investigated as a function of mining and milling operations and of dust suppression techniques:

1. Particle number size distribution and particle mass size distribution,
2. Mass Median Aerodynamic Diameter (MMAD),
3. Activity Median Aerodynamic Diameter (AMAD),
4. Long-Lived Radioactive Dust (LLRD) concentration, [LLRD],
5. Total dust, respirable dust, and silica dust concentrations,
6. Radionuclide identification.

In order to accomplish items 1 to 6, a variety of instrumentation was used such as cascade impactors, horizontal elutriators, nylon cyclones, CAMPEDS (102), and optical particle counters.

In addition, and because of the importance of the electrical charge associated with LLRD, the determination of LLRD electric charge versus particle size has been conducted for a number of mining operations such as crushing and ore transportation by conveyor belts (40). Particle charge is important because it influences the behaviour (e.g., collection characteristics of dust samplers), and the deposition of dust in the respiratory tract (42-44,70).

As anticipated, in the above studies, the size distributions (particle number, mass, and electrical charge), the MMAD, AMAD, [LLRD], and total dust and silica dust concentrations depend on the mine and mill operation monitored, and on the type of dust suppression technique used. What follows is a summary of the work conducted in Canadian uranium mines and uranium mills. For simplicity, the discussion below will be divided into the work

conducted by ELL (with and without dust suppression techniques) and work carried out by other organizations.

A. LONG-LIVED RADIOACTIVE DUST STUDIES CONDUCTED AT THE ELLIOT LAKE LABORATORY

Size characterization studies of LLRD were initiated at the ELL early in 1979 by the author, and have subsequently continued up to the present. Early measurements of LLRD size distribution were conducted with in-house built size selective dust samplers with mid-cut sizes ranging from 1.25 μm to 7.1 μm. These samplers were optimized for collection of dust passing the particle size selectors on back-up filters with subsequent assessment of dust by weighing and X-ray diffraction (XRD) analysis, and also radioactivity measurements on the filters by conventional total α-particle activity techniques.

Some size selective samplers used horizontal elutriators whose size selection characteristics were calculated from theory (73,100). In addition, in-house designed and built impaction size selectors (six and eight stages) were employed in several underground uranium mines (101). Respirable (total) LLRD was determined by means of single stage impactor size selective samplers such as CAMPEDS (102), and nylon cyclones. Shortly after these initial studies, LLRD size characterizations have been carried out with commercial 10-stage cascade impactors (Sierra model 210), and 8-stage cascade Marple impactors model 290. Furthermore, Long-Lived Radioactive Dust measurements in the (total) respirable range (~1 to 10μm) have been conducted preferentially with optical particle counters (OPC) and nylon cyclones. Optical particle counters have also been used extensively for particle size characterization in addition to mass size characterization by cascade impactors. A summary of early work on the characterization of LLRD can be obtained from refs. 6,9,103. More recent work is described below.

1. Surveys and Characteristics. Numerous LLRD surveys have been done over the last decade in underground (U/G) uranium mines and uranium mills in order to gain information regarding airborne concentration ranges of LLRD characteristic of distinct mining and milling operations. In most cases, concentration data have been supplemented with particle (number and mass) size distribution information as well as (in specific instances) with electrical particle charge distribution data. Some of this work is documented in refs. 6,9,40,103. Because of the potential occupational health hazards associated with the inhalation and injection of industrial dusts, the main emphasis has been placed in monitoring mining (and milling) operations which generate large amounts of dust such as rock breaking, rock crushing, and transportation of mineral ores and rock waste by conveyor belts. A brief summary of the data compiled over the last few years is given below (see also Figs. 23-31 and Tables 2-7). For a more detailed account and explanation of the data the reader should examine the above references. Some of the most relevant features and conclusions of these studies are:

1. In the great majority of cases the AMAD is higher than the MMAD of the carrier dust.
2. There seems to be, in general, a simple relationship or correlation between AMAD and MMAD, namely, the AMAD increases or decreases with increasing or decreasing MMAD, respectively.
3. Large variability in MMAD, AMAD, and airborne LLRD concentration, [LLRD], data depending on underground conditions, such as airflow rate, and the nature of mining and milling operations.
4. Item 3 depends greatly, quantitatively, and qualitatively speaking, on special working practices adopted by the mining and milling companies such as reduction, suppression, or, in general, airborne pollutant control techniques, e.g., water sprays, wet scrubbers, electrostatic precipitators, filtering techniques, etc.

5. Airborne [LLRD] depends on the grade of the ore mined or milled.
6. The specific activity (SA) of the LLRD collected in air samples (i.e., the ratio of the long-lived α-particle radioactivity measured in the sample and the mass of dust collected in the sample) was, in general, significantly higher for physico-chemical milling operations (acid leaching, decantation, extraction, precipitation) than for mechanical mining and milling operations (rock crushing, transportation, screening, and other operations). This is to be expected because of the extracting, concentrating and refining nature of some physico-chemical milling operations. An exception to the above is yellowcake packaging, a mechanical milling operation, which yielded by far the highest SA of any mechanical or milling operation in mines or mills, i.e., 1.0×10^4 - 2.0×10^4 mBq/mg (see Tables 2 and 3) (104).
7. For similar ore grades, mechanical operations in mines and mills gave similar results. Differences observed can be attributed to differences in airflow rates, airflow patterns, and due to geometrical considerations.

Broadly speaking, the data collected in the various surveys conducted over extended periods can be summarized as follows:

a) For underground uranium mines the following ranges for [LLRD] and AMAD were obtained:

[LLRD] : very low to >250 mBq/m^3

AMAD : 2.5 μm to ~6.0 μm

b) For uranium mills the ranges were:

[LLRD] : ~30 mBq/m^3 to ~1.3×10^5 mBq/m^3

AMAD : ~3 μm to >15 μm.

It is worthwhile noting that parallel sampling of LLRD atmospheres with different types of instruments produced different results. This was particularly true when comparisons were made of mass (and α-particle activity)

size distributions using two different kinds of cascade impactors, namely, the Sierra 210 and the Marple 290. Furthermore, the total LLRD collected using nylon cyclones and the two types of cascade impactors indicated above differed substantially. This can be understood because of the different size-selective characteristics of cyclones and cascade impactors. The discrepancies observed between the Sierra and the Marple impactors deserve serious consideration and this is one of the purposes of phase II of this project.

2. Effectiveness of Dust Abatement Techniques in Reducing Airborne Long-Lived Radioactive Dust Concentrations. A variety of dust abatement techniques have been tried, aimed at studying their effectiveness in reducing the airborne LLRD concentration produced in the course of some mining operations which generate large amounts of dust, e.g., rock breaking and rock crushing, ore transportation by conveyor belts, and dust exhaust galleries where dust produced in the above operations is discharged. The following dust abatement techniques have been studied (105-109):

a) wet scrubbers,

b) water sprays,

c) electrostatic collection methods,

d) filtering (fan/filter systems).

A summary of the above studies is presented in Table 6. It can be seen that, in general, a quite significant effect (reduction) is brought about by wet scrubbing, electrostatic precipitation and water sprays on the Long-Lived Radioactive Dust concentration, [LLRD], the Mass Median Aerodynamic Diameter (MMAD), and the Activity Median Aerodynamic Diameter (AMAD). The effectiveness of the fan/filter system for respirable dust and LLRD could not be ascertained because hardly any dust producing mining operations took place during this particular study. Most mining activities were restricted to heavy dieselized vehicle traffic whose exhaust is mainly made up of particles in the

sub-micron range. Because the filter installed in the filter/fan system was particularly intended for large particles, sub-micron size particles had little difficulty in passing through the filter, and hence, the dust abatement system. However, the filter had a noticeable although small effect on the AMAD, MMAD and [LLRD] associated with the small size particle clouds.

The effectiveness of the wet scrubber, electrostatic precipitator and water sprays in reducing LLRD and other variables is summarized in Tables 6 and 7.

3. Long-Lived Alpha-Particle Activity Associated with Dust Samples. Considerable effort has gone into the measurement of the long-lived α-particle activity associated with dust samples from hard rock uranium mines. The idea behind this work was to investigate whether a reasonable relationship could be established between long-lived radioactivity in dust samples and respirable dust mass (total or silica dust) reliable enough for α-particle dosimetry applications. This is important in view of new regulations by the responsible regulatory agency (AECB) which may require uranium mining and milling operators to report airborne long-lived α-particle activity for radiation exposure estimation purposes. Because dust mass in air samples from local underground uranium mines is routinely assessed at the Elliot Lake Laboratory as part of a collaborative agreement, a reliable relationship between long-lived radioactivity and dust mass would greatly facilitate the determination of personnel exposure levels by measurement of dust mass alone. Furthermore, not only could this method be applied routinely in the future, but it also could be used to calculate earlier long-lived airborne radioactivity by using past dust measurement records.

Data collected in two underground uranium mines during the period 1983 to 1985 were analyzed. Total respirable dust, silica dust, and long-lived α-particle activity were measured. Total respirable dust was estimated by

conventional weighing techniques. Respirable quartz (silica) dust was measured using X-ray diffraction techniques. The long-lived α-particle activity (gross α-count) was determined by conventional gross α-particle counting methods. A large number of samples were taken on silver membrane filters (5 μm mean pore size) using gravimetric dust samplers (101,103) and nylon cyclones. Long-lived α-particle activity versus total respirable dust, and long-lived α-particle activity versus quartz dust mass were analyzed by linear regression analysis using the Least Squares Method. Poor correlation was found between long-lived α-particle activity and total respirable dust mass. A much better correlation (~0.75 correlation coefficient) was found between long-lived α-particle activity and silica dust mass. The best fitted data for the two mines can be represented by the following two expressions (110) (see also Figs. 30 and 31):

$$A(mBq) = 156.92\ W_Q + 3.44 \quad \text{for mine B, and}$$

$$A(mBq) = 160.25\ W_Q + 7.87 \quad \text{for mine A.}$$

Subsequent studies on samples taken with nylon cyclones have shown similar relationships, although subtle differences have been found which are at present under investigation. These studies represent a continuing effort aimed at establishing a reliable and consistent relationship between [LLRD] and silica dust mass concentration suitable for practical applications. Such a relationship would prove very useful for occupational exposure purposes in the uranium industry.

B. LONG-LIVED RADIOACTIVE DUST STUDIES CONDUCTED BY OTHER ORGANIZATIONS IN CANADA

As previously indicated, other LLRD studies have been conducted, or are in progress, by organizations other than the Elliot Lake Laboratory. All these other studies have been, or are being, sponsored by the AECB. Work in progress includes LLRD characterization surveys as well as investigations on

the health effects of uranium ore dust inhaled by rats, and LLRD solubility studies with MacLaren Plansearch Inc. (Toronto) as the main contractor.

A study aimed at determining the contribution of LLRD to the committed dose equivalent received by uranium mine and mill workers in the Elliot Lake area was completed in 1985 by the Canadian Institute for Radiation Safety (CAIRS) under the technical direction of P. Duport and sponsorship of the AECB (8).

The work conducted at CAIRS consisted mainly in determining the [LLRD], AMAD and MMAD from field samples taken at the local Elliot Lake uranium mines and mills, using one cascade impactor (Sierra 210). From the radionuclide make-up of LLRD, the AMADs, and a lung dosimetry model proposed by the International Commission on Radiological Protection (ICRP) (document ICRP 30, ref. 111), the Derived Air Concentration (DAC) and the Annual Limit on Intake (ALI) were calculated. The main conclusions of the study were as follows. In underground mine locations, the AMADs were in the range 5 to 10 μm, whereas in mills the AMAD was close to 7 μm. Furthermore, the DAC was in the range 1.29×10^3 to 1.64×10^3 mBq/m^3, whereas in mill working areas the DAC was about 2.4×10^3 mBq/m^3.

Despite the large number of measurements carried out by the Elliot Lake Laboratory and CAIRS, more documentation is needed, particularly in view of the discrepancies observed using different instrumentation, and also because of varying working environmental conditions and the implementation of better quality control measures and stricter occupational exposure levels.

C. LONG-LIVED RADIOACTIVE DUST STUDIES OUTSIDE CANADA

There have been a number of studies on LLRD characterization, solubility, and other related topics outside Canada, particularly in uranium producing countries and/or countries with significant nuclear power

consumption such as the U.S.A., France, Australia, and other countries. Although of great interest, these studies are of limited practical interest in the context of the Canadian experience because the working parameters, ore grades, and other considerations are somewhat different. However, the reader is urged to consult the pertinent literature and references therein (112-117), and other important contributions on the subject.

FINAL COMMENTS

In this report a number of topics of practical interest have been discussed such as the production of dust in uranium mining and milling operations, as well as the properties, characterization and measurement of dust clouds, the criteria for the measurement of dust, and instrumentation in common use for dust monitoring and characterization purposes. Finally, a brief summary of work done on the characterization of Long-Lived Radioactive Dust in Canada, and outside Canada, has been presented.

From a review of the above subjects two major issues stand out clearly in the context of occupational exposure, namely:

1. The need for a rapid and accurate determination of Long-Lived Radioactive Dust concentrations [LLRD] at the work place; and
2. The complete and reliable characterization (AMAD, MMAD, and other variables) of LLRD.

Pertinent information on item 1 can be realized by direct measurement of airborne LLRD. However, this is an expensive and time-consuming process, and hence labour intensive. There is, however, an indirect but promising way to gain this kind of information, namely, from dust mass measurements of dust samples taken routinely by mining and milling companies for dust compliance purposes in accordance with the pertinent governmental regulatory agencies. This method is based on the reasonable premise that a relationship exists

between total respirable dust (or silica dust) and LLRD α-particle activity, or γ-activity, which can be predicted on theoretical grounds, or better still, which can be determined experimentally with the desired degree of accuracy. In order to be of practical use for compliance purposes, as well as for occupational exposure applications, the above relationship should not only have a high degree of correlation, but it should also be capable of revealing differences between various mining and milling operations, and occupational categories, provided such differences truly exist and are relevant enough to play a significant practical role.

As previously discussed, experimental work aimed at establishing a relationship between respirable dust (total and silica dust) and Long-Lived Radioactive Dust has been initiated by the Elliot Lake Laboratory some time ago. However, despite a fairly large data base already existing on the subject, much more work will be necessary before it is possible to establish beyond doubt that such a relationship exists, and that it can be used for occupational exposure applications and other purposes.

Various dust chacterization studies have revealed the disturbing fact that different instruments designed for the same or similar purpose produce different results. Hence, the need for instrument standardization and a standard method that can be reliably used to characterize dust emissions, e.g., LLRD, is therefore, of utmost importance. In many applications, certain cascade impactors are used as the standard instrument for dust characterization purposes. However, most cascade impactor systems require rather complex experimental procedures which make dust characterization rather cumbersome and time-consuming.

Because of practical constraints, the need for simplification in field operations is an important practical consideration. Hence, if use could be made of field measurements which are currently and routinely conducted by mining and milling companies in order to characterize dust generated in the

course of mining and milling operations, this would result in a great economic advantage and a significant reduction in the level of effort. One way of accomplishing the above objective is by comparing the performance of instruments and methodologies which are currently used in routine field measurements of dust with standard techniques for precise dust characterization. This is precisely the purpose of the second phase of this project. If successful, it will be possible to use the data collected by means of several instruments and techniques in common use by the uranium mine and mill companies to obtain a better representation of the experimental field conditions in the above working locations.

REFERENCES

1. National Research Council: Measurement and Control of Respirable Dust in Mines. (N.G.W. Cook, ed.), Report NMAB-363, National Academy of Sciences, Washington, D.C., 1980.

2. Walton, W.H., ed. Inhaled Particles III. vol. 1, Unwin Brothers Limited, Surrey (England), 1971.

3. Walton, W.H., ed. Inhaled Particles IV. vol. 1, Pergamon Press, Oxford (England), 1977.

4. Walton, W.H., ed. Inhaled Particles V. vol. 26, No. 1-4 (The Annals of Occupational Health), Pergamon Press, Oxford (England), 1982.

5. Marple, V.A. and B.Y.H. Liu, eds. Aerosols in the Mining and Industrial Work Environments. vol. 1 (Fundamentals and Status), Ann Arbor Science, Ann Arbor (Mich.), 1983.

6. Bigu, J. and Grenier, M. Studies of Radioactive Dust in Canadian Uranium Mines. CIM Bulletin vol. 77, No. 869, pp. 62-68, 1981.

7. Paschoa, A.S. et al. Uranium Bearing Particles in Miners' and Millers' Lungs. In: Occupational Radiation Safety in Mining. H. Stocker, ed. pp. 511-517, Canadian Nuclear Association, Toronto (Canada), 1984.

8. Duport, P.J. and Edwardson, E.E. Determination of the Contribution of Long-Lived Dust to the Committed Dose Equivalent Received by Uranium Miners and Mill Workers in the Elliot Lake Area. Atomic Energy Control Board Information Reports INFO-0167-1 and INFO-0167-2, Ottawa (Canada), 1985.

9. Bigu, J. and Grenier, M. Characterization of Dust in Canadian Underground Uranium Mines. In: Proc. of 2nd U.S. Mine Ventilation Symp. (P. Mousset-Jones, ed.), pp. 269-277, A.A. Baldema (Rotterdam/Boston), 1985.

10. The International Commission on Radiological Protection (ICRP):

Radiation Protection of Workers in Mines. ICRP Committee, ICRP Publication No. 47, Pergamon Press, Oxford (England), 1986.

11. Green, H.L. and Lane, W.R. Particulate Clouds: Dusts, Smokes and Mists. 2nd edition, E. & F.N. Spon Ltd., London (England), 1964.

12. Friedlander, S.K. Smoke, Dust and Haze - Fundamental of Aerosol Research. John Wiley & Sons, Inc., New York (U.S.A.), 1977.

13. Billings, C.E. and Gusman, R.A. Dynamic Behaviour of Aerosols. In: Handbook of Aerosols. (R. Dennis, ed.), pp. 40-65, Technical Information Center (U.S. Department of Energy), TID-26608, 1976.

14. Davies, C.N. Deposition from Moving Aerosols. In: Aerosol Science (C.N. Davies, ed.), pp. 393-446, Academic Press, London/New York, 1966.

15. Strauss, W. Industrial Gas Cleaning. Pergamon Press, Oxford (England), 1975.

16. Hamaker, H.C. Physica, vol. 4, p. 1058, 1937.

17. Bradley, R.S. Trans. Faraday Soc., vol. 32, p. 1088, 1936.

18. Corn, M. Adhesion of Particles. In: Aerosol Science. (C.N. Davies, ed.), pp. 359-392, Academic Press, London and New York, 1966.

19. Reeks, M.W., Reed, J. and Hall, D. On the Resuspension of Small Particles by a Turbulent Flow. Journal of Physics D: Applied Physics, vol. 21, No. 4, pp. 574-589, 1988.

20. Fuchs, N.A. The Mechanics of Aerosols. MacMillan, New York (U.S.A.), 1964.

21. Herdan, G. Small Particle Statistics. Butterworths, London (England), 1960.

22. Kaye, B.H. Direct Characterization of Fineparticles. John Wiley & Sons, New York (U.S.A.), 1981.

23. Schwartz, H.P. and Shane, K.C. Measurement of Particle Shape by Fourier Analysis. Sedimentol. vol. 13, pp. 213-231, 1969.

24. Sutton, H.M. and Bundalli, N. A Suggestion for the Exact Determination

of Particle Size and Shape. In: Proc. of the Soc. for Analytical Chemistry, pp. 13-17, Jan. 1973.

25. Ehrlich, R. and Weinberg, B. An Exact Method for Characterization of Grain Shape. J. of Sedimentary Petrol., vol. 40, No. 1, pp. 205-212, 1970.

26. Kaye, B.H. and Wright, C.D. Decision Matrix Design and Cybernetic Mode Operation of SHADOW, a System for Fineparticle Shape Characterization. Powder Technology, vol. 18, No. 1, pp. 27-30, 1977.

27. Naylor, A.G. Optical Information Procedures Applied to Powder Science and Technology. Ph.D. Thesis, Reading University (England), 1973.

28. Redman, J.D. Optical Aids to Pattern Recognition. In: House Journal of the Atomic Weapons Research Establishment, Aldermaston, Berkshire (England), June 1967.

29. Murphy, R. Optical Information Processing Procedures for Determining the Essential Features of Particle Size. M.Sc. Thesis, Laurentian University, Sudbury (Canada), 1972.

30. Mandelbrot, B.P. Fractals, Form, Chance, and Dimensions. W.H. Freeman, San Francisco (U.S.A.), 1977. (See also New Scientist, pp. 808-810, June 2, 1978).

31. Mandelbrot, B.P. The Fractal Geometry of Nature. W.H. Freeman and Co., New York (U.S.A.), 1983.

32. Da-hong Li and Ganczarczyk, J. Fractal Geometry of Particle Aggregates Generated in Water and Waste Water Treatment Processes. Environ. Sci. Technol., vol. 23, No. 11, pp. 1385-1389, 1989.

33. Schaefer, D.W. Polymers, Fractals and Ceramic Materials. Science, vol. 243, pp. 1023-1027, 1989.

34. Patterson, H.S., Whytlaw-Gray, R. and Cawood, W. The Structure and Electrification of Smoke Particles. Proc. Roy. Soc., vol. 124, pp. 523-532, 1929.

35. Kunkel, W.B. The Static Electrification of Dust Particles on Dispersion into a Cloud. J. Appl. Phys., vol. 21, pp. 820-832, 1950.

36. Kunkel, W.B. Charge Distribution in Coarse Aerosols as a Function of Time. J. Appl. Phys., vol. 21, pp 833-837, 1950.

37. Johnston, A.M., Vincent, J.H. and Jones, A.D. Measurements of Electric Charge for Workplace Aerosols. Ann. Occup. Hyg., vol. 29, pp. 271-284, 1985.

38. Johnston, A.M., Vincent, J.H. and Jones, A.D. Electrical Charge Characteristics of Dry Aerosols Produced by a Number of Laboratory Mechanical Dispensers. Aerosol Sci. Tech., vol. 6, pp. 115-127, 1987.

39. Bigu, J. Some Observations on the Electrical Charge Characteristics of Radioactive (^{222}Rn Progeny) and Non-Radioactive Aerosols. Health Physics, vol. 58, No. 1, pp. 21-36, 1990.

40. Bigu, J. Electrical Charge Characteristics of Long-Lived Radioactive Dust. Health Physics, vol. 58, No. 3, pp. 341-350, 1990.

41. Billard, F. and Madelaine, G. Etude de la Charge Electrique porteé par les Aerosols. In: Assessment of Airborne Radioactivity, STI/PUB/159, IAEA, Vienna (Austria), 1967.

42. Prodi, V. and Mularoni, A. Electrostatic Lung Deposition Experiments with Humans and Animals. Ann. Occup. Hyg., vol. 29, pp. 229-240, 1985.

43. Liu, B.Y.H. et al. Electrostatic Effects in Aerosol Sampling and Filtration. Ann. Occup. Hyg., vol. 29, vol. 2, pp. 251-269, 1985.

44. Briant, J.K. and Moss, O.R. The Influence of Electrostatic Charge on the Performance of 10 mm Nylon Cyclones. Am. Ind. Hyg. Assoc. J., vol. 45, No. 7, pp. 440-445, 1984.

45. Porstendörfer, J. and Mercer, T.T. Influence of Electric Charge and Humidity upon the Diffusion Coefficient of Thoron Decay Products. Health Physics, vol. 37, pp. 191-199, 1979.

46. Dua, S.K. and Kotrappa, P. Comment on the Charge of Decay Products of

Thoron and Radon. Am. Ind. Hyg. Assoc. J., vol. 42, pp. 242-243, 1981.

47. Dua, S.K., Kotrappa, P. and Bhanti, D.P. Electrostatic Charge on Decay Products of Thoron. Am. Ind. Hyg. Assoc. J., vol. 39, pp. 339-345, 1978.

48. Bricard, J. et al. Spectre des Aerosols Naturels Radioactifs. In: Proc. Symp. on La Pollution Radioactive des Milieux Gazeux, 1964.

49. Hoppel, W. Ion-Aerosol Attachment Coefficient, Ion-Depletion, and Charge Distribution on Aerosols. J. Geophys. Res., vol. 90, pp. 5917-5923, 1985.

50. Whitby, K.T. and Liu, B.Y.H. The Electrical Behaviour of Aerosols. In: Aerosol Science (C.N. Davies, ed.), pp. 59-86, Academic Press, London and New York, 1966.

51. Bricard, J. and Pradel, J. Electric Charge and Radioactivity of Naturally Occurring Aerosols. In: Aerosol Science (C.N. Davies, ed.), pp. 87-110, Academic Press, London and New York, 1966.

52. Jonassen, N. The Effect of Electric Fields on ^{222}Rn Daughter Products in Indoor Air. Health Physics, vol. 45, pp. 487-491, 1983.

53. Bigu, J. Effects of Electric Fields on ^{220}Rn Progeny Concentration. Health Physics, vol. 49, pp. 512-516, 1985.

54. Gunn, R. Diffusion Charging of Atmospheric Droplets by Ions, and the Resulting Combination Coefficients. J. of Meteorology, vol. 11, pp. 339-347, 1954.

55. Liu, B.Y.H. and Pui, D.Y.H. Electrical Neutralization of Aerosols. Aerosol Science, vol 5, pp. 465-472, 1974.

56. Yeh, H. A Theoretical Study of Electrical Discharging of Self-Charging Aerosols. J. Aerosol Sci., vol. 7, pp. 343-349, 1976.

57. Fleischer, R.L. Theory of Alpha-Recoil Effects on Radon Release and Isotropic Disequilibrium. Geochimica et Cosmochimica Acta, vol. 47, pp. 779-784, 1983.

58. Van de Hulst, H.C. Light Scattering by Small Particles. Dover Publications Inc., New York (U.S.A), 1981.

59. Particle Size-Selective Sampling in the Workplace. Report of the American Conference of Governmental Industrial Hygienists (ACGIH) Technical Committee on Air Sampling Procedures. Published by ACGIH, Cincinnati, (OH, USA), 1985.

60. Morrow, P.E. et al. Deposition and Retention Models for Internal Dosimetry of the Human Respiratory Tract. Report of the International Commission on Radiological Protection (ICRP) Task Group on Lung Dynamics. Health Physics, vol. 12, pp. 173-207, 1964.

61. Barth, H.G. and Sun, S. Particle Size Analysis. Analytical Chem. vol. 57, pp. 151R-175R, 1985.

62. Modern Methods of Particle Size Analysis. (Chemical Analysis Monograph, vol. 73), H.G. Barth (ed.), John Wiley & Sons, New York (U.S.A.), 1984.

63. Allen, T. Particle Size Measurement. (Powder Technology Series), 3rd Ed., Chapman & Hall, London (England), 1981.

64. Aerosols in the Mining and Industrial Work Environments, vol. 3 (Instrumentation), Marple, V.A. and Liu, B.Y.H. (eds.), Ann Arbor Science, Ann Arbor (MI, U.S.A.), 1983.

65. Advances in Air Sampling. (Industrial Hygiene Science Series), American Conference of Governmental and Industrial Hygienists (ACGIH), 2nd printing, Lewis Publishers, Chelsea (MI, U.S.A.), 1989.

66. Air Sampling Instruments for Evaluation of Atmospheric Contaminants, 7th Ed., S.V. Hering (ed.), American Conference of Governmental Hygienists, Cincinnati (OH, U.S.A.), 1989.

67. John, W. and Reischl, G. A Cyclone for Size Selective Sampling of Ambient Air. J. Air Pollution Control Assoc., vol. 30, p. 872, 1980.

68. Lippmann, M. and Chan, T.L. Cyclone Sampler Performance. Staub-Reinhalt, Luft, vol. 39, p. 7, 1979.

69. Saltzman, B.E. Generalized Performance Characteristics of Miniature Cyclones for Atmospheric Particulate Sampling. Am. Ind. Hyg. Assoc. J.,

vol. 45, p. 671, 1984.

70. Almich, B.P. and Carson, G.A. Effects of Charging on 10 mm Nylon Cyclone Performance. Am. Ind. Hyg. Assoc. J., vol. 35, p. 603, 1974.

71. Hering, S.V. Inertial and Gravitational Collectors. In: ref. 66, pp. 337-364.

72. Claassen, B.J., Jr. Experimental Determination of Vertical Elutriator Particle Transfer Efficiency. Am. Ind. Hyg. Assoc. J., vol. 42, No. 4, pp. 305-309, 1981.

73. Walton, B.H. Theory and Size Classification of Airborne Dust Clouds by Elutriation. Brit. J. of Appl. Physics, Supplement No. 3, paper A.5, pp. S29-S40, 1954 (Also given as p. 529).

74. Mercer, T.T. Aerosol Technology in Hazard Evaluation. Academic Press, New York (U.S.A.), 1979.

75. Stöber, W. and Flaschsbart, H. Size Separating Precipitation in a Spinning Spiral Duct. Envir. Sci. Technol., vol. 3, p. 1280, 1969.

76. Stöber, W. Design, Performance and Applications of Spiral Duct Aerosol Centrifuges. In: Fine Particles, Aerosol Generation, Measurement, Sampling and Analysis (B.Y.H. Liu, ed.), pp. 351-398, Academic Press, New York (U.S.A.), 1976.

77. Hoover, M.D., Morawietz, G. and Stöber, W. Optimizing Resolution and Sampling Rate in Spinning Duct Aerosol Centrifuges. Am. Ind. Hyg. Assoc. J., vol. 44, p. 131, 1983.

78. Goetz, A., Stevenson, H.J.R. and Preining, O. The Design and Performance of the Aerosol Spectrometer. J. Air Pollution Control Assoc., vol. 10, p. 378, 1960.

79. Gerber, H.E. The Goetz Aerosol Spectrometer. In: Aerosol Measurement (Lundgren, F.S. et al. eds.), pp. 36-55, University Presses of Florida, Gainesville (FL, U.S.A.), 1979.

80. Stöber, W. and Flachsbart, H. Aerosol Size Spectrometry With a Ring Slit

Centrifuge. Envir. Sci. Tech., vol. 3, p. 641, 1969.

81. Hollaender, W. et al. Very High Volume Aerosols Sampling With a Novel Drum Centrifuge. Aerosol Sci. Tech., vol. 7, p. 67, 1987.

82. Tillery, M.I. Concentric Aerosol Spectrometer. Am. Ind. Hyg. Assoc. J., vol. 35, p. 62, 1974.

83. Hochrainer, D. and Brown, P.M. Sizing of Aerosol Particles by Centrifugation. Envir. Sci. Tech., vol. 3, p. 830, 1969.

84. Keskinen, J., Janka, K. and Lehtimäki, M. Virtual Impactor as an Accessory to Optical Particle Counters. Aerosol Sci. Tech., vol. 6, pp. 79-83, 1987.

85. McFarland, A.R., Ortiz, C.A. and Bertch, R.W., Jr. Particle Collection Characteristics of a Single Stage Dichotomous Sampler. Envir. Sci. Technol., vol. 12, p. 679, 1978.

86. Lioy, P.J. et al. An Intercomparison of the Indoor Air Sampling Impactors and the Dichotomous Sampler for a 10 μm Cut Size. J. Air Pollution (JAPCO), pp. 668-670, 1988.

87. Ono, D. and Chang, D.P.Y. Electrets as a Cascade Impactor Substrate. J. Aerosol Sci., vol. 15, No. 6, pp. 647-656, 1984.

88. Tuchmann, D.P., Esmen, N.A. and Weyel, D.A. Design and Calibration of a Low Flow Parallel Stage Impactor. Am. Ind. Hyg. Assoc. J., vol. 47, No. 1, pp. 55-58, 1986.

89. Lippmann, M. Sampling Aerosols by Filtration. In: ref. 66, pp. 305-336.

90. Dorman, R.G. Filtration. In: Aerosol Science (C.N. Davies, ed.), pp. 195-221, Academic Press, New York (U.S.A.), 1966.

91. Pich, J. Theory of Aerosol Filtration by Fibrous and Membrane Filters. In: Aerosol Science (C.N. Davies, ed.), pp. 223-280, Academic Press, New York (U.S.A.), 1966.

92. Aitken, I. Collected Sci. Papers. (C.S. Knot, ed.), Cambridge U.P., Cambridge (England), 1923.

93. Watson, H.H. The Thermal Precipitator. Trans. Inst. Mining Metal., vol. 46, p. 176, 1936.

94. Green, H.L. and Watson, H.H. Special Report Series No. 199, Medical Research Council, London (England), 1935.

95. Swift, D.L. and Lippmann, M. Electrostatic and Thermal Precipitators. In: ref 66, pp. 387-403.

96. Kasper, G. Hot-Wire Precipitator With Low Inlet Losses and Low Size Selectivity. Rev. Sci. Instrum., vol. 53, No. 1, pp. 79-82, 1982.

97. White, H.J. Industrial Electrostatic Precipitation. Addison-Wesley Publishing Co., Reading (MA, U.S.A.), 1963.

98. Brown, E.L. Electrostatic Precipitators. In: Dust Control and Air Cleaning (R.G. Dorman, ed.), pp 280-317, Pergamon Press, Oxford/New York, 19 ?

99. Gottschlich, C.F. Source Control by Electrostatic Precipitation. In: Air Pollution, vol. III, 2nd Ed., A.C. Stern (ed.), Academic Press, New York/London, 1968.

100. Mercer, T.T., Tillery, M. and Newton, G.J. A Multistage Low Flow Rate Cascade Impactor. J. Aerosol Sci., vol. 1, p. 9, 1970.

101. Knight, G., Bigu, J., Mogan, P. and Steward, D.B. The Size distribution of Airborne Dust in Mines. In: Int. Symp. on Aerosols in the Mining and Industrial Working Environment, pp. 25-1/25-4, Minneapolis (MI, U.S.A., Nov. 1-6), 1981.

102. Knight, G. Mine Dust Sampling Systems - CAMPEDS. CANMET Report 78-7, Energy, Mines and Resources Canada, Ottawa, 1978.

103. Bigu, J. and Kirk, B. Experimental Determination of the Unattached Radon Daughter Fraction and Dust Distribution in Some Canadian Uranium Mines. Can. Mining J., vol. 103, No. 8, pp. 39-45, 1982.

104. Bigu, J. and Duport, P. Characterization of Long-Lived Radioactive Dust Clouds Generated in Uranium Mill Operations. Division Report MRL 87-105

(TR), CANMET, Energy, Mines and Resources Canada, Ottawa, Jan. 1987.

105. Bigu, J., Grenier, M. and Hardcastle, S. Effectiveness of a Wet Scrubber in Reducing Radioactive Aerosol and Dust Concentrations in Underground Uranium Mines. Am. Ind. Hyg. Assoc. J., vol. 49, No. 11, pp. 572-578, 1988.

106. Grenier, M.G., Hardcastle, S. and Bigu, J. Evaluation of a Water-Type Dust Collector at an Underground Crushing Operation. Am. Ind. Hyg. Assoc. J., vol. 49, No. 3, pp. 101-107, 1988.

107. Grenier, M.G. and Bigu, J. Suppression of Airborne Dust in Hard Rock Mines by Means of Electrostatic Water Sprays. Appl. Ind. Hyg., vol. 3, No. 9, pp. 251-257, 1988.

108. Bigu, J. and Grenier, M. Reduction of Airborne Radioactive Dust by Means of a Charged Water Spray. Am. Ind. Hyg. Assoc. J., vol. 50, No. 7, pp. 336-345, 1989.

109. Bigu, J. and Grenier, M. Performance of a Fan/Filter Ventilation System for Reducing Radon (Thoron) Progeny and Respirable Dust in an Underground Uranium Mine. Division Report MRL 88-26(TR), CANMET, Energy, Mines and Resources Canada, Ottawa, March 1988.

110. Bigu, J. Long-Lived Alpha-Particle Activity in Dust Samples from Hard Rock Uranium Mines. Am. Ind. Hyg. Assoc. J., vol. 49, No. 11, pp. 566-571, 1988.

111. The International Commission on Radiological Protection (ICRP): Limits for Intake of Radionuclides by Workers. ICRP Committee, ICRP Publication No. 30, Pergamon Press, Oxford (England), 1978.

112. McGuire, S.A. The NRC's Limit on Intake of Uranium Ore Dust. U.S. Nuclear Regulatory Commission (Washington) Report NUREG-0941, 1983.

113. Knuth, R.H. and George, A.C. Uranium Mill Ore Dust Characterization. Environmental Measurements Laboratory (U.S. Dept. of Energy) Report EML-384, 1980.

114. Sill, C.W. Simultaneous Determination of U-238, Th-230, Ra-226, and Pb-210 in Uranium Ores, Dusts and Mill Tailings. Health Physics, vol. 33, p. 393, 1977.

115. Barzic, J.Y. Etude de l'aerosol d'une mine d'uranium. Ph.D. Thesis, L'Universite de Bretagne Occidentale (France), 1975.

116. Kalkwarf, D.R. Solubility of Airborne Products from Uranium Ores and Tailings Piles. Pacific Northwest Laboratory Report PNL-2870 (CA, U.S.A.), 1979.

117. Woods, D.A. Final Product Dust Activity Median Aerodynamic Diameters in the Product Packing Areas of Two Australian U Mills. Health Physics, vol. 51, No. 3, pp. 352-356, 1986.

Table 1 - Terminal velocities, relaxation times and diffusivities of spherical particles of unit density at 1 atm and 20°C (11,12,14).

Particle Diameter μm	Relaxation Time τ(s)	Terminal Velocity υ(cm/s)	Diffusivity $D(cm^2/s)$
0.1	8.67×10^{-8}	8.6×10^{-5}	6.75×10^{-6}
0.2	2.29×10^{-7}	2.3×10^{-4}	2.22×10^{-6}
0.3	4.28×10^{-7}	4.2×10^{-4}	--
0.5	1.02×10^{-6}	1.0×10^{-3}	6.32×10^{-7}
1	3.57×10^{-6}	3.5×10^{-3}	2.77×10^{-7}
2	1.30×10^{-5}	1.3×10^{-2}	1.28×10^{-7}
3	2.80×10^{-5}	2.7×10^{-2}	--
5	7.95×10^{-5}	7.8×10^{-2}	--
10	3.06×10^{-4}	0.31	2.41×10^{-8}
15	6.93×10^{-4}	0.68	--
20	1.22×10^{-3}	1.22	--
25	1.94×10^{-3}	1.90	--
30	2.75×10^{-3}	2.70	--
50	7.34×10^{-3}	7.58	--
100	2.55×10^{-2}	30.3	--
150	4.69×10^{-2}	46	--
200	7.13×10^{-2}	70	--
300	0.117	115	--
500	0.204	200	--
1000	0.392	385	--

Table 2 - Cascade impactor data for several mechanical operations in a uranium mill.

Mechanical Operation	Impactor	MMAD (μm)	Dust σg	AMAD(LLRD) (μm)	LLRD σg	Dust Conc. (mg/m^3)	LLRD Conc. (mBq/m^3)	LLRD(S.A.) (mBq/mg)
Grizzly	C	15.4	2.8	15.3	3.4	12.51	1090	87
"	EMR	14.5	2.4	19.0	3.0	8.99	1570	175
Jaw Crusher	C	12.8	3.0	12.3	3.3	2.70	380	141
" "	EMR	8.4	2.7	7.6	3.7	1.53	380	248
Cone Crusher	C	5.4	2.6	5.7	2.8	0.84	190	226
" "	EMR	6.6	2.4	6.2	3.4	0.86	270	314
Screens	C	5.3	2.3	5.8	2.6	1.69	390	231
"	EMR	6.2	2.4	5.7	3.[illegible]	1.49	520	349
Top Fine Ore Bin/	C	4.0	3.3	4.0	3.3	0.30	180	600
Conveyor Belt	EMR	3.7	4.5	4.1	3.5	0.37	230	605
" "	EMR	3.4	2.8	3.8	3.1	0.08	100	1250
Grinding	EMR	-	-	3.7	5.8	-	48	-
"	M_2	-	-	10.0	2.3	-	59	-
Yellowcake Packaging	C	10.2	3.1	11.1	3.5	12.43	1.3×10^5	1.05×10^4
" "	EMR	12.3	3.7	11.8	2.6	6.21	1.25×10^5	2.01×10^4

Notes: a) C and EMR are Sierra impactors. M_2 is a Marple impactor

b) σg represents geometric standard deviation.

c) S.A. indicates specific activity.

Table 3 - Cascade impactor data for several physico-chemical operations in a uranium mill.

Operation	Impactor	MMAD (μm)	Dust σg	AMAD(LLRD) (μm)	LLRD σg	Dust Conc. (mg/m^3)	LLRD Conc. (mBq/m^3)	LLRD(S.A.) (mBq/mg)
Acid Leaching	C	6.9	2.4	6.6	3.5	0.30	252	840
" "	C	7.4	2.8	9.5	4.0	0.23	181	787
Counter-Current Decantation (CCD)	EMR	8.3	3.0	10.2	3.6	0.40	266	665
"	M_1	-	-	12.8	1.7	-	394	-
"	M_2	-	-	10.5	1.8	-	371	-
	M_1	-	-	13.1	1.8	-	160	-
Solvent Extraction	EMR	4.5	5.3	2.9	3.7	0.06	39	650
" "	M_2	-	-	3.8	3.9	-	31	-
Yellowcake Precip.	C	7.0	4.0	16.2	3.8	0.34	2110	6206
" "	EMR	9.0	2.8	13.2	3.6	0.31	1890	6097
" "	C	5.4	6.3	9.0	4.7	0.30	134	447
" "	M_1	-	-	13.2	1.8	-	106	
" "	C	4.0	3.8	6.6	4.9	0.06	35	583
Yellowcake Packaging	C	10.5	3.1	11.1	3.5	12.43	1.30×10^5	1.05×10^4
" "	EMR	12.3	3.7	11.8	2.6	6.21	1.25×10^5	2.01×10^4

Notes: a) C and EMR are Sierra impactors; M_1 and M_2 are Marple impactors.

b) σg represents geometric standard deviation.

c) S.A. indicates specific activity.

d) Yellowcake packaging data have been included for completeness.

Table 4 - Data for several mining operations.

Mining Operation	AMAD*(σg)	MMAD*(σg)	[LLRD] (mBq/m^3)	Total Dust (mg/m^3)	Quartz Dust (mg/m^3)	[Dust]$^+_{CI}$ (mg/m^3)	Specific Activity (mBq/mg)
Ore transportation (Conveyor belt)	4.79 (2.79)	3.97 (2.85)	83.72±20.7	0.53	0.24	1.05	78.72
Rock Crushing (Crusher platform)	5.30 (2.84)	4.40 (2.90)	126.30±25.1				
Rock Crushing (mechanics workbench)	4.90 (3.18)	2.40 (5.40)	34.90±17.8				
Dust Discharge (gallery)[1]	4.00 (2.50)		238.6				
Air Filtering (filter/fan system)[2]	Uncertain	0.11 (7.34)	very low				

* in μm.

\+ from cascade impactor (C.I.) measurements.

[1] Dust discharge from a rock breaking/conveyor belt transportation operation (airflow rate: 1.64 m^3/s).

[2] COGEMA fan/filter system (measurements after air filtering).

Table 5 - Dust and radioactive dust data taken in several underground uranium mines.

Date	[U] ($\mu g/m^3$)	[Th] ($\mu g/m^3$)	RD (mg/m^3)	SD (mg/m^3)	CD (mg/m^3)	[Ra-226]* (mBq/m^3)
Dec 1/83	3.11±0.3	<0.43	-	-	-	10.12±1.47
Dec 15/83	-	-	1.05±0.3	0.12±0.02	0.93±0.3	-
Dec 21/83	-	-	1.69±0.4	0.04±0.04	1.65±0.4	-
Jan 4/84	-	-	1.94±0.5	0.10±0.03	1.74±0.5	-
Nov 1/84	0.72±0.01	0.32±0.03	-	-	-	6.71±0.71
Nov 2/84	0.81±0.01	0.18±0.02	-	-	-	4.79±0.48
Average:	0.77**	0.25**	1.56	0.07	1.41	5.75**

Remark: The square brackets stand for concentration. RD, SD and CD stand, respectively, for total respirable dust, silica dust and combustible dust. The values given are averages from a substantial number of samples.

*Ra-226 is given in α-activity concentration.

**Average from Nov. 84 data taken at the same location.

Table 6 - Effect of dust abatement methods on AMAD, MMAD and [LLRD].

Variable	Dust Abatement Method	% Reduction	Location
[LLRD]	Wet Scrubber	68.1	Crusher platform
		39.0	Mechanics workbench
		87.6	Crusher itself.
MMAD		63.6	Crusher platform
		54.2	Mechanics workbench
AMAD		48.1	Crusher platform
		47.1	Mechanics workbench.
MMAD	Electrostatic Precipitator	26.3-35.7	Downstream of precipitator
AMAD	" "	"	" " "
MMAD	Water Sprays	35.3	Downstream of spray
MMAD	No Water Spray	21.8*	" " "

*Reduction due to gravitational settling.

Table 7 - Effect of dust abatement method on MMAD*, AMAD* and [LLRD]*

Dust Abatement	System in Operation	Mining Operation	Mining Location	MMAD[3] (σg) (μm)	AMAD[3] (σg) (μm)	[LLRD] (mBq/m^3)
Wet Scrubber	No	Rock crushing	Crusher Platf.[1]	4.40 (2.90)	5.30 (2.84)	126.3±25.1
" "	No	" "	M.W.B.[2]	2.40 (5.40)	4.90 (3.18)	34.9±17.8
" "	Yes	" "	Crusher Platf.	1.60 (5.30)	2.75 (3.98)	40.3±14.4
" "	Yes	" "	M.W.B.	1.10 (6.50)	2.59 (4.21)	21.3±8.1
" "	Yes	" "	Crusher Platf.	--	2.50 (2.00)	226.0
" "	Yes	" "	M.W.B.	--	0.44 (3.01)	28.0
Electrostatic Precipitator	No[4]	Rock breaking/ ore transportation	Dust discharge exhaust gallery	3.76 (2.46)	3.20 (2.50)	163.4
"	Yes[5]	"	"	3.05 (2.41)	2.85 (2.40)	151.3
"	Yes[4]	"	"	3.04 (2.73)	3.20 (2.30)	123.0
Water Sprays	No[4]	"	"	3.76 (2.46)	3.20 (2.50)	163.4
" "	Yes[6]	"	"	3.12 (2.88)	3.55 (2.20)	139.6

[1] stands for platform

[2] stands for mechanics workbench

[3] measurements carried out with Sierra cascade impactors

[4,5,6] Airflow rate conditions: 0.61, 1.02, and 0.82-1.02 m^3/s, respectively.

* stands for Mass Median Aerodynamic Diameter (MMAD), Activity Median Aerodynamic Diameter (AMAD), and Long-Lived Radioactive Dust Concentration, [LLRD].

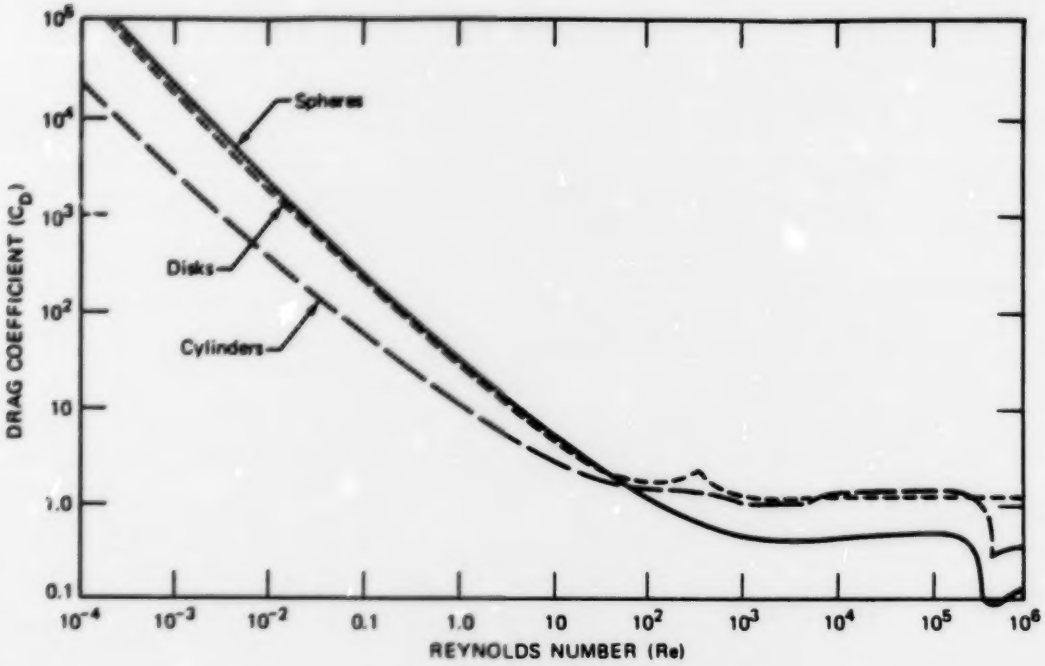

Fig. 1 - Drag coefficient versus Reynolds number for spheres, cylinders and disks.

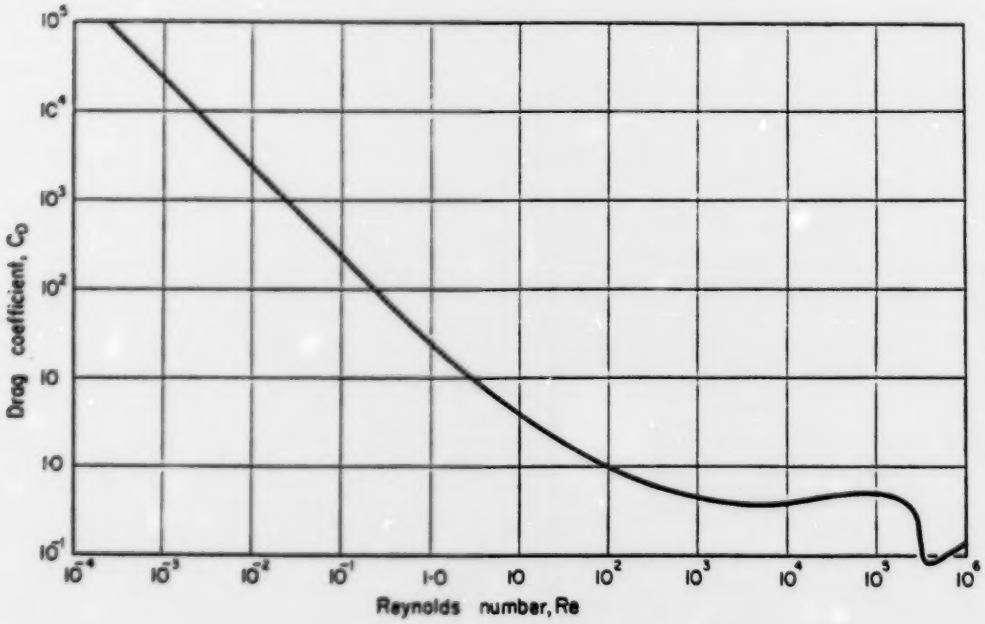

Fig. 2 - Drag coefficient versus Reynolds number.

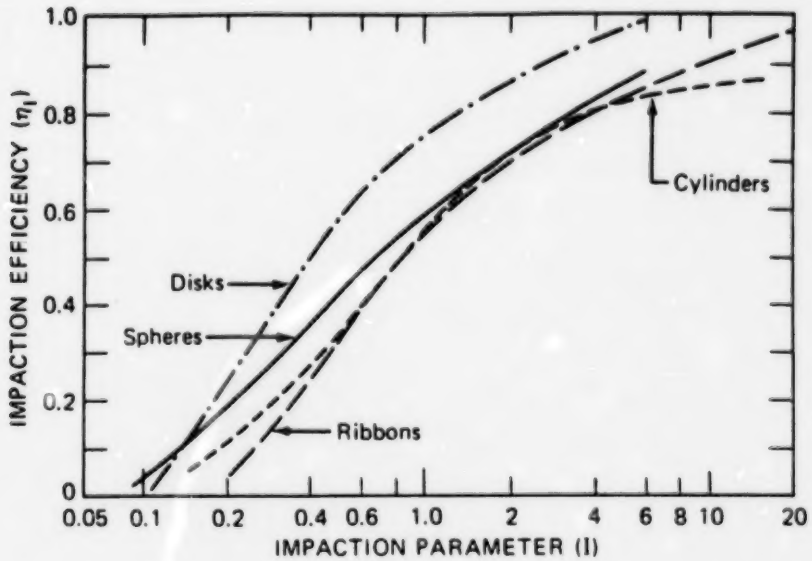

Fig. 3 - Impaction efficiencies for cylinders, spheres, ribbons, and disks.

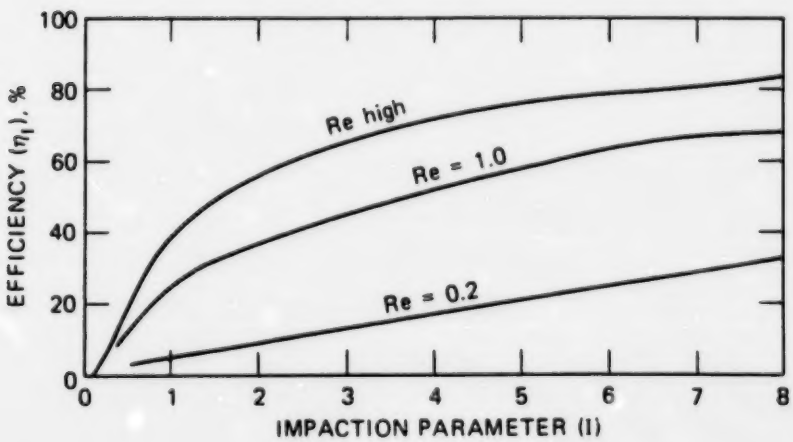

Fig. 4 - Theoretical impaction efficiency on cylinders at low Reynolds numbers.

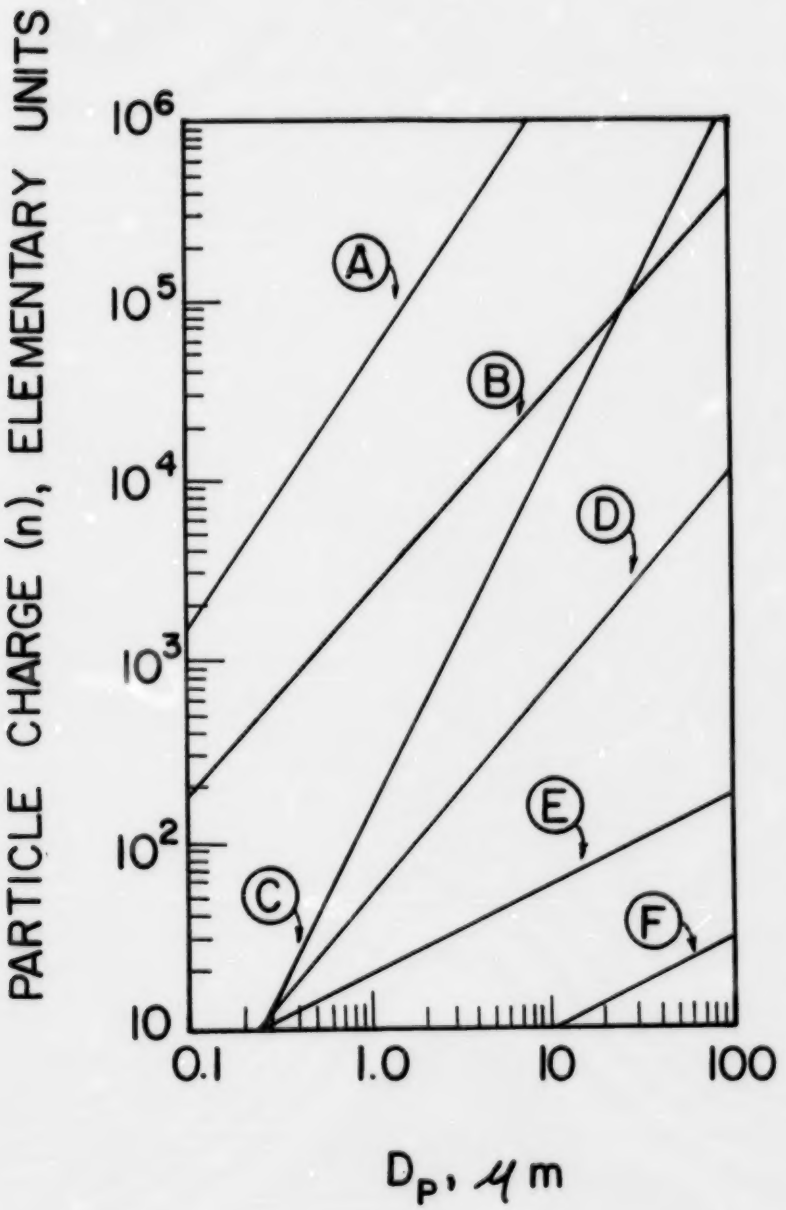

Fig. 5a - Particle electrical charge versus particle diameter: Rayleigh limit (A), contact charging (B), field charging (C), diffusion charging (D), maximum charge on atomized droplets (E), and charge for Boltzmann's equilibrium (F).

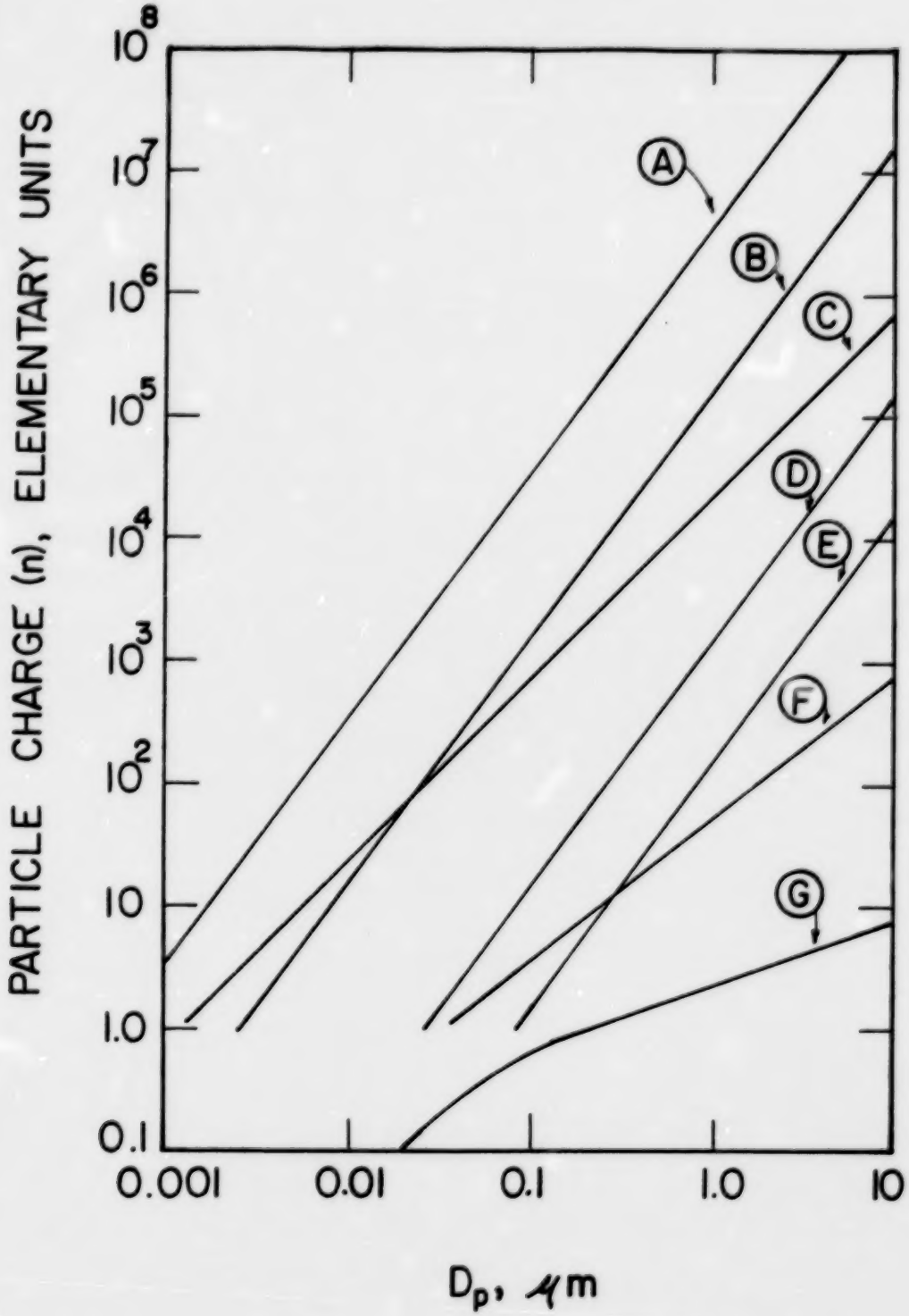

Fig. 5b - Particle electrical charge versus particle diameter for the ion limit (A), electron limit (B), Rayleigh limit (C), field charging (D) and (E), diffusion charging (F), and bipolar equilibrium (G).

NASAL INHALATION DEPOSITION

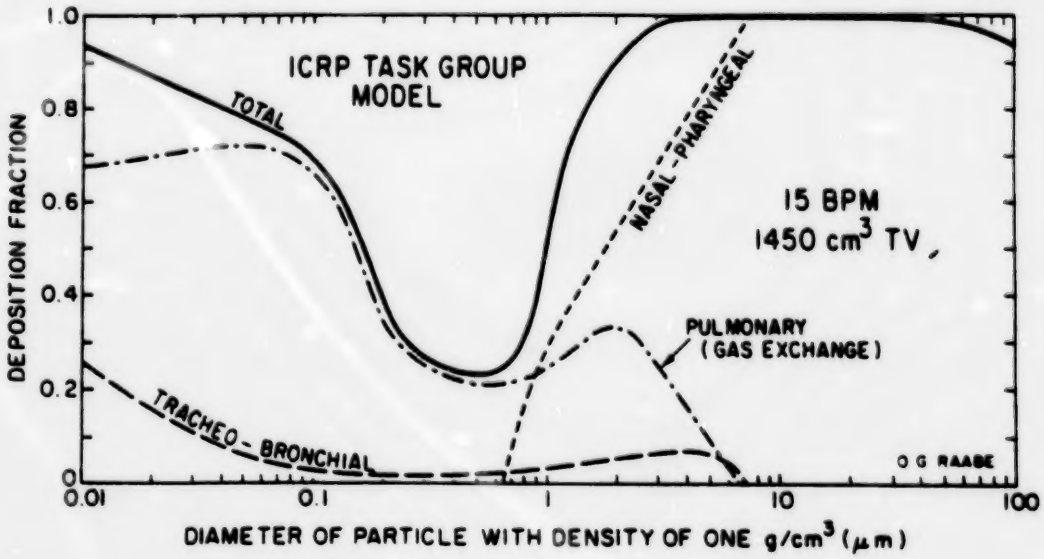

Fig. 6 - Total and regional deposition fractions for various sizes of inhaled airborne spherical particles with physical density of 1.0 g/cm^3 in the human respiratory tract as calculated by the International Commission on Radiological Protection (ICRP) Task Group on Lung Dynamics for nasal breathing at a rate of 15 breaths per minute (BPM) and tidal volume (TV) of 1450 cm^3.

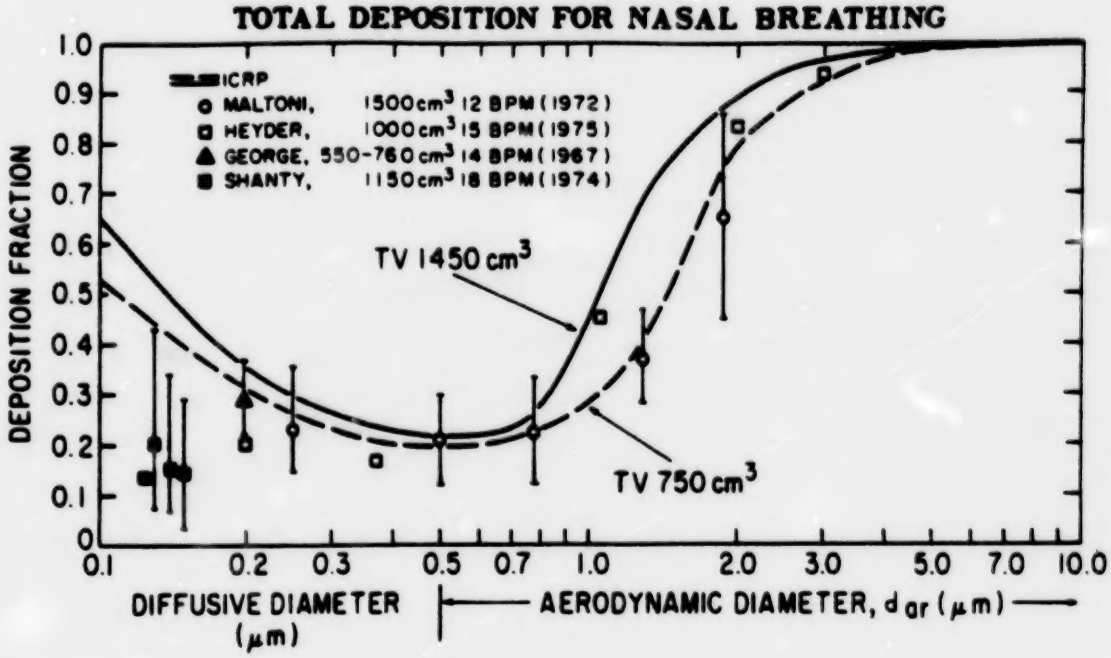

Fig. 7 - Selected data reported for the deposition in the entire respiratory tract of monodisperse aerosols inhaled by persons via the nose from Giacomelli-Maltoni et al., Heyder et al., George and Breslin, and Shanty, compared with predicted values calculated by the ICRP Task Group on Lung Dynamics for tidal volumes (TV) of 750 cm^3 (dashed line) and 1450 cm^3 (solid line).

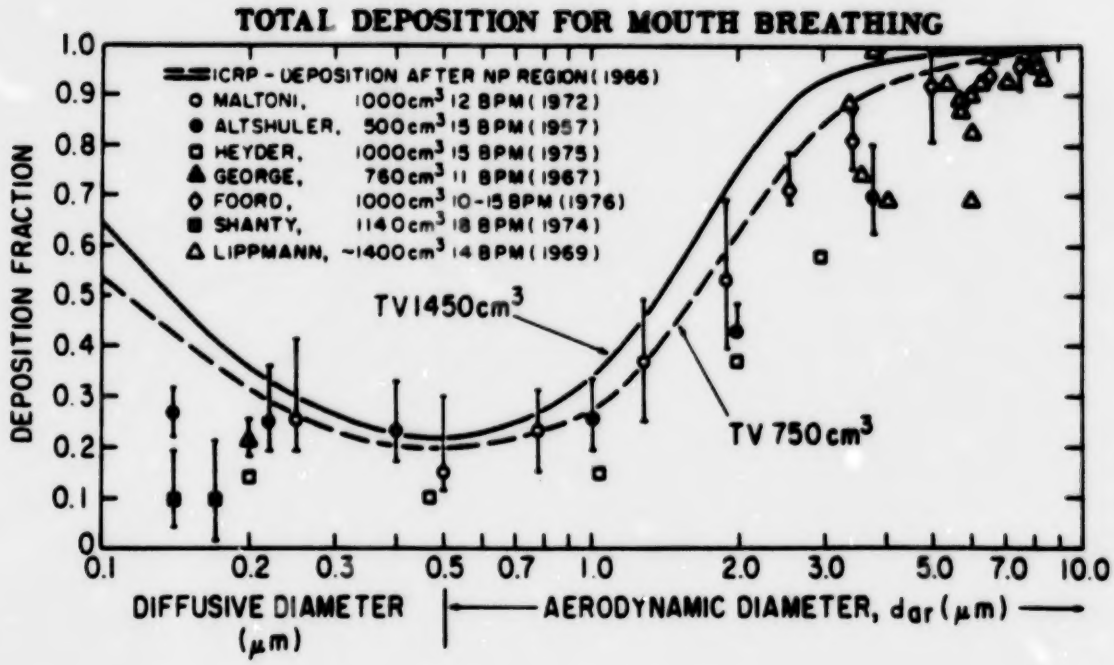

Fig. 8 - Selected data reported for the deposition in the entire respiratory tract of monodisperse aerosols inhaled by persons through the mouth from Giacomelli-Maltoni et al., Altshuler et al., Heyder et al., George and Breslin, Foord et al., Shanty, and Lippmann and Albert compared with predicted values calculated by the ICRP Task Group on Lung Dynamics for tidal volumes (TV) of 750 cm^3 (dashed line) and 1450 cm^3 (solid line).

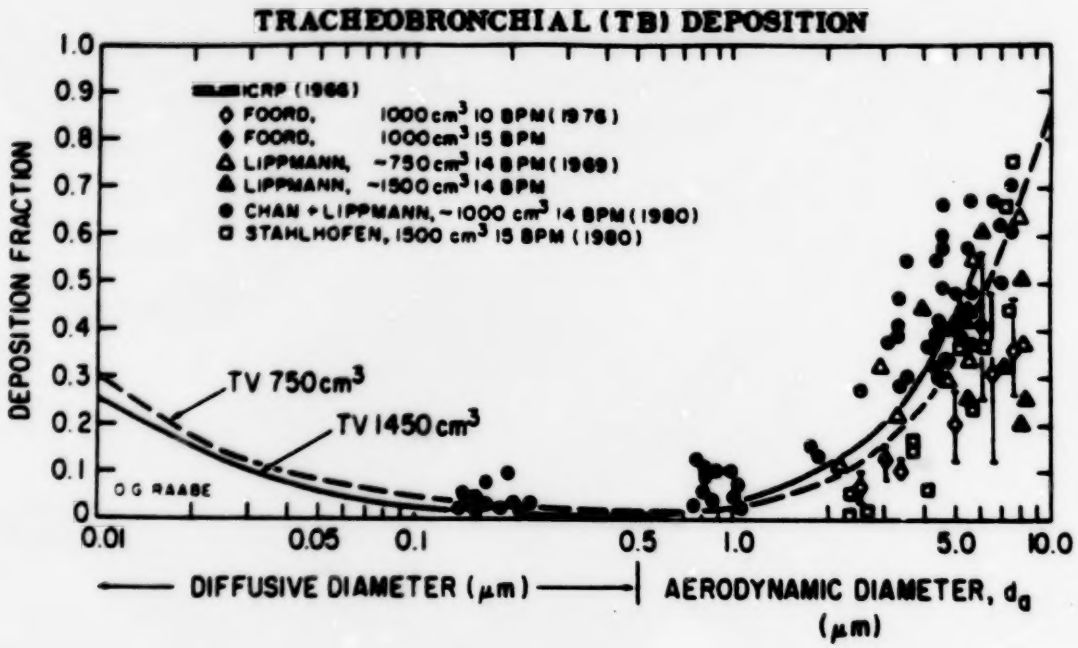

Fig. 9 - Selected data reported for the deposition in the human tracheobronchial region (TBR) as fraction of monodisperse aerosols entering the trachea reported by Foord et al., Lippmann and Albert, Chan and Lippmann, and Stahlhofen et al. compared with predicted values calculated by the ICRP Task Group on Lung Dynamics for tidal volumes of 750 cm^3 (dashed line) and 1450 cm^3 (solid line).

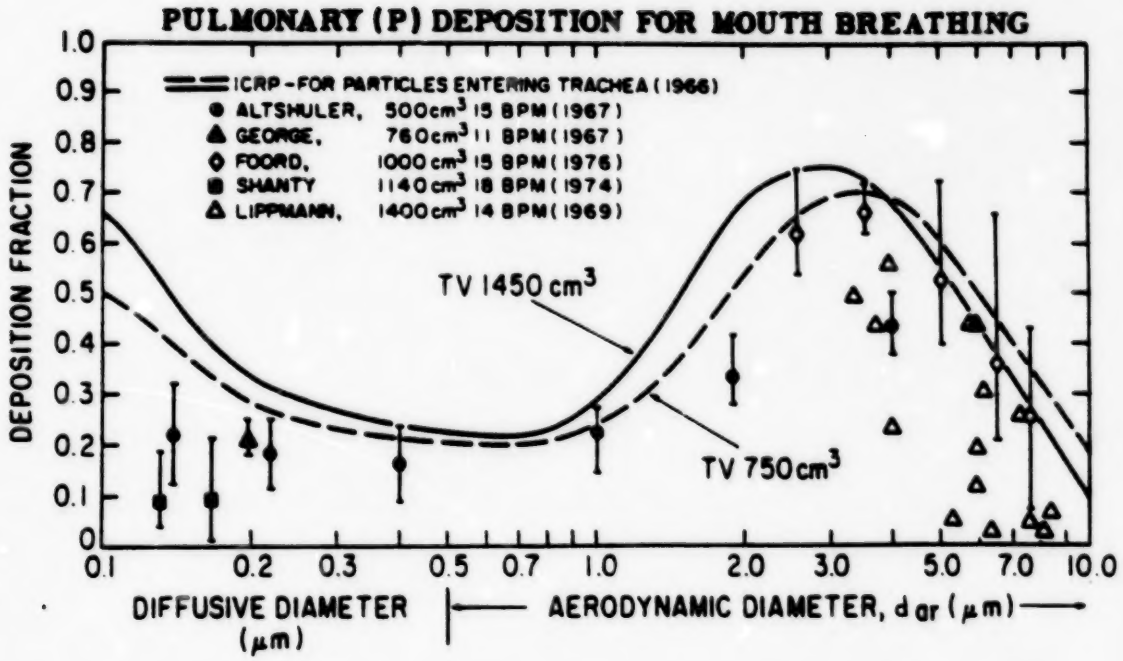

Fig. 10 - Selected data for pulmonary (P) gas exchange region (GER) deposition of monodisperse aerosols inhaled through the mouth by people reported by Altshuler et al., George and Breslin, Foord et al., Shanty, and Lippmann and Albert, compared with predicted values calculated by the ICRP Task Group on Lung Dynamics for tidal volumes (TV) of 750 cm^3 (dashed line) and 1450 cm^3 (solid line).

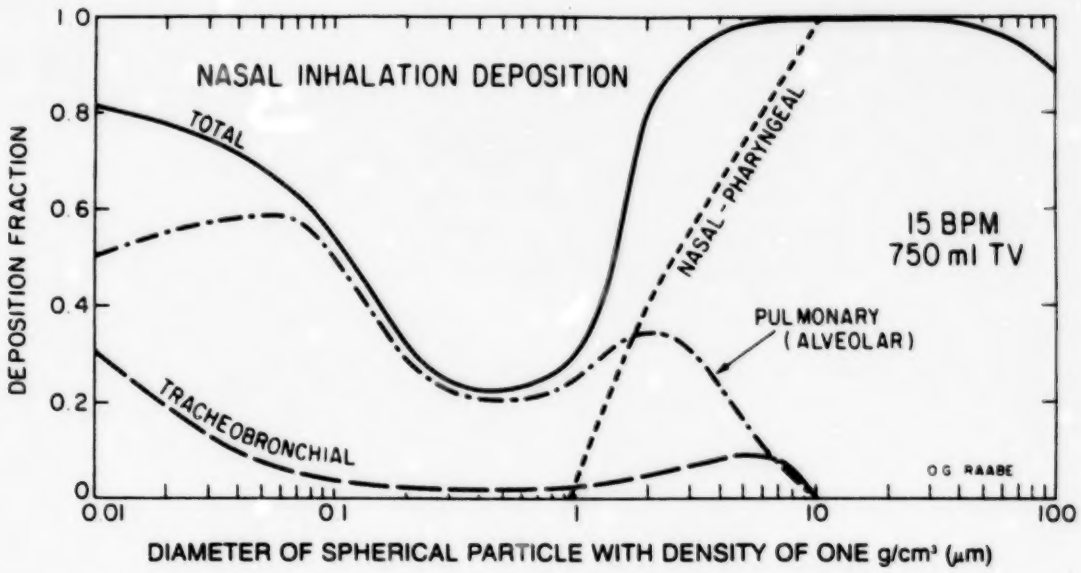

Fig. 11 - Nasal Inhalation Deposition: Total and regional deposition fractions for aerosols entering the nose for various sizes of inhaled airborne spherical particles with physical density of 1 g/cm^3 in the human respiratory tract as calculated by the International Commission on Radiological Protection (ICRP) Task Group on Lung Dynamics for nasal breathing at a rate of 15 breaths per minute (BPM) and tidal volume (TV) of 750 mL.

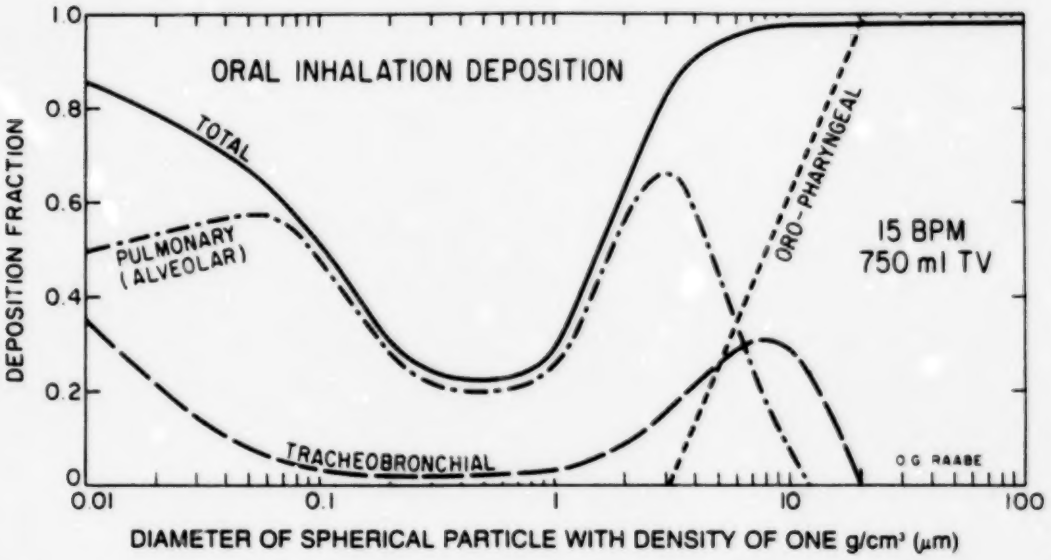

Fig. 12 - Oral Inhalation Deposition: Total and regional deposition fractions for aerosols entering the mouth for various sizes of inhaled airborne spherical particles with physical density of 1 g/cm^3 in the human respiratory tract as calculated by the International Commission on Radiological Protection (ICRP) Task Group on Lung Dynamics with the head airway deposition function given by Raabe for oral breathing at a rate of 15 breaths per minute (BPM) and tidal volume (TV) of 750 mL.

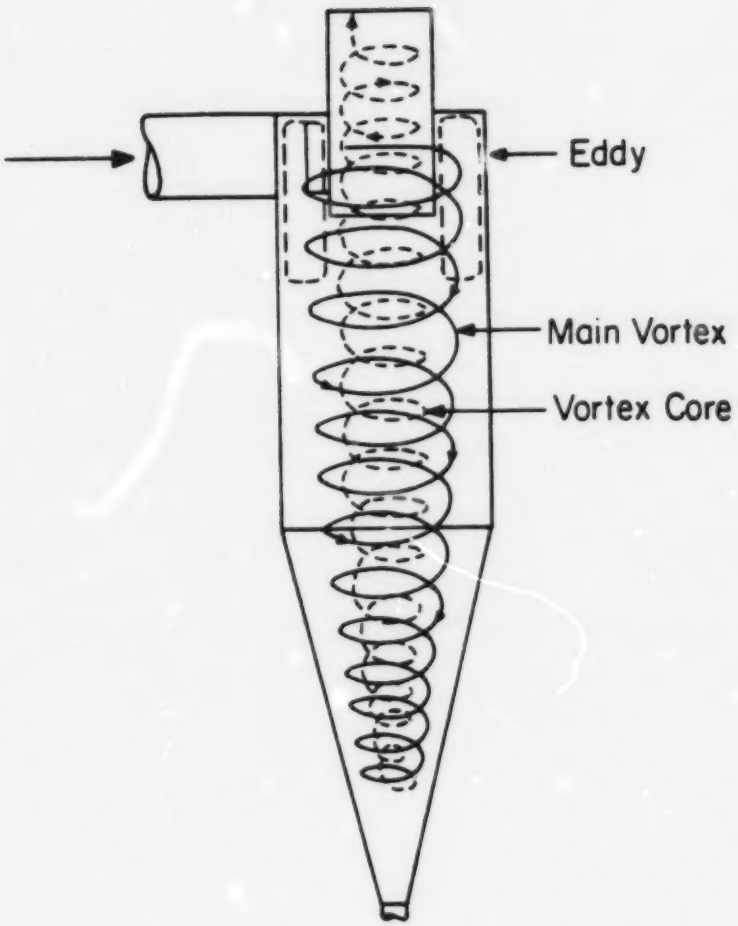

Fig. 13 - Flow patterns in a cyclone collector.

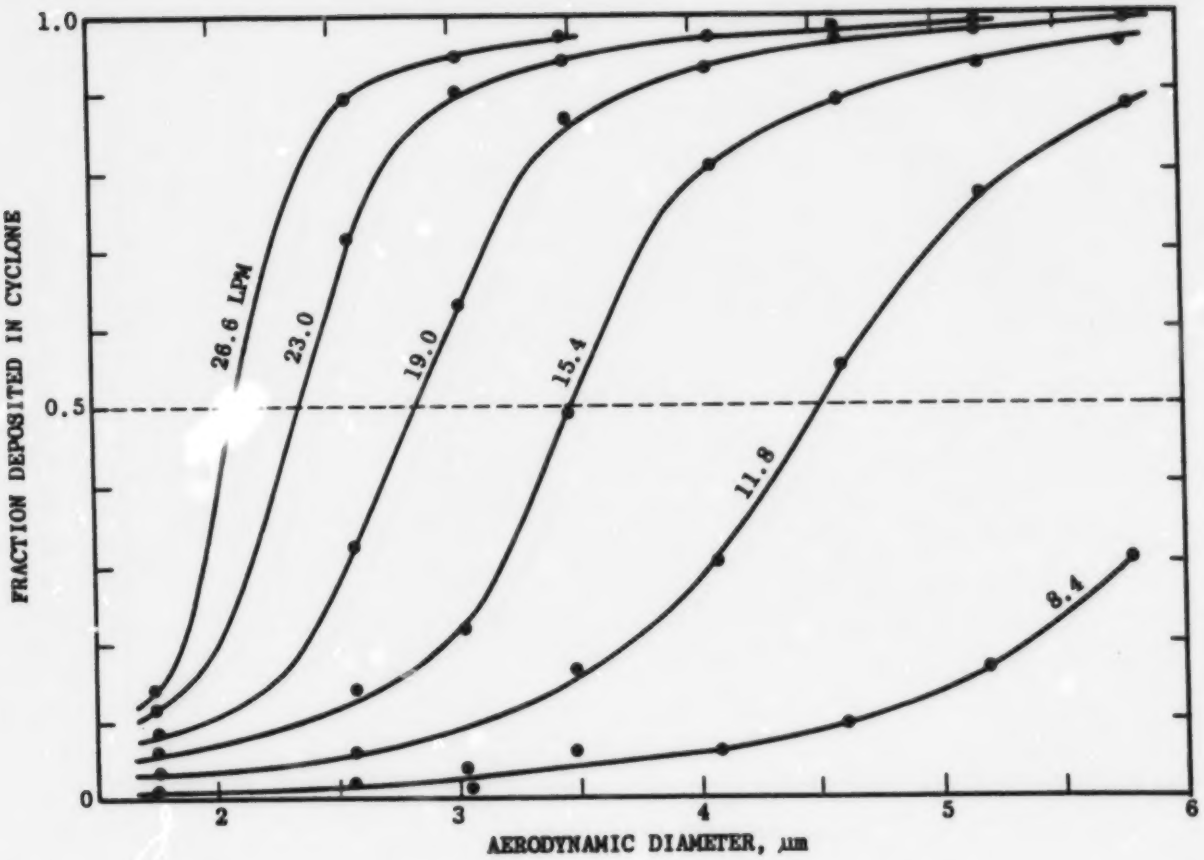

Fig. 14 - Fraction of solid particles deposited in the AIHL cyclone as a function of particle aerodynamic diameter. The curves are labelled with the flow rate.

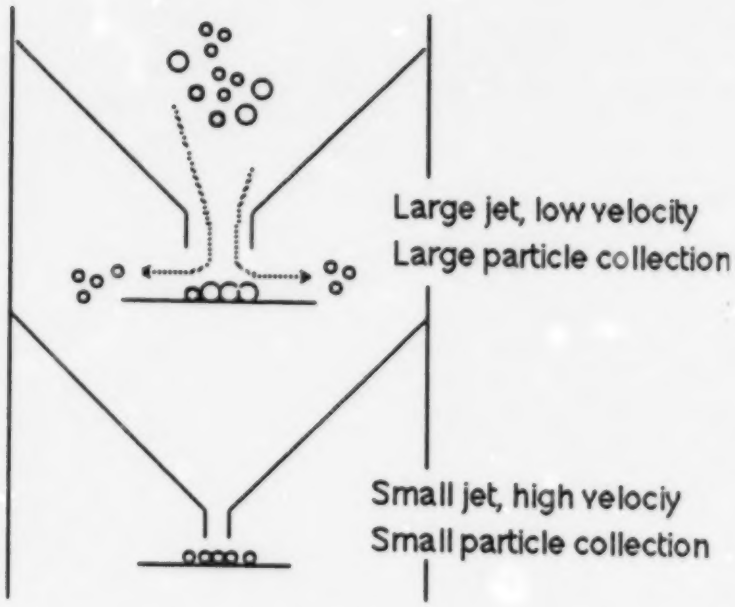

Fig. 15 - Schematic of two impactor stages showing large and small particle trajectories.

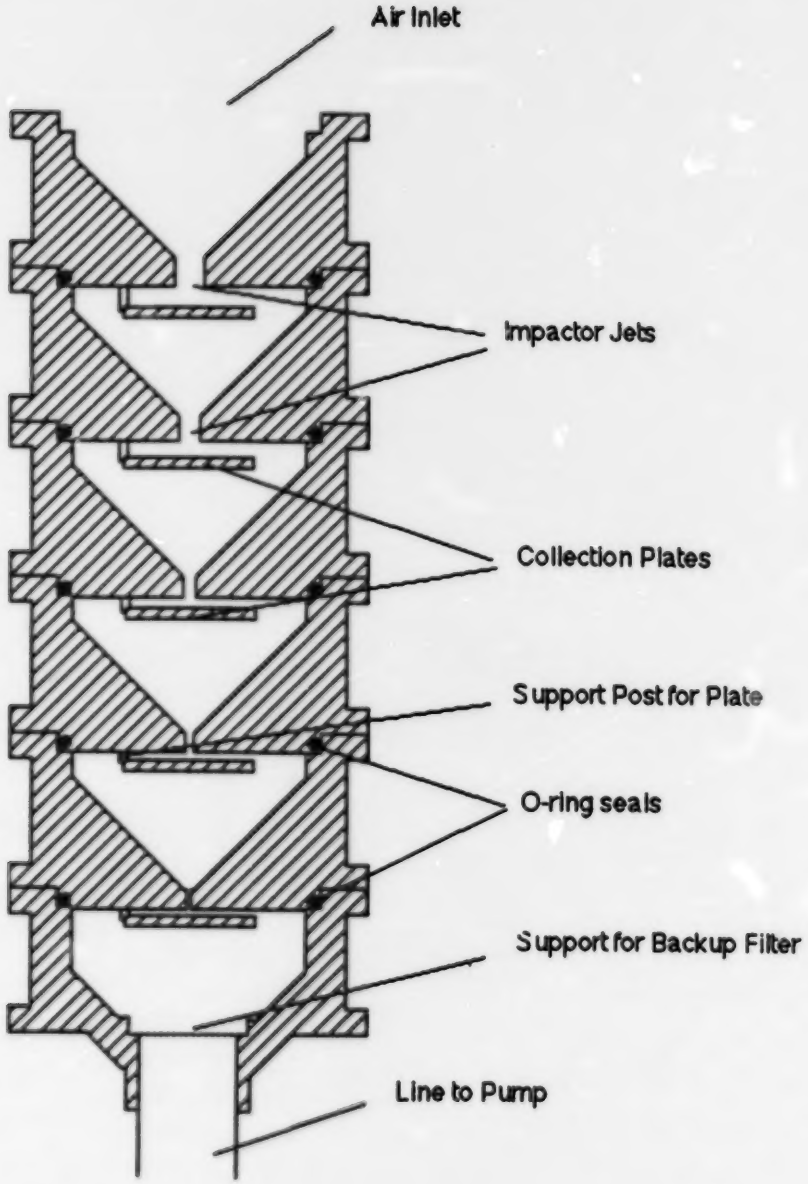

Fig. 16 - A single-jet, five-stage cascade impactor.

Fig. 17 - Sierra/Marple Series 210 Ambient Cascade Impactor.

Fig. 18 - Marple personal sampler, Series 290.

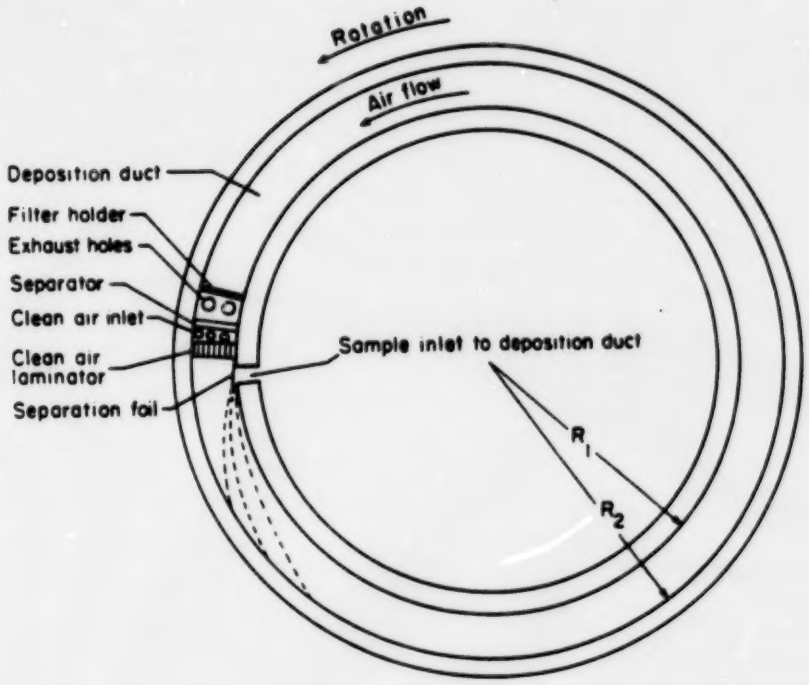

Fig. 19 - Top view of a cylindrical duct aerosol centrifuge with particle trajectories shown by dashed lines.

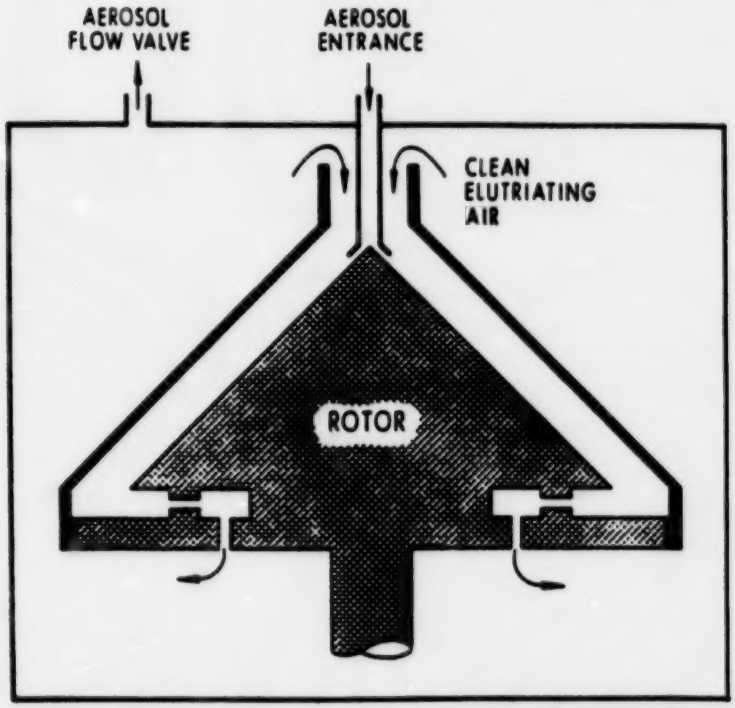

Fig. 20 - Schematic of the conifuge.

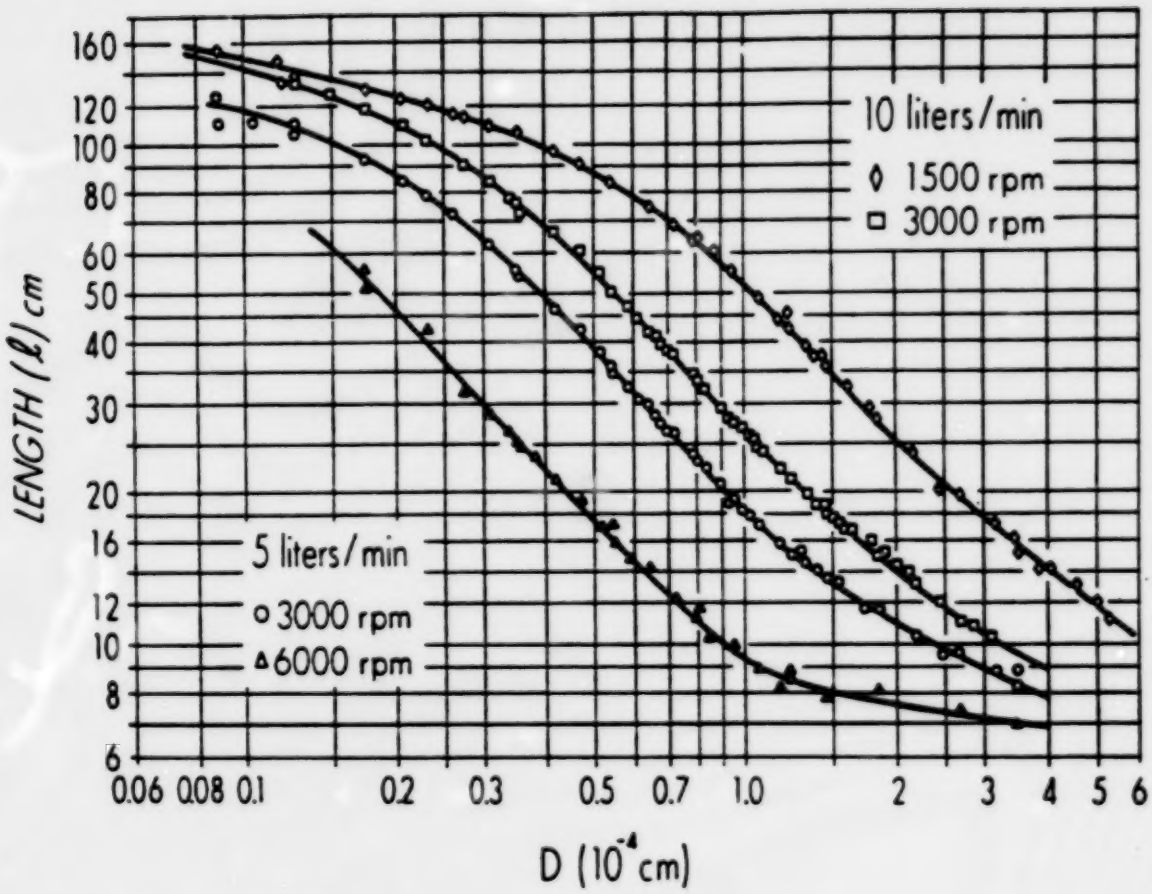

Fig. 21 - Calibration curves for the Stober spiral duct centrifuge at different rotation rates and at different total flow rates. Total flow refers to both aerosols sample flow plus the particle-free sheath air flow.

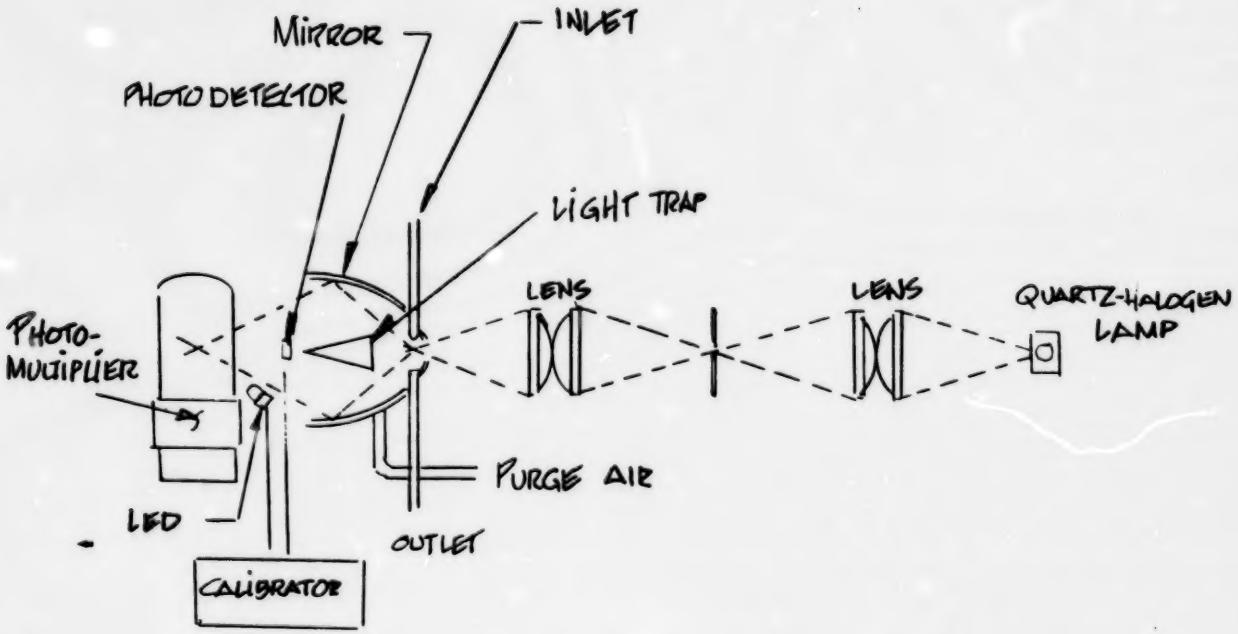

Fig. 22 - CLIMET Model CI-7300 optical particle counter optical system.

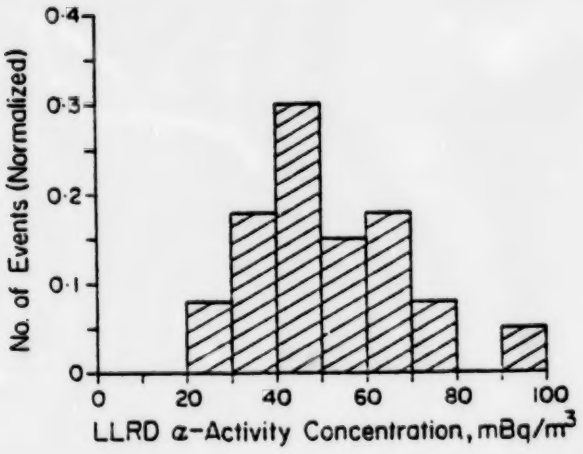

Fig. 23a - LLRD α-activity concentration in mine air. Same general area of an U/G U-mine collected over several months, Elliot Lake Laboratory.

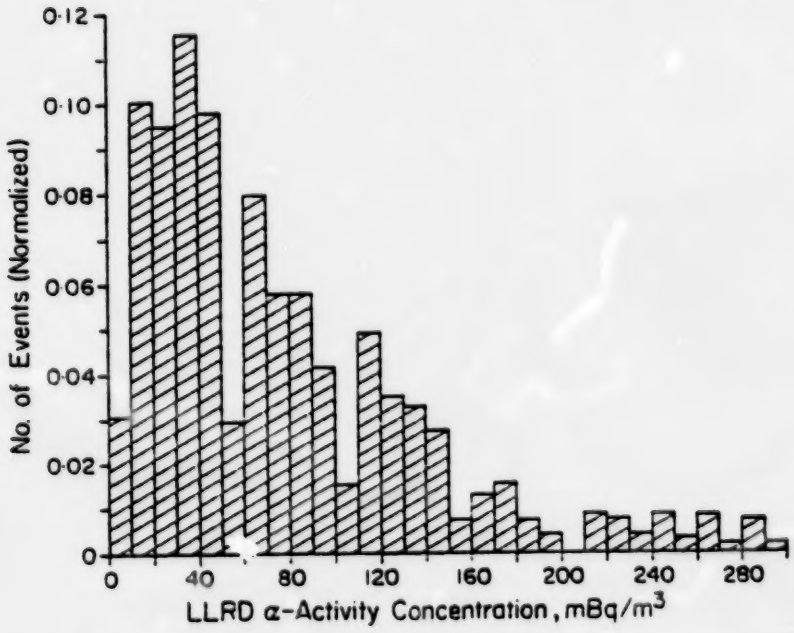

Fig. 23b - LLRD α-activity concentration in mine air. Different mines, different locations (taken over two years), Elliot Lake Laboratory.

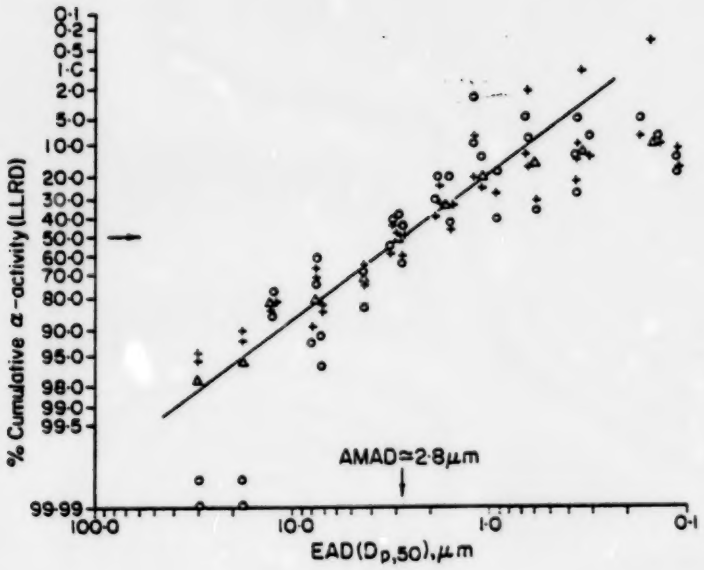

Fig. 24 - Percentage (%) cumulative LLRD α-particle activity corresponding to dust of size $<D_{p,50}$ versus EAD for several independent measurements by cascade impactors.

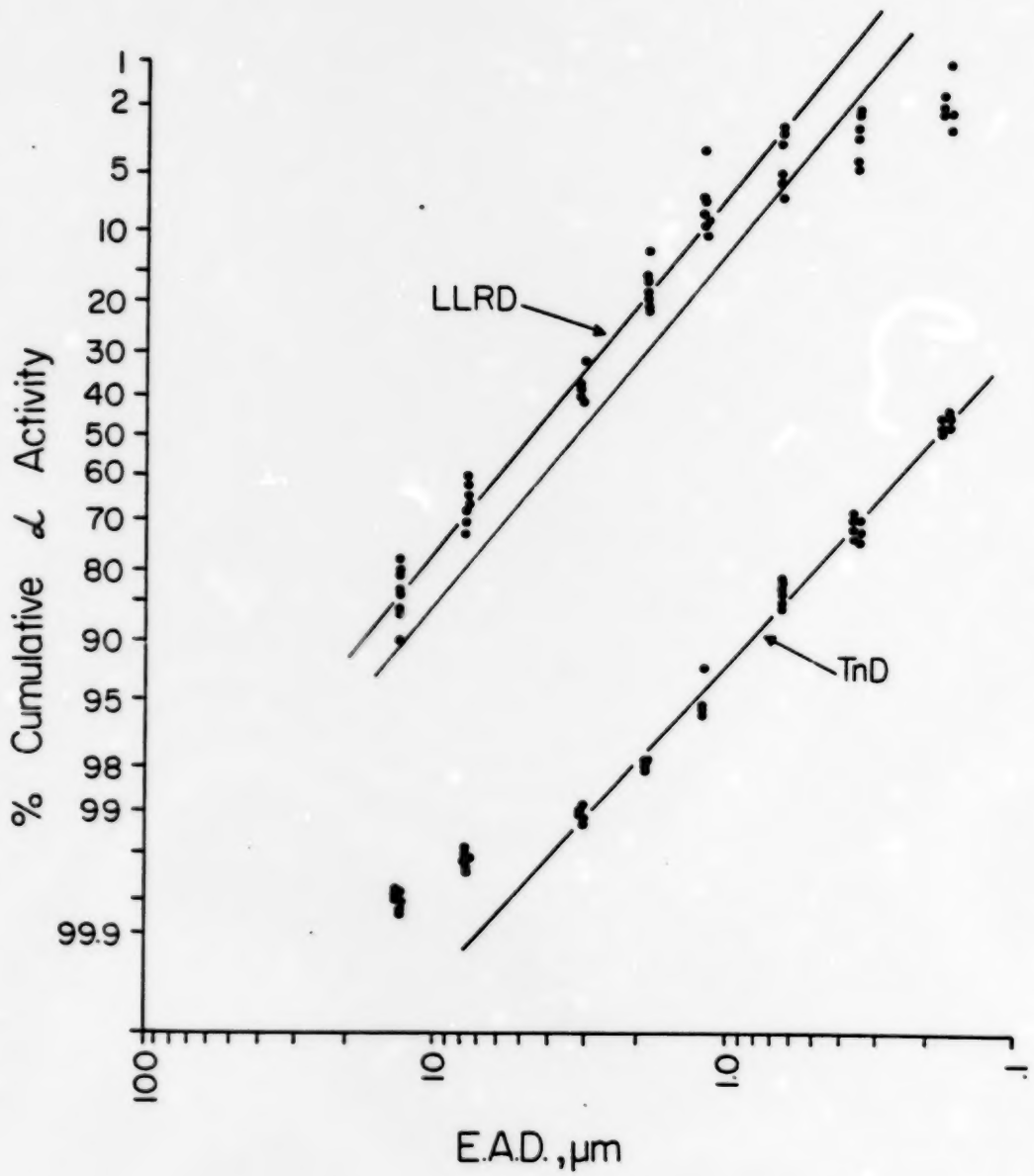

Fig. 25 - Cumulative α-particle activity versus Equivalent Aerodynamic Diameter (EAD) for long-lived radioactive dust (LLRD) and thoron progeny (TnD), for different days. (Conveyor Belt).

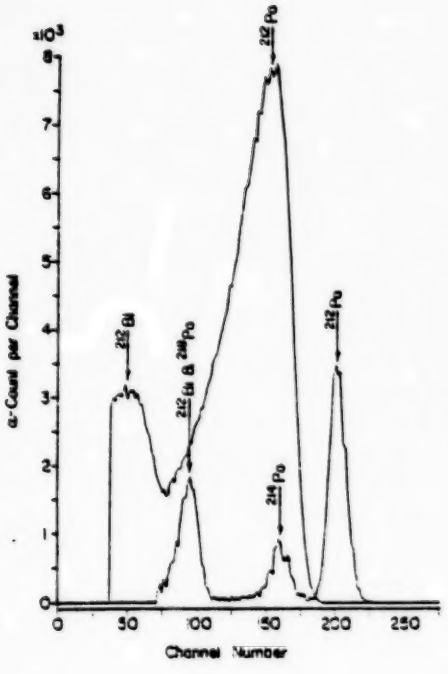

Fig. 26a - TnD α-spectrum from a radioactive dust sample. Also shown is the α-spectrum from a RnD + TnD reference source.

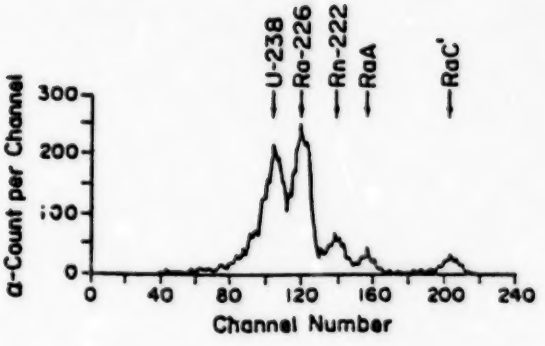

Fig. 26b - LLRD α-spectrum from a radioactive dust sample from U/G U-mine (tentative identification). Silicon barrier detector, under vacuum.

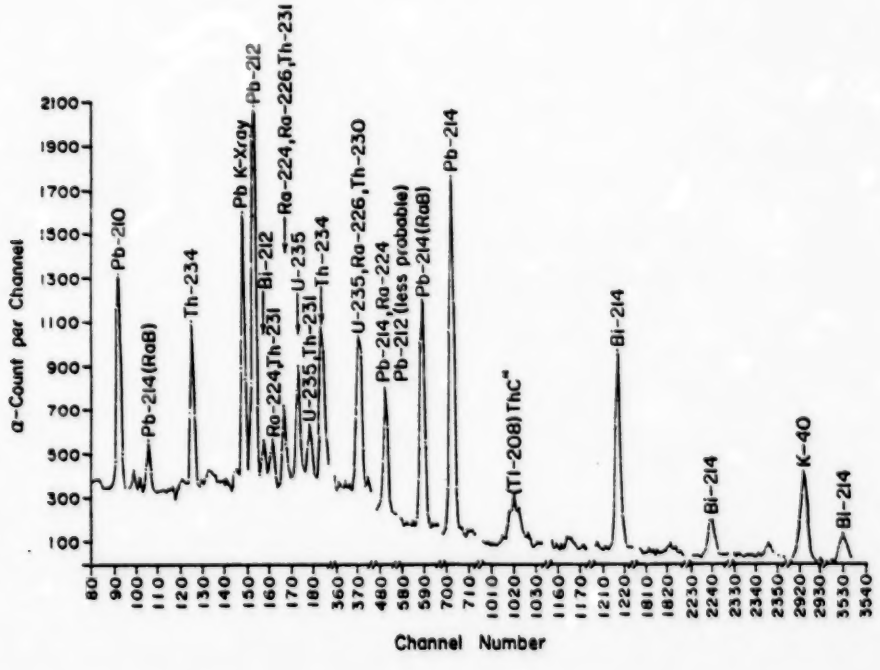

Fig. 26c - LLRD γ-spectrum, taken with a HPGe, from a radioactive dust sample.

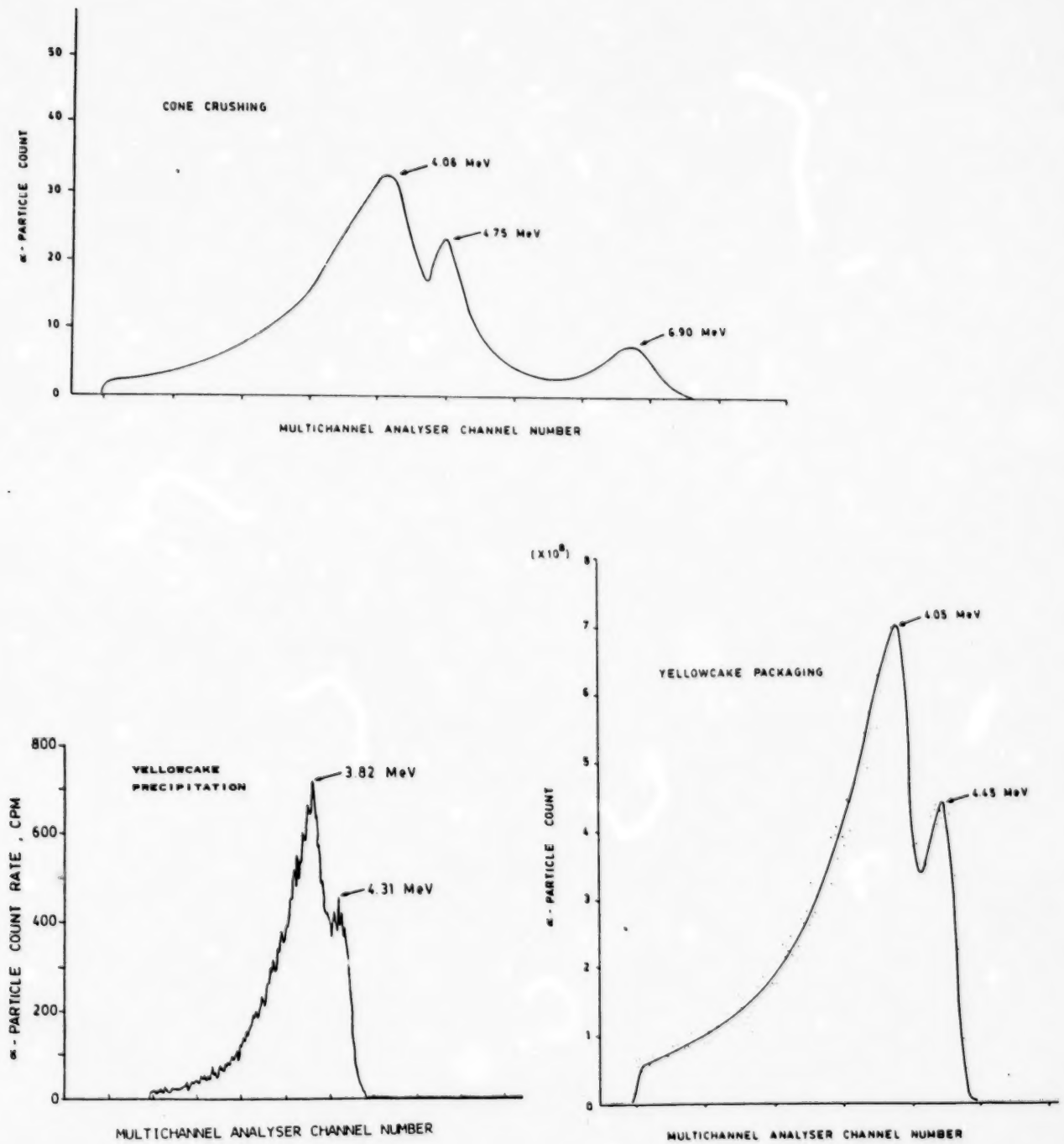

Fig. 27 - Alpha-particle spectra corresponding to different mill operations.

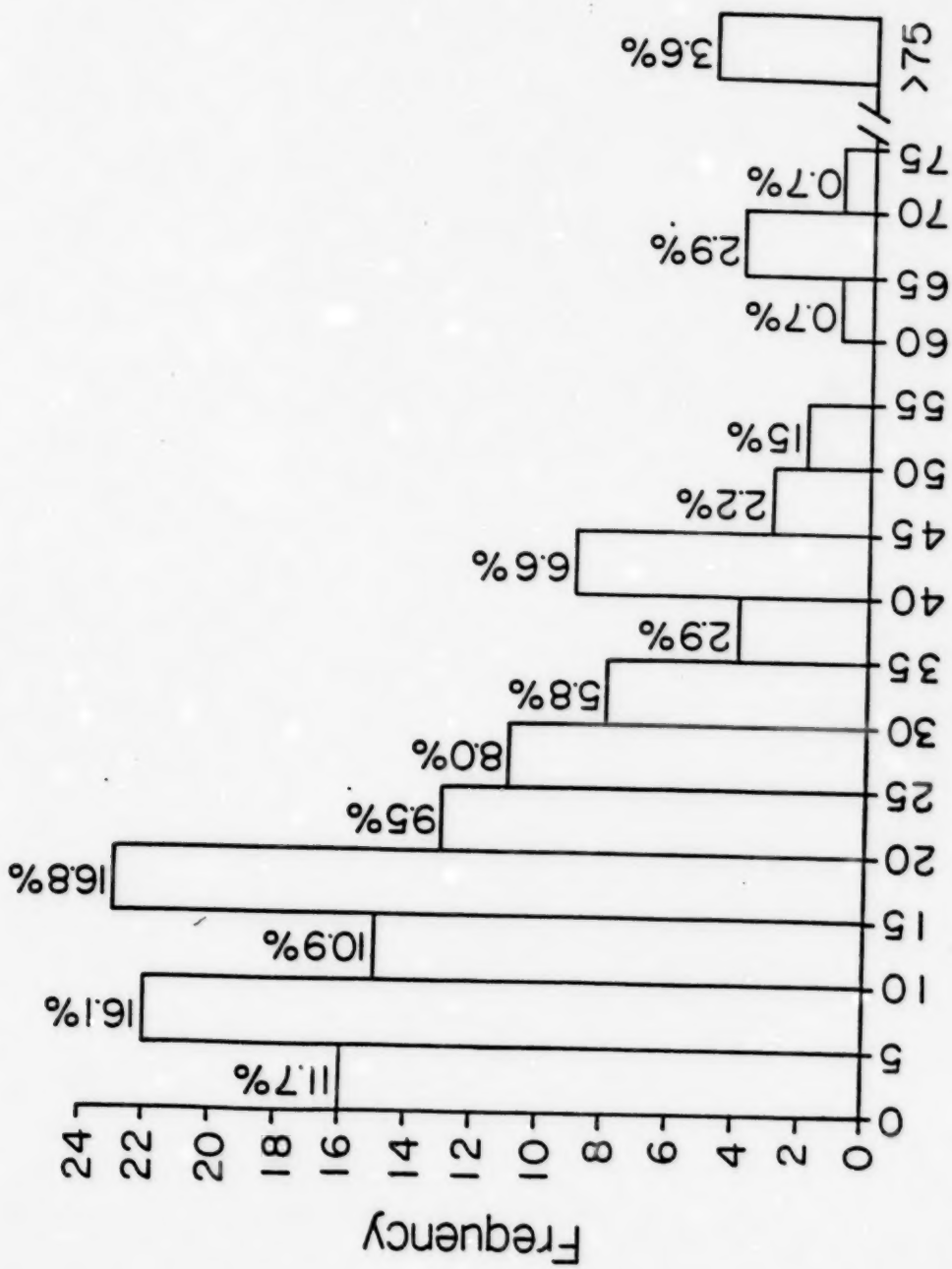

Fig. 28 - Frequency (distribution) versus α-particle activity concentration for LLRD samples collected in an U/C U-mine. Also shown are the frequency percentages of the total number of measurements (Mine A).

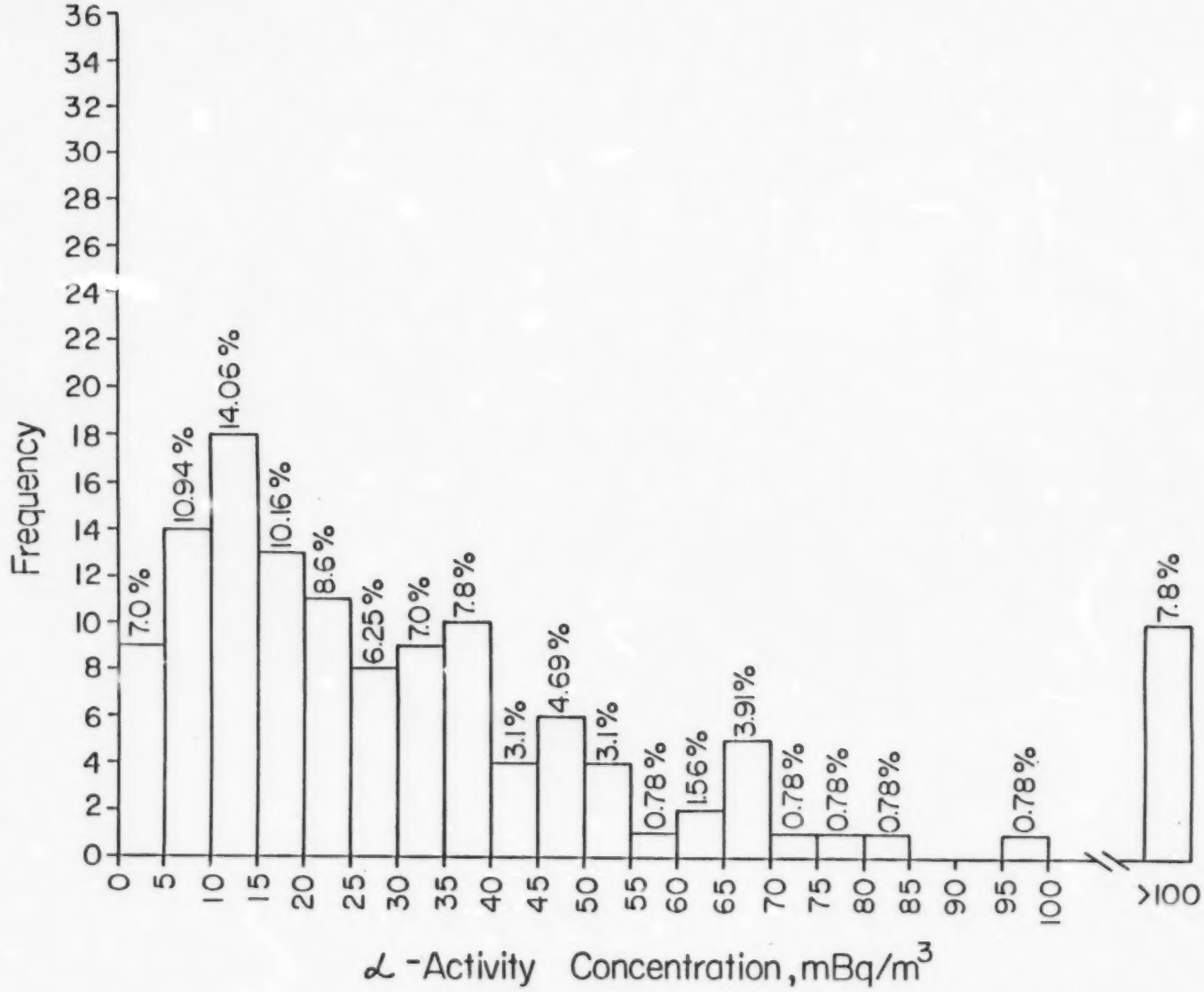

Fig. 29 - Frequency (distribution) versus α-particle activity concentration for LLRD samples collected in an U/G U-mine. Also shown are the frequency percentages of the total number of measurements (Mine B).

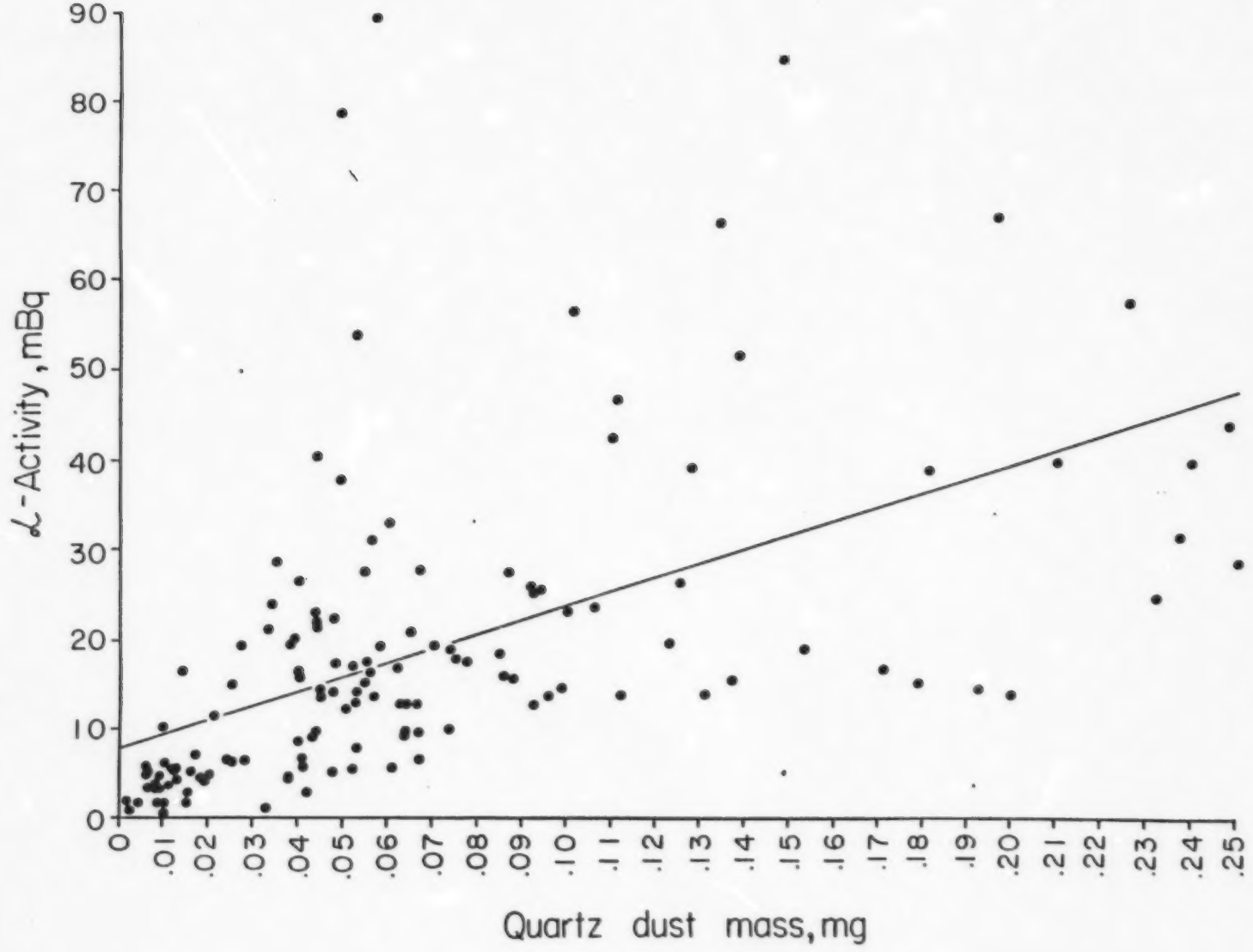

Fig. 30 - LLRD α-particle activity versus quartz dust mass for the period 1983-1985 (Mine A).

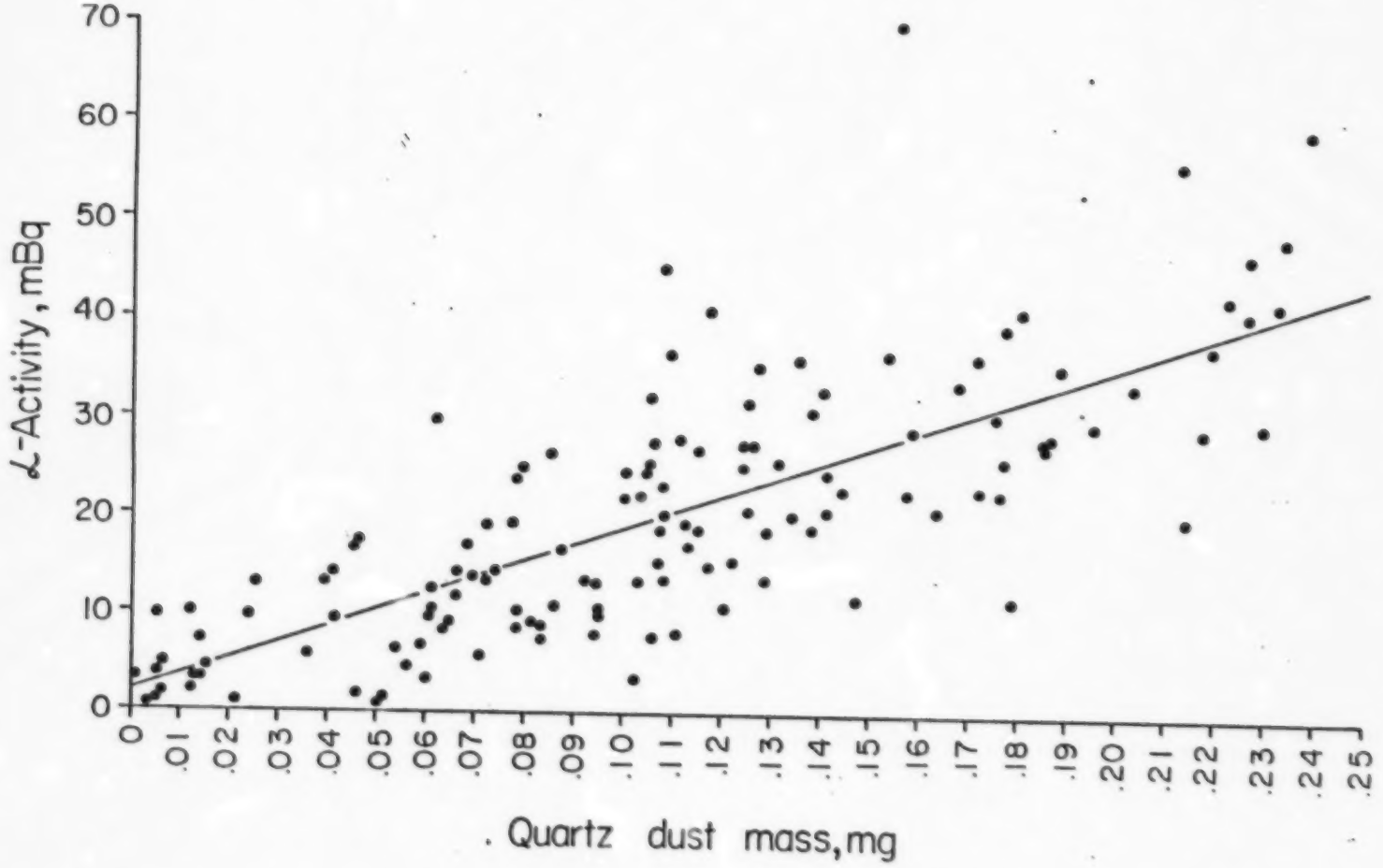

Fig. 31 - LLRD α-particle activity versus quartz dust mass for the period 1983-85 (Mine B).

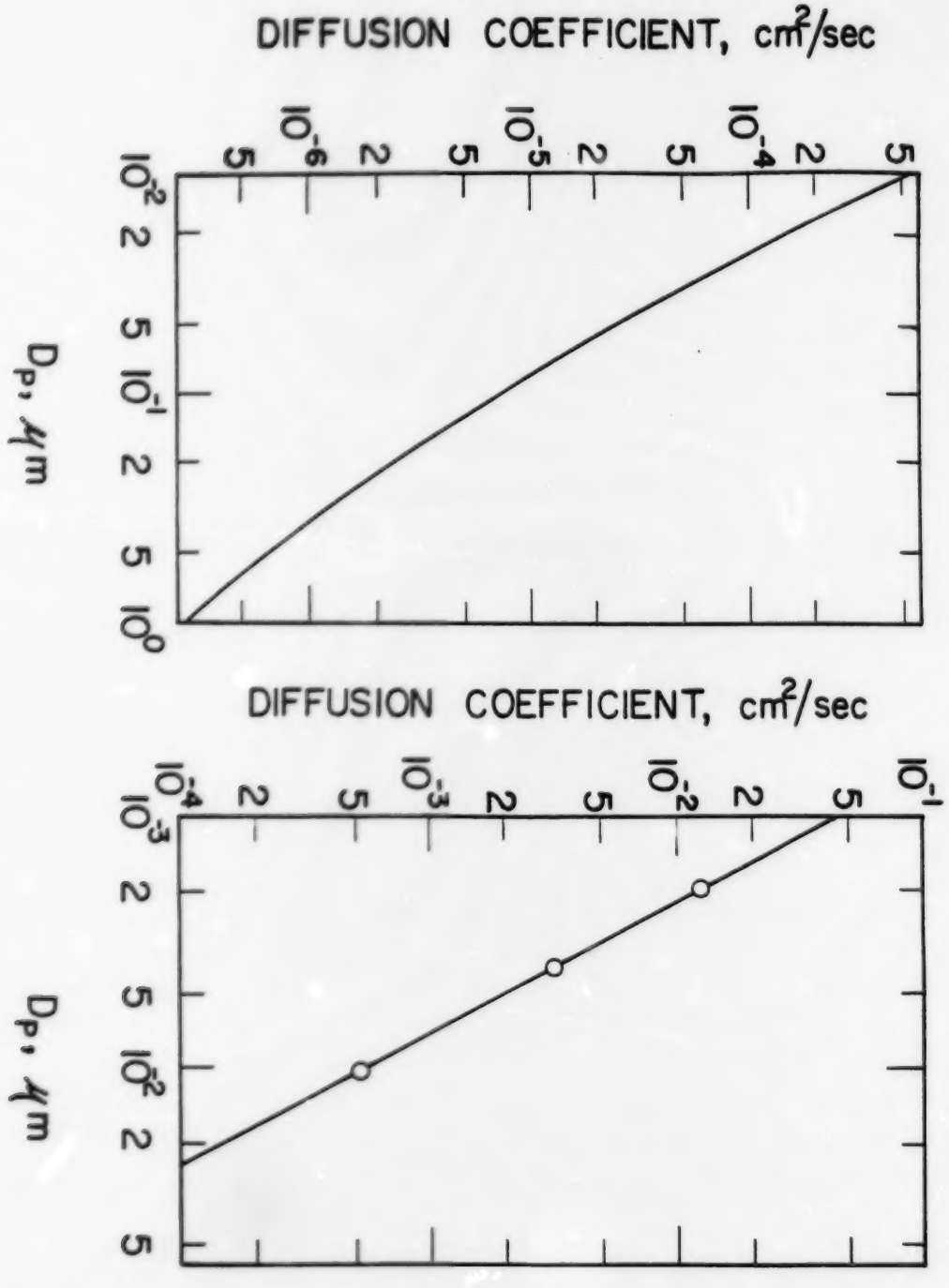

Fig. 32 - Diffusion coefficient for particles of diameter Dp.

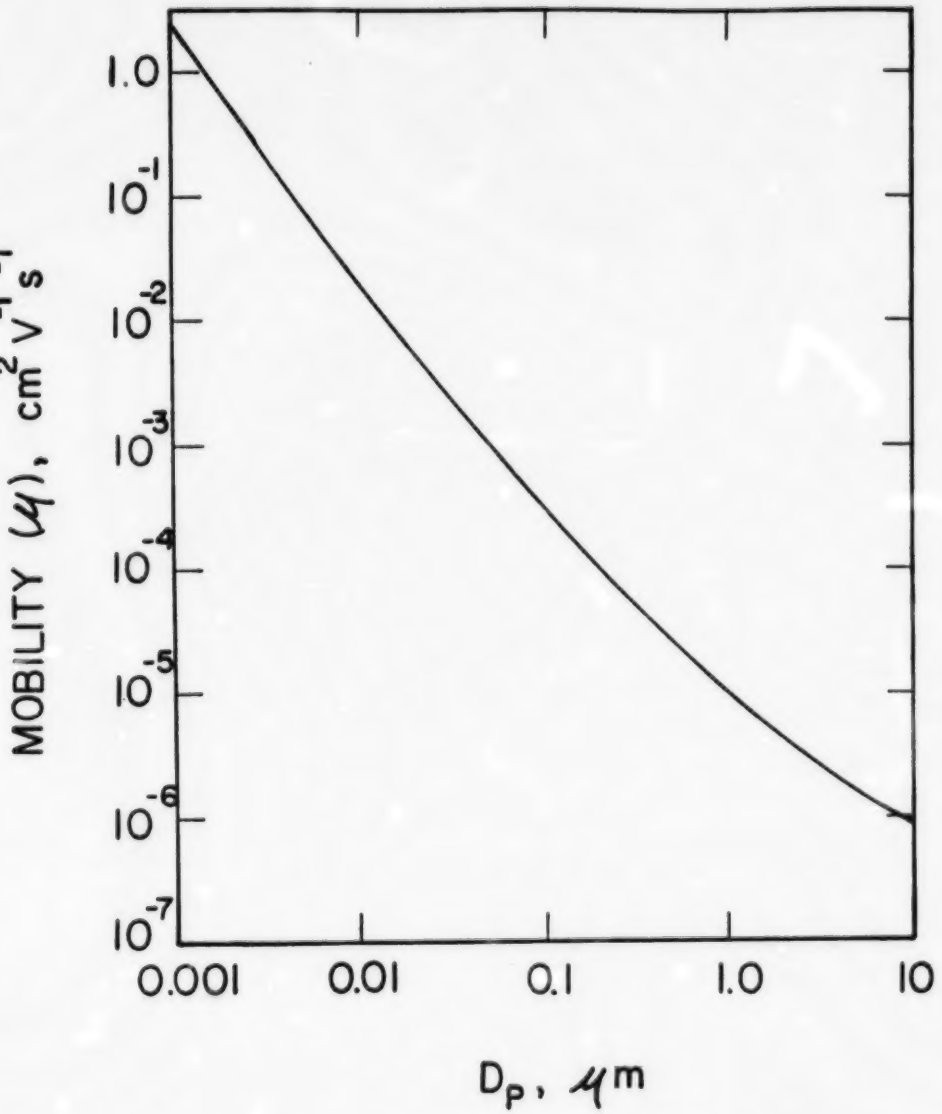

Fig. 33 - Electrical mobility for particles of diameter D_p.

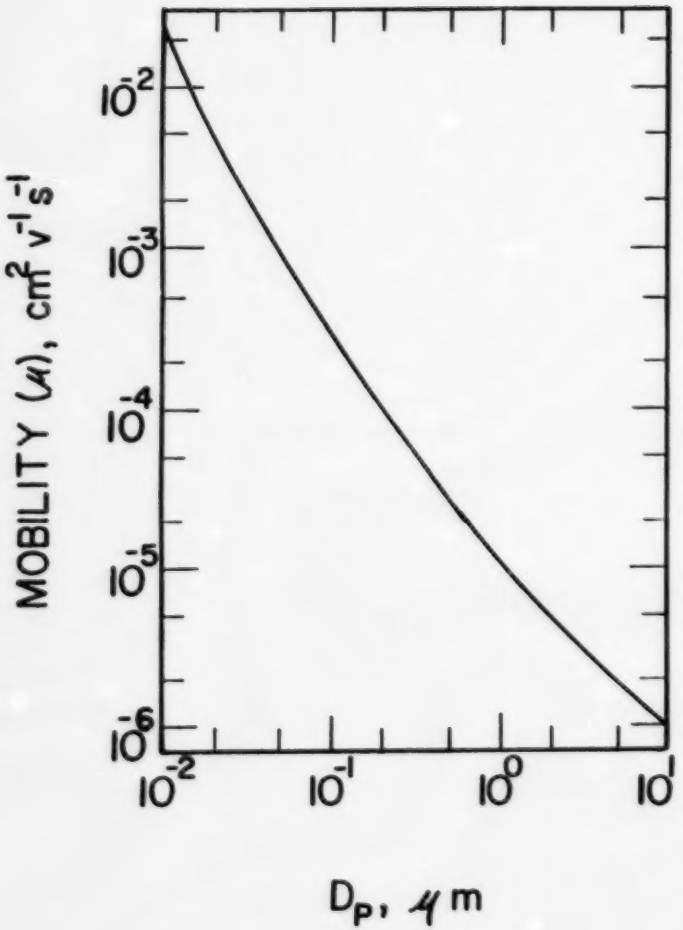

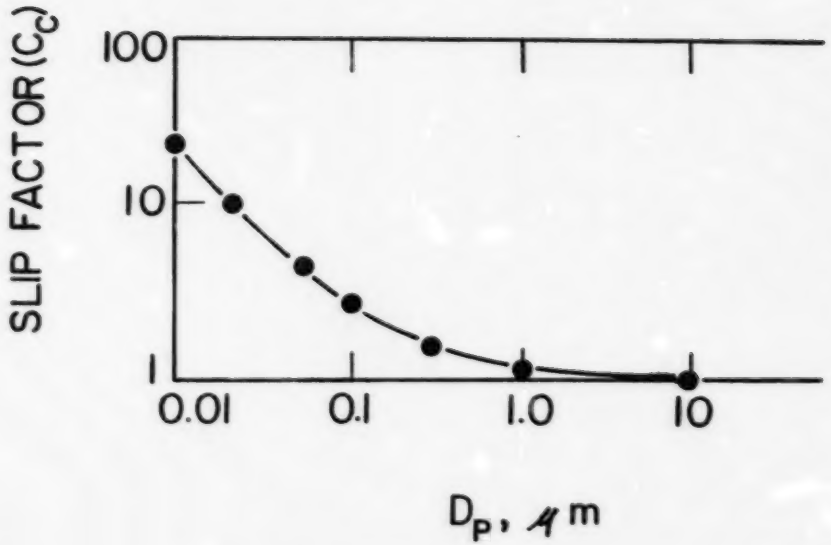

Fig. 34 - Electrical mobility for particles of diameter Dp (left hand side) and slip factor for particles of diameter Dp (right hand side).